Analysis and Evaluation of Transactive Energy Control in Active Distribution Systems

by

Matt Gray

A Thesis Submitted in Partial Fulfillment
of the Requirements for the Degree of

Doctor of Philosophy in Electrical Engineering

in

The Faculty of Engineering and Applied Science

in The Department of Electrical, Computer and Software Engineering

University of Ontario Institute of Technology

October 2016

Certificate of Approval

Abstract

The electric power distribution system is experiencing significant operational changes due to the integration of plug-in electric vehicles and intermittent distributed energy resources such as rooftop solar photovoltaics. As plug-in electric vehicle charging represents a significant increase in system loading, both distribution transformers and substation transformers are subject to overload conditions which rapidly degrade transformers lifetime. Furthermore, the increased penetration of rooftop solar photovoltaic in the residential sector may lead to bi-directional power flow and may additionally cause overload to the distribution transformers. In order to accommodate the growing market penetration of plug-in electric vehicles and rooftop solar photovoltaics, the electric utility must employ energy management to prolong the transformers lifetime. Given that transformers represent one of the most expensive assets in the distribution system, failure to resolve transformer lifetime degradation issues require the electric utility to incur the costs of transformer replacement or upgrading. The work in this dissertation proposes a transactive energy control methodology to perform residential energy storage system control as a means of reducing transformer lifetime degradation. The results have shown that the proposed framework may extend median annual distribution transformer lifetime by nearly double the expected lifetime of distribution transformers without transactive energy control. Finally, the proposed transactive control scheme has also been found to reduce active power losses within the system.

Acknowledgements

I would like to thank my supervisor, Dr. Walid Morsi Ibrahim. Your support, guidance, and genuine interest in the work has both motivated me and enhanced the depth of my research, allowing me to progress further than I had imagined.

I would also like to acknowledge NSERC for supporting my work and ultimately allowing me to pursue research in my field of interest.

Table of Contents

List of Tables

List of Figures

Nomenclature

AC – Alternating Current

AEP – American Electric Power

AMI – Advanced Metering Infrastructure

ANN – Artificial Neural Networks

c_t^{import} – Cost to Import Power at the Substation Transformer ($/kWh)

c_t^{DAM} – Cost to Import Power From the Transmission System ($/kWh)

CAES – Compressed Air Energy Storage

CDF – Cumulative Distribution Function

CPEVS – Canadian Plug-in Electric Vehicle Survey

CPP – Critical Peak Pricing

CPR – Critical Peak Rebate

d – Day Index

D – Set of All Days

DC – Direct Current

DG – Distributed Generation

DLMP – Distribution Locational Marginal Pricing

DR – Demand Response

DSO – Distribution System Operator

EPRI – Electric Power Research Institute

ESS – Energy Storage System

$F_{AA,t}$ – Accelerated Aging Factor

F_{EQA} – Equivalent Aging Factor

F_{Inv} – Inverter Efficiency Factor

F_T – Temperature Factor

FIPA – Foundation for Intelligent Physical Agents

FIT – Feed-In Tariff

GWAC – GridWise Architectural Council

h – Hour Index

H – Set of All Residential Homes

HAT – Home Arrival Time

HEM – Home Energy Manager

HEV – Hybrid Electric Vehicles

HP – Hourly Pricing

HVAC – Heating, Ventilation, and Air Conditioning

i – Bus Index

I – Current (A)

ICE – Internal Combustion Engine

IEC – International Electrotechnical Commission

IED – Intelligent Electronic Device

IEEE – Institute of Electrical and Electronics Engineers

IESO – Independent Electricity System Operator

IRR_t – Irradiance Seen on Solar Panel (kW/m^2)

k – Downstream Bus Index

K_i – Ratio of Initial Load to Rated Load

K_S – Ratio of Stable Load to Rated Load

KKT – Karush-Kuhn-Tucker

LMP – Locational Marginal Price

LoL – Loss of Life (%)

LTEP – Long Term Energy Plan

m – Empirically Derived Change in Winding Temperature to Change in Load Constant

MAE – Mean Absolute Error

MAPE – Mean Absolute Percent Error

MAS – Multi-Agent System

MPPT – Maximum Power Point Tracking

n – Empirically Derived Change in Top-Oil Temperature to Change in Load Constant

N_{Homes} – Number of Residential Homes

N_V – Number of Plug-in Electric Vehicles

OEV – Ontario's Electric Vehicles

ONAN – Oil Natural Air Natural

OLTC – On-Load Tap Changer

P – Active Power (kW)

$P_{e,t}^{Ch}$ – Energy Storage Unit e Charging Power at time t (kW)

$P_{e,t}^{Dis}$ – Energy Storage Unit e Discharging Power at time t (kW)

P_p^{rated} – Nameplate Rating of Solar Array p (kW)

$P_{p,array}$ – Real Power Output of Solar Array p (kW)

$P_{p,pu}$ – Per Unit Output of Solar Array p

PAPR – Peak-to-Average Power Reduction

PBEV – Plug-in Battery Electric Vehicles

PCC – Point of Common Coupling

PEV – Plug-in Electric Vehicles

PHEV – Plug-in Hybrid Electric Vehicles

PSH – Pumped Storage Hydropower

PV – Photovoltaic

Q – Reactive Power (kVAR)

r_v^{tot} – Maximum Driving Range of Plug-in Electric Vehicle v (miles)

R – Ratio of Rated Load Losses to No Load Losses

RTP – Real-Time Pricing

S – Apparent Power (kVA)

SOC – State of Charge

SQP – Sequential Quadratic Programming

t – Time Index

T – Set of All Time Steps

T_t – Temperature at Time Interval t (°C)

TFS – Transactive Feedback Signal

TIS – Transactive Information Signal

TSO – Transmission System Operator

TOU – Time of Use

TXF – Transformer

TXFCT – Center-Tapped Distribution Transformer

ν_i – Set of Input Predictors for Artificial Neural Network Model

ν_o – Set of Target Variables for Artificial Neural Network Model

V_i –Voltage at Bus i (kV)

VLN_{abc} – Vector of Line-to-Neutral Voltages for Phases A, B, and C

VT – Voltage Transformer

w – Weighting Values in Artificial Neural Network Model

δ_v – Driving Distance of Plug-in Electric Vehicle v (miles)

Δt – Duration of Time Interval (h)

$\Delta\theta_H$ – Change in Hottest-Spot Temperature (°C)

$\Delta\theta_{H,S}$ – Stable Hottest-Spot Temperature (°C)

$\Delta\theta_{H,i}$ – Initial Increase in Hottest-Spot Temperature (°C)

$\Delta\theta_{TO}$ – Change in Top-Oil Temperature (°C)

$\Delta\theta_{TO,i}$ – Initial Increase in Top-Oil Temperature (°C)

$\Delta\theta_{TO,R}$ – Top-Oil Increase Above Ambient Temperature at Rated Load (°C)

$\Delta\theta_{TO,S}$ – Stable Top-Oil Temperature (°C)

γ_v – Specific Energy of Plug-in Electric Vehicle v (kWh/mile)

η_e – Efficiency of Energy Storage Unit e

η_v – Efficiency of Vehicle Charger Used to Charge Plug-in Electric Vehicle v

ρ – Phase Index

ς –Artificial Neural Network Node Index

θ_A – Ambient Temperature (°C)

θ_H – Hottest-Spot Temperature (°C)

τ_{TO} – Top-Oil Thermal Time Constant (h)

τ_w – Winding Thermal Time Constant (h)

Ξ – Set of All Hours a PEV is Disconnected

1 Introduction

1.1 Background

Due to the integration of information technology within the power system, alongside economic and environmental concerns, ongoing research continues to assess the capabilities of adapting the existing power system infrastructure for improved reliability and efficiency through the use of intelligent decision making techniques, referred to as the Smart Grid. As defined by the US Department of Energy, the Smart Grid vision "uses digital technology to improve reliability, resiliency, flexibility, and efficiency (both economic and energy) of the electric delivery system" [1]. In this respect many stakeholders have established Smart Grid initiatives such as Ontario's Long Term Energy Plan (LTEP), to promote the reduction of energy costs and incorporate community engagement [2]. While the LTEP has resulted in the creation of a Smart Grid Fund to increase penetration of distributed renewable energy resources and electric storage devices [3], further initiatives are targeted directly towards residential customers. Programs such as Ontario's Electric Vehicles (OEV) [4] and MicroFIT [5] encourage residential customer plug-in electric vehicle and rooftop solar photovoltaic (PV) growth. While Government initiatives provide significant incentive for residential customers to actively produce power in addition to power consumption, traditional power consumers are transformed into prosumers, defined as customers capable of both producing and consuming power; the electric utilities are tasked with the responsibility of adapting the power system infrastructure to accommodate this new power system landscape which has not been experienced before.

In consideration of the growing penetration of plug-in electric vehicle charging, probabilistic impact penetration studies have determined that plug-in electric vehicle charging may increase voltage unbalance and neutral current within the distribution system [6], and additionally cause transformer overload resulting in reduced transformer lifetimes [7]. While electric utilities may employ a number of solution methodologies to mitigate voltage unbalance and neutral current issues, such as phase reconfiguration [8], few solution methodologies have been discussed to reduce transformer loss of life. Despite previous research showing the ability of rooftop solar photovoltaic generation to reduce transformer loss of life [9], in many cases transformer lifetime remains below the typical lifetime expected in systems design. As transformers constitute one of the most expensive components within distribution systems, the electric utility must pursue an additional form of control to alleviate loss of life impact.

More recently a term known as transactive energy has been proposed, which outlines an emerging concept of performing control actions within the power system [10]. As defined by the GridWise Architectural Council (GWAC), "Transactive energy refers to the use of a combination of economic and control techniques to improve grid reliability and efficiency" [11]. As the economics of distribution system operation consist of day-ahead energy markets, which look to buy and sell power at an hourly resolution over a 24-hour period in advance, and real-time energy markets, which look to buy and sell power over a 5-minute interval in real-time; transactive energy naturally integrates control into these energy markets to benefit the systems operation.

1.2 Problem Statement

Given financial incentive for residential customers to purchase plug-in electric vehicles (PEVs), rooftop solar photovoltaics (PVs) and energy storage systems (ESS), the increasing penetration of these technologies at residential homes results in different residential load and load growth patterns versus the predictable static growth models electric utilities were accustomed to. For example, plug-in electric vehicle forecasts vary wildly in PEV penetration estimates, with one source estimating the number of PEV's in Ontario increasing as low as triple the number of PEVs (status quo estimate), up to 50 times (100% growth estimate) the number of PEV's between 2015-2020 [12]. Rooftop solar photovoltaic penetration also expects significant growth, having 1.7GW solar capacity seen in 2015 (approximately 4.5% of Ontario's installed capacity) with another 3GW expected by 2040 [13]. Lastly, due to the recent emergence of retail energy storage systems such as the Tesla Powerwall, residential customers are now able to improve their home energy reliability and reduce electricity costs through managing the charging and discharging of household ESS. Having recently entered the retail market, total rated capacity of home ESS is projected to grow in North America up to 40 times between 2016 to 2025 [14].

As residential homeowners load profiles are now changing to incorporate intermittent large power consuming/generating devices, such as PEV and rooftop solar PV, previous research has suggested the distribution system will experience operational issues during excessive generation/demand periods. The resultant increase in PV penetration has been found in impact studies to cause reverse power flow and transformer overload [15], which represent abnormal system conditions and may result in undesired protection relay tripping [16]. Due to

the increased load demand of PEV charging, PEV have been found to cause distribution transformer overload [17], ultimately degrading transformer lifetimes in the primary distribution system [7]. The impact of PEV charging has been further found to be larger in magnitude considering second generation PEV's emerging on the market, due to higher charging powers and larger battery capacities [18].

In order for electric utilities to adapt to accommodate PEV and PV penetration growth within the distribution system, electric utilities may benefit from using the rapidly growing penetration of residential energy storage systems as a means of controlling the power flowing through the transformer, and consequently reducing the rate at which transformers degrade within the system. Given that energy storage systems must first charge electrical energy before power may be later discharged back into the power system; transactive control, which is any control scheme adhering to transactive energy, considering energy storage systems is naturally suited to the day-ahead energy market, which establishes the procurement of generation and load resources over a 24-hour time window versus the 5-minute horizon used in the real-time market.

1.3 Objectives

The main objective of this dissertation looks to address a transactive energy control solution for the electric utility to support the rapidly growing penetration of prosumer-based devices (specifically PEV's, PV's, and ESS). In order to achieve this goal, the following objectives are addressed:

1. Evaluate transformer loss of life to identify when distribution utility control action must be taken to mitigate transformer loss of life limit violation within the day-ahead energy market
2. Design of a transactive control framework and establish a game theoretic method to quantify the costs of bidding placed by the electric utility in the day-ahead scheduling problem to reschedule prosumer energy storage system resources for transformer loss of life reduction
3. Investigate the effectiveness of the proposed transactive energy control framework in terms of transformer loss of life reduction and active power loss reduction in order to assess the technical benefits and limitations of such control schemes
4. Determine the effectiveness of the transactive control framework under varying plug-in electric vehicle and rooftop solar photovoltaic penetrations, as well as time-of-use and distribution locational marginal pricing residential customer pricing schemes, to evaluate the proposed transactive energy scheme under varying conditions.

1.4 Proceeding Chapters

Chapter 2 of this dissertation investigates literature surrounding emerging Smart Grid technologies, specifically considering residential customer PEV, PV, and ESS in terms of transformer loss of life impact and solution methodologies. The resultant literature review will establish transactive energy methodologies used in ensuring power systems reliable operation, and detail a comparison of solution methodologies effectively employed in literature as the utilities means of reliability.

Chapter 3 provides a background on distributed energy resources within active distribution systems, including: primary energy storage systems, distributed generators (DG), plug-in electric vehicle charging, and rooftop solar photovoltaic generation.

Chapter 4 discussed the economic interactions of distribution systems operation. Specifically, this chapter provides an overview of energy markets, locational marginal pricing, distributed generation costs, and distribution locational marginal pricing based on previously reported literature.

Chapter 5 initially provides a discussion of distribution system power flow, specifically the modeling of distribution systems as well as the forward/backward sweep algorithm. Mathematical relationships have further been discussed as a means of estimating the transformers lifetime. The next section discusses the usage of artificial neural networking as a forecasting technique. Furthermore, a framework for transactive energy control of residential energy storage systems is presented, which seeks to minimize peak-to-average power. Finally, a game theoretic approach is used to determine the optimal costs incurred by the distribution utility to residential customers for the ability to perform residential energy storage system control.

Chapter 6 presents the implementation of the proposed transactive energy control methodology on a test system. The performance of the proposed transactive energy control scheme in terms of the technical and economic performance has further been discussed.

Lastly, Chapter 7 summarizes the significant findings seen in this work, providing recommendations for appropriate usage of a transactive energy control scheme, and offers potential future extensions for future studies.

2 Literature Review

2.1 Introduction

As the composition of residential household loads is changing to adapt with emerging technologies, residential customers power consumption habits are rapidly changing from the traditional predictive models employed by electric utilities. One such change is seen in residential customers whom are now beginning to drive plug-in electric vehicles, which draw significant power when charging their battery from the distribution power system. Consumers are also capable of employing small scale generation sources, rated up to a maximum of 10kW [19], of which the majority are rooftop solar photovoltaic installations. Traditionally, residential homeowners, referred to as consumers, had the capability of connecting loads which consume electrical power from the distribution system. When residential homeowners install generation at the household, the opportunity exists for the homeowner to both produce and consume power, transforming the homeowner from a consumer into a prosumer, defined as a combination of producer and consumer. Lastly, the recent emergence of household energy storage systems (ESS) combine the characteristics of both load and generation resources, as these storage systems draw significant amounts of power used to store energy for discharging back into the system at a future point in time. While these residential customers, whom reside at the end of the power system, are undergoing rapid changes in energy use patterns; the power system itself, specifically the distribution system which is used to supply power to these consumers, must perform energy management in order to accommodate the change in energy consumption habits.

The distribution system, which forms the last section of the power system and delivers power to end-use residential customers, expects significant investment in infrastructure required to accommodate the rapidly changing demand. Considering the infrastructure upgrades required to perform distribution automation, advanced metering, and other energy management functions; the Electric Power Research Institute (EPRI) estimates a total investment of $167-$249 billion in Smart Grid costs by 2030 [20]. Despite the large up-front cost of distribution system infrastructure, the resultant benefit-to-cost ratio is approximately 4:1, by considering both public and electric utility benefits such as prolonged asset lifetimes, increased reliability, and increased productivity [21]. Furthermore, the increased efficiency and inclusion of renewable generation estimates a 58% reduction in carbon dioxide (CO_2) by 2030 as compared to CO_2 emissions in 2005 [22]. In order to fully realize these projected benefits, the distribution system must effectively and economically use the emerging Smart Grid technology to limit reliability impact on distribution systems operation.

2.1.1 Impact of Plug-in Electric Vehicle Charging on Voltage Unbalance and Neutral Current

Preliminary work investigating the impact of plug-in electric vehicle charging on secondary distribution systems has determined through a probabilistic study that Level 1 (120V) PEV charging with as low as 50% penetration levels results in secondary system voltage unbalance violations as shown in Table 2.1 [6]. The results of [6] have further determined that at high penetration levels, distribution transformer neutral current may exceed allowable levels, resulting in neutral overload conditions, visualized in Fig. 2.1, and may consequently trip protection devices. Similar studies performed in [23] and [24] have further

reported that increasing plug-in electric vehicle penetration results in voltage unbalance conditions near the feeder at which plug-in electric vehicles charge, with a reported 27.1% chance of voltage unbalance violation with plug-in electric vehicle penetrations as low as 10%.

Table 2.1 Number of Hours Voltage Unbalance Violation Occurs on Secondary System Due to PEV Charging

PEV Penetration	Number of Hours of Voltage Unbalance Violation
50%	3
100%	7
200%	12

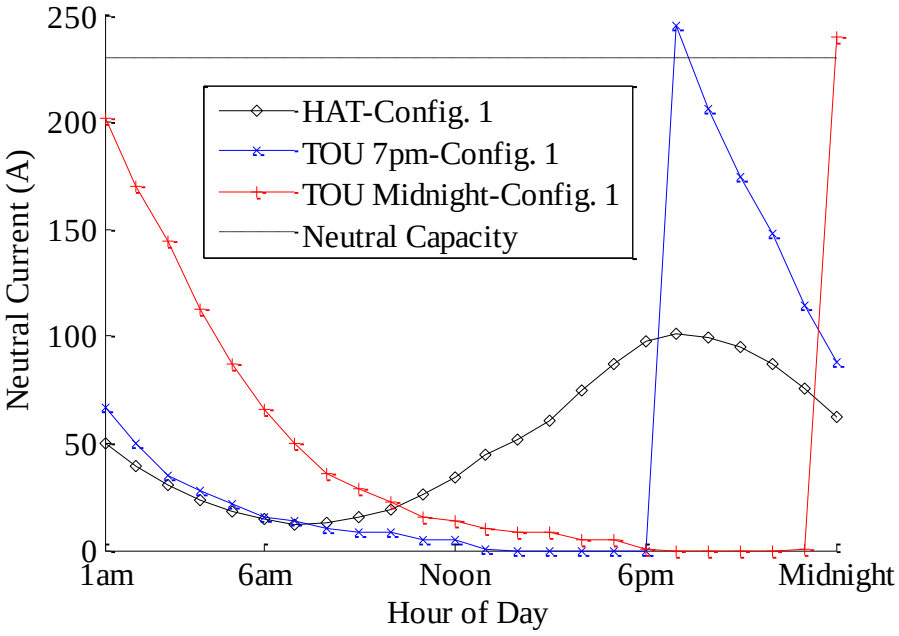

Fig. 2.1: Neutral Current Seen at Distribution Transformer

2.1.2 Impact of Plug-in Electric Vehicle Charging on Distribution System Losses

Studies investigating the impact of plug-in electric vehicle charging on system efficiency have found that uncoordinated plug-in electric vehicle charging strategies result in increased line losses [23, 25]. Transformer losses have also been found to increase due to plug-in electric vehicle charging, which has been reported to triple in the presence of 40% PEV penetration [26]. Such losses have further been attributed towards the temporal coincidence of plug-in electric vehicle charging [27], which has shown that losses are significantly increased due to the simultaneous charging of numerous plug-in electric vehicles.

2.1.3 Impact of Plug-in Electric Vehicle Charging on Transformer Overload

In secondary distribution systems, consisting of the low-voltage system connecting the secondary of distribution transformers to end-use residential customers, distribution transformers are typically sized to accommodate the expected load growth of residential systems. Many studies have reported the potential for transformer overload to occur in secondary systems which supply the charging of plug-in electric vehicles [7, 17, 18, 26, 28, 29], with [17] reporting 100% of 50kVA distribution transformers must be upgraded to a larger size for secondary systems feeding 1 PHEV/House, to mitigate overload occurrences. The work of [17] also indicates an increase in peak demand of the substation transformer by 132% at 100% PHEV penetration, resulting in substation transformer overload. Such overloading conditions are typically the result of temporal coincidence, in which the majority of plug-in electric vehicles are expected to begin charging at similar hours at the end of the work day [30].

2.1.4 Impact of Plug-in Electric Vehicle Charging on Transformer Loss of Life

Contrary to the term transformer overload, indicating a transformer is supplying power beyond its nameplate rating, transformers are capable of operating under overload conditions at the cost of significantly increased heating, therefore increasing the speed at which the transformers lifetime degrades [31]. The work of [15] has found that more than 90% of distribution transformers feeding 1 PEV/House considering 3.7kW Level 2 charging are subject to overload during the hours of 7pm-9pm, resulting in daily distribution transformer loss of life ranging between 0.006%-0.013% when house peak loading is assumed 6.64kVA, and 0.120%-0.268% in the case of 8.65kVA peak loading. Given a daily loss of life limit of 0.013% [31], distribution transformers will experience loss of life violation unless corrective measures are performed. Such loss of life violation has been further reported in [7], preliminary work of which plug-in battery electric vehicles have been found to be more detrimental to distribution transformer loss of life. Through the study in [7], summarized in Table 2.2, distribution transformer loss of life values were found to be 150% greater than would be seen by plug-in hybrid electric vehicles.

Table 2.2 Distribution Transformer Loss of Life Considering PEV Type and Charging Level

PEV Considered	Charging Level Considered	Mean Distribution Transformer Loss of Life (%)
PHEV Only	Level 1 (120V)	0.0057
PHEV and PBEV	Level 1 (120V)	0.0064
PBEV Only	Level 1 (120V)	0.0073
PHEV Only	Level 2 (240V)	0.0066
PHEV and PBEV	Level 2 (240V)	0.0082
PBEV Only	Level 2 (240V)	0.0107

A study performed in [18] extends upon plug-in electric charging impact to suggest that second generation plug-in electric vehicles, which have larger battery capacities, may double the expected loss of life on distribution transformers when compared to first generation PEV counterparts. Moreover, [18] reports increased transformer loss of life at high power ratings, as the plug-in electric vehicle charging impact increases from 2.90% annually to 3.11% annually when considering 3.7kW and 6.6kW charging powers respectively in the case of 50% PEV penetration of Nissan Leaf plug-in battery electric vehicles.

2.2 Plug-in Electric Vehicle Charging Impact Mitigation Techniques

As plug-in electric vehicles are growing in penetration and have been predicted to cause numerous reliability issues, prior research had begun to investigate effective methods of reducing the impact caused by plug-in electric vehicles, without compromising the energy requirements of the plug-in electric vehicle owner. The majority of literature focuses on scheduling plug-in electric vehicle charging, while other research works have investigated the addition of rooftop solar panels to directly mitigate the effects of PEV charging.

2.2.1 Phase Reconfiguration of Secondary Systems

In order to reduce the voltage unbalance neutral current within the secondary system, preliminary work in [8] has proposed a phase reconfiguration solution. Through the application of phase reconfiguration devices, the work in [8] establishes an economic quantification of the benefits of phase reconfiguration in terms of voltage unbalance and neutral current reduction. The results of [8] have moreover investigated the economic feasibility of applying such a method, summarized in Table 2.3, which reports the annualized net profit to distribution utilities through application of the phase reconfiguration devices.

Table 2.3 Expected Annual Net Profit Due to Addition of Phase Reconfiguration Into Secondary System

Number of Phase Reconfiguration Devices	Annual Net Profit Considering Home Arrival Time PEV Charging	Annual Net Profit Considering Time-of-Use PEV Charging
1	$41.36	$393.90
2	$63.38	$395.50
3	$48.16	$374.50
4	$29.67	$342.10
5	$12.62	$310.10

While the results of [8] have been shown to mitigate voltage unbalance and neutral overload conditions, the phase reconfiguration devices may only adjust which phase a load draws power from, and does not remove the significant PEV charging load which results in increased transformer loss of life.

2.2.2 Plug-in Electric Vehicle Charging Scheduling and Aggregation

Given that 84% of all plug-in electric vehicle charging occurs at home [32], typically after returning home from work [33], plug-in electric vehicle scheduling methods look to schedule the combined charging of all plug-in electric vehicles to minimize power system impact. Taking into account the potential inconvenience to the customer [34], most plug-in electric vehicle scheduling methods aim to disperse the cumulative plug-in electric vehicle charging demand as much as possible while retaining the total charge energy and connection time parameters set by the PEV owner [35]. Practically, such methods either assume the electric utility is responsible for coordinating the plug-in electric vehicle charging schedules,

or alternatively, an intermediate plug-in electric vehicle aggregator performs scheduling operations while adhering to grid constraints [36].

The work of [37] considers a different perspective on plug-in electric vehicle charging scheduling by establishing a theoretical limit on the maximum number of simultaneous PEVs which may charge at any given time, considering transformer loss of life and CO_2 emission constraints via optimal scheduling. Having performed optimization using Karush-Khan-Tucker, the results of [37] suggest that no greater than 20% household penetration of plug-in electric vehicles (2.1) may be supported simultaneously at any given hour.

$$Household\ Penetration(\%) = \frac{N_V}{N_{Homes}} \times 100 \tag{2.1}$$

Where N_V and N_{Homes} are the number of plug-in electric vehicles and residential homes respectively. As 20% simultaneous plug-in electric vehicle charging limit restricts charging to one vehicle per five houses, this solution methodology may be infeasible at larger vehicle penetrations, given that the majority of homeowners perform PEV charging at overnight hours.

In order to reduce the computational cost required to solve the scheduling of a large number of PEV's, convex relaxation was used in [38] to simultaneously minimize charge duration and maximize the final state of charge of plug-in electric vehicles. Convex optimization considered in this work aimed to limit total transformer power to the maximum value (peak load) expected without PEV in the system. While this charge scheme successfully limited PEV charging to the peak transformer loading, transformer peak loading is typically larger than the transformer rating, and the resultant optimal solution may significantly degrade transformer lifetime.

Following the notion that plug-in electric vehicle owners respond to time-of-use (TOU) customer pricing by programming PEV to charge during off-peak hours [39], PEV charging control may be performed indirectly through changing the times considered as off-peak hours in the TOU pricing scheme as studied in [40]. Through delaying the time at which the TOU off-peak rate begins later in the night starting at 11pm, the simulated 5 house secondary system fed by a 50kVA distribution transformer found a reduction in peak loading from 48kW to 40kW with minimum voltage increased from 113V to 115.5V. Despite positive impact mitigation seen, the impact of modifying the TOU rate with respect to the impact of charging plug-in electric vehicles seen on the primary system, which is highly susceptible to large numbers of simultaneous vehicle charging, has not been investigated. Furthermore, the work of [40] has not considered the resultant impact of changing TOU rates on non-PEV residential demand and may be optimistic in reporting mitigation.

While plug-in electric vehicle scheduling methods under idealized scenarios have shown the ability to reduce the impact expected in uncoordinated plug-in electric vehicle charging scenarios, such scheduling methods typically rely on residential customers' willingness to perform demand response. Furthermore these solutions, which provide a benefit to the electric utility, require economic consideration to the plug-in electric vehicle owner for their participation, a business case which has not been successfully proven in literature.

2.3 Impact of Rooftop Photovoltaics on Transformer Lifetime

Rooftop solar photovoltaics (PV) represent an emerging technology which allows homeowners to become power producers alongside traditional household power consumption. Given that household generation locally supplies household consumption, rooftop solar PV

generation acts to improve voltage profiles [41] and reduce transformer loss of life [42]. Such benefits may be seen in prior literature, as [43] reports that 17% rooftop solar PV penetration may supply up to 55% of system loading during peak sunlight hours in July. Furthermore, the work of [15] suggests that 50% PV penetration is capable of reducing the expected loss of life of 25kVA and 50kVA distribution transformers by 60% throughout a typical year.

Despite the benefits offered by PV generation, the work in the literature also suggests that excess generational capabilities may result in significant voltage rise, which may limit total installable capacity [43], and is further concluded by overvoltage issues found in the IEEE 13 Bus Test System when modified to include 40% PV penetration [44]. Such overvoltage issues have resulted in the recommendation that voltage rise impact studies be performed on any feeder exceeding an average of 5kW PV/House [45].

2.3.1 Mitigating the Impact of Plug-in Electric Vehicle Charging using Rooftop Solar Photovoltaic

Considering rooftop solar photovoltaic is growing in penetration, a number of articles [15, 41, 42, 46] have investigated the ability of household rooftop solar PV generation as a means of mitigating the increased load demand due to plug-in electric vehicle charging.

The work of [46] considers a Monte Carlo simulation to study the combined effects of rooftop solar PV with plug-in electric vehicles in an Ontario based distribution power system. While this study has concluded that rooftop solar PV generation is not capable of mitigating transformer overload resulting from plug-in electric vehicle charging due to a lack of chronological coincidence, this study has not further investigated the resultant impact of solar generation to address plug-in electric vehicle impact on transformer lifetime degradation. Such

loss of life impact was further neglected in [41], which has determined the times of peak solar panel generation does not occur at the same time of peak plug-in electric vehicle charging and therefore transformer overload persists.

The work of [42] looks to quantify the transformer loss of life improvement, through the addition of solar panel generation to reduce the impact of plug-in electric vehicle charging loads as a stochastic Monte Carlo simulation. It was found in this work that 27% penetration of plug-in electric vehicles on a 200kVA transformer may expect loss of life reduction from 125% to 110% when 27% solar panel penetration is added. Less optimistic findings are reported in [15] which conclude that when 50% solar penetration is added to 50% plug-in electric vehicle penetration, the resultant loss of life of the distribution transformer is reduced by only 1%.

Further preliminary work in [9] has further detailed an investigation into the synergy between rooftop solar PV as a solution to the increased transformer loss of life seen with PEV charging. The results of [9] have revealed that PV penetration is capable of reducing the loss of life incurred by transformers, but the loss of life reduction is limited due to the time-mismatch between PV generation and peak transformer loading as exemplified in Fig. 2.2.

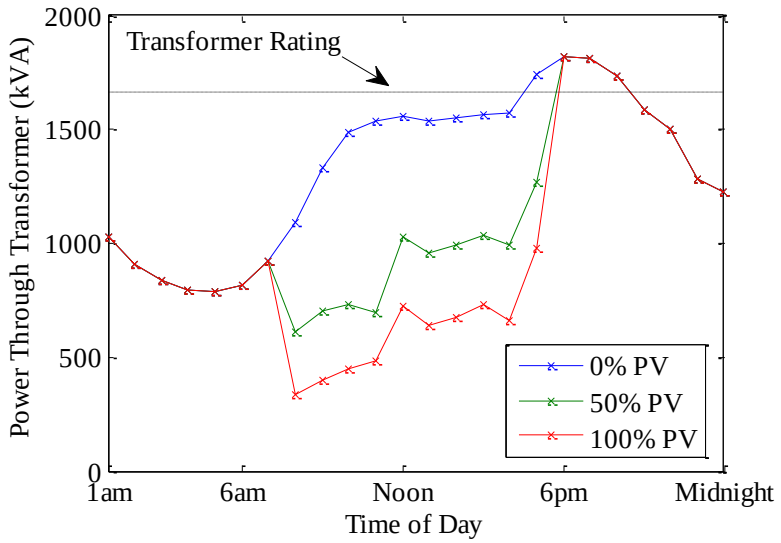

Fig. 2.2: Exemplified Mismatch between PV Generation and Peak Transformer Loading Times

2.4 Impact Mitigation Techniques in the Presence of Rooftop Solar PV

In order to effectively mitigate voltage rise issues occurring due to large PV penetrations, a number of mitigation techniques have been proposed in previous literature, including: dispatch of PV generation [47, 48], controllable reactive power banks [49], demand side management [50-52], and energy storage system control [53-55].

Literature investigating PV dispatch investigate the benefits of allowing PV systems to output a controllable amount of real (P) and reactive (Q) power based on grid operational conditions. While such schemes have proven to be effective in mitigating voltage rise issues with load tap changer control in the primary system [47] and without load tap changer control in the primary system [48], reactive power output of PV systems as an impact mitigation solution suffers from a number of practical issues preventing widespread deployment. Firstly, the governing IEEE standard for interconnecting distributed resources with electric power

systems (IEEE 1547 [56]) does not permit PV inverters to regulate voltage through reactive power injection for reasons of electric utility predictability. Furthermore the PV system owner, whom receives financial compensation for active power generation only, must reduce their active power generation in order to provide reactive power and therefore decreasing revenue for the PV owner. Similar economic issues are faced in the reactive power bank control scheme of [49], which suggests the PV owner pay additional installation costs to control reactive power as a means of regulating power quality, despite not being responsible for power quality control.

Demand side management techniques look to increase the system loading during hours of peak PV generation, by shifting deferrable loads to the times of high PV output [50]. While the usage of load shifting techniques has played a role in the mitigation of PV issues in high penetrations [51], the low turnout rate of demand response participants [52] suggests that distributed generation dispatch may be more effective than load shifting in resolving voltage rise issues caused by PV generation.

Prior literature [53-55] has begun to investigate the benefits of pairing energy storage systems (ESS) with residential PV systems behind the residential customers' meters, to alleviate PV generational impact. The most simple control scheme looks to shift the PV generation profile by storing the excess power generation from rooftop solar PV into the ESS during midday, the time at which voltage is expected to rise above normal operating limits [53]. The energy stored in the ESS through rooftop solar PV generation may then be discharged throughout the evening, the time at which voltage magnitudes are expected to be lowest. While this simple charge/discharge scheme is capable of shifting a portion of the generated PV energy to later points in time, the work of [54] suggests that on-load tap changers (OLTC) must be equipped with communication to all ESS to reduce unnecessary load tap changes and therefore

relieve strain on OLTC devices. While such a solution focuses on prolonging the utility equipment's lifetime, the economic costs associated with the communication system would expectedly exceed the benefits of prolonged OLTC life, rendering the solution impractical.

A more practical economic ESS case has been suggested in [55], which looks to use ESS behind the residential customers meter to increase the self-consumption of the customer, which measures the percentage of PV energy generated that is consumed locally or alternatively stored in an energy storage device [57]. The study of [55] considers the German power system, in which the price of selling rooftop solar PV generation to the electric utility is less than the cost of purchasing energy. Due to higher energy purchase costs than the price of selling PV generation, there is more economic benefit to the residential customer if PV generation is used to feed the residential customers own load demand than to export generated PV power to the grid. The results of [55] have shown that while using ESS for self-consumption is economical to the residential customer, the study has not considered the possibility of additional economic motivation for the residential customer to use their ESS for electric utility control, resulting in a mutual benefit to the ESS owner and electric utility.

2.5 Transactive Energy for Distribution System Control

In May 2004, the GridWise Architecture Council (GWAC) formed from the need to define interoperability frameworks to address the growing number of technologies being deployed on the electric grid. In response to the observation that technology on the grid edge is significantly increasing, and distributed energy resources such as intermittent resources add significant complexity to the grid, GridWise referred to "Transactive Energy" to address growing control required of a Smart Grid. As defined by GWAC, transactive energy is "the

combination of economic and control techniques to improve grid reliability and efficiency" [11]. One such application of transactive energy is through establishing a transactive market between the distribution system operator and residential customers.

The work of [58] outlines three markets which are used to tie central controllers to end-use loads and describes the difference between transactive energy control with respect to previous demand response measures taken by electric utilities: active markets, interactive markets, and transactive markets. An active market represents one-way communication between the central controller and end-use loads, where the central controller sends pricing information to end-use loads, and the end-use loads may react to the pricing scheme imposed. Time-of-use pricing is an example of demand response typically used by electric utilities, which employs an active market; as the electric utility imposes a pricing scheme on the residential customer, but the electric utility is not aware in advance of how the pricing will impact residential customer demand. Extending on an active market is an interactive market, which involves two-way communication as end-use loads may return information back to the central controller, potentially resulting in changes to the original pricing signal. Finally, a transactive market advances on an interactive market by including end-use loads which are capable of performing automatic actions to pursue the interests of the end-use loads.

While the definition of transactive energy is still open to interpretation, it may be given that control schemes may follow the ideas of transactive energy as long as economics, control, grid reliability, and efficiency are objectives outlined in the control scheme. Furthermore a transactive market, which is one application employing transactive energy, requires end-use loads to: employ two-way communications, react to price changes, return information to a central controller, and act automatically on behalf of the end-use load owner. In recent

literature, a number of transactive energy experiments have been performed on utility systems, primarily focusing on double-auction bidding transactive markets for transactive control.

The most notable transactive energy project is the Pacific Northwest National Laboratories "Olympic Peninsula Project" [59], which employed a 5-minute real-time pricing signal via double auction bidding in order to determine the effectiveness of two-way communications between the electric grid and capable distributed resources. In this respect, controllable load and generation devices were capable of submitting bids for the price and quantity of power supply/demand (with uncontrollable loads and generators bidding at $9,999 and $0 representing the maximum and minimum allowable bid values respectively), with the market determining the appropriate clearing point to match supply and demand at each 5 minute interval. In this experiment, the major controllable load consisted of heating, ventilation, and air conditioning (HVAC) as controlled using smart thermostats, which provided residential customers with a "comfort setting" (desired level of comfort versus cost savings) and automatically controlled residential customers thermostat levels in response to real-time prices. Throughout the recorded dataset spanning a year in duration, the transactive control scheme was able to maintain feeder capacity within limits for the entire year except for a single 5-minute interval. Furthermore, 5% to 20% peak load reductions were achievable using the real-time pricing method, through shifting of thermostatic loads to early morning hours when prices were low.

PowerCentsDC [60] performed a customer pricing response experiment in 2009 to compare residential customer response to different consumer pricing schemes including critical-peak pricing (CPP), critical-peak rebate (CPR), and hourly pricing (HP). Through this experiment, PowerCentsDC found that time-based consumer pricing plans play a noticeable

role in peak reduction; with CPP, CPR, and HP reducing summer peak consumption by 34%, 13%, and 4% respectively. Such results further determined that smart thermostats, which automatically adjust homeowners' temperature set point based on electricity pricing, were capable of reducing peak loading beyond normally achievable levels obtained when homeowners manually adjust thermostats in response to pricing schemes. While this form of control allows end-use loads to act automatically and react to price changes, the smart devices were not reported to provide two-way communications and return information to central controllers, and therefore the project established an active market as opposed to a transactive market. Furthermore, while the control scheme used in this work aimed to combine economics and control, this work only provides analysis to residential customer response to different pricing plans, and therefore did not consider grid reliability and efficiency as required by transactive energy ideals.

American Electric Power (AEP) Ohio attempted a larger scale transactive energy project, spanning 11 electric utilities in the Pacific Northwest region, to incorporate price-responsive devices including large and small demand resources [61]. Large demand resources included: DG's, heating ventilation and air conditioning (HVAC), renewable generation, and battery energy storage devices. Small demand resources consider: communicating thermostats, water heater controllers, and smart appliances. Furthermore, AEP Ohio integrated SMART Choice home energy management systems to some residential customers, which allows the residential customers to automatically bid for power in the real-time market and therefore has established a transactive market. While this project employs a transactive market, and considers grid reliability in terms of power-outages in the real-time market, the AEP Ohio project does not

consider the effects of transactive energy in the day-ahead market, including reliability issues such as transformer lifetime degradation.

In the most recent transactive energy experiment to date, PNNL established the gridSMART Smart Grid demonstration project, which provides participants with a home energy manager (HEM) as a combination of advanced metering infrastructure (AMI) and smart thermostat communication [62]. Through allowing residential customers to set their desired comfort settings (desired level of comfort versus cost savings), the HEM competed in a double-auction market with generation resources to employ a transactive market for increased grid reliability. Through the gridSMART experiment, it was found that congestion reduction was achievable while retaining positive impressions on residential customers, as 76.3% of customers reported positive feedback versus 11.8% giving negative feedback. Moreover, the real-time pricing strategy resulted in monthly electricity bill savings to 51.4% of customers (at an average of $22.15 saved per month) versus 9.5% experiencing increased costs (at an average of $22.23 per month). Another interesting finding by the gridSMART project was the technical limitations of real-time pricing, in which the processing and communication times of the market were too large in duration to meet 5-minute intervals in real-time, and as such the 5 minute real-time prices were calculated and set based on the results of the double-auction market clearing value in the interval performed 10 minutes prior. Despite employing a transactive market, the grid reliability application was limited to customer interruptions, and did not assess the long term reliability effects of transformer lifetime degradation. Furthermore, grid efficiency in terms of losses was not reported. Finally, while the transactive market outlined in [62] considered energy storage systems, the transactive market was employed in

the real-time energy market and therefore may not have found a long term optimal solution more appropriately given in day-ahead market scheduling.

The concept of transactive energy has also been gaining attention in academic literature, as a means of minimizing economic risk to the electric utility [63], and is traditionally employed as a feedback loop between transactive information signals (TIS) and transactive feedback signals (TFS) [64]. The majority of academic literature pertaining to transactive energy focuses on the economic case, thermodynamic controls, PEV scheduling, or microgrid cluster control.

Recent literature focusing on economics [65] and [66] aim to provide a business case to incentivize residential customers to install distributed energy resources. Such literature has considered the cost/benefit analysis of photovoltaic and energy storage systems in residential homeowners [65], as well as employing game theory for energy market bidding in commercial businesses [66]. While these studies detail economic benefit to residential customers through PV generation, these studies limit the ability of the distributed resources to provide control signals to the electric utility. Despite these works claiming transactive energy methodologies; a lack of two-way communication, and therefore the lack of an established transactive market, results in the studies only employing active market control and therefore does not follow transactive energy ideals.

Studies which consider demand response in appliances [58, 67, 68], typically focused on smart thermostats and investigated the ability of demand response on distribution system control to maintain grid reliability. While such forms of control are capable of reducing peak loading (to as much as 17% reduction given 25% smart thermostat penetration [58]), these

studies rely on active residential customer participation into demand response programs, which typically receive low response rates.

Scheduling of plug-in electric vehicles in transactive energy schemes has been considered in [69] and [70]. Since PEV are expected to park for a longer time duration than required to fully charge [69], transactive energy schemes in PEV exploit the customers' ability to wait for reduced pricing times in order to charge their plug-in electric vehicle. Charge scheduling of PEV has been performed at the individual level in [69] and as fleets in [70], however the act of scheduling electric vehicles may delay or limit the consumers ability to reliably charge, resulting in inconvenience to the plug-in electric vehicle owner [34].

Lastly, literature has investigated the impact of transactive energy on microgrid clusters, as a set of interacting microgrids which exchange power between each other in order to balance generation and demand as performed in [71] and [72]. While the microgrid cluster power exchange method has been shown to reduce microgrid operating costs by up to 15.34% [71]; similarly to PEV literature, these studies do not consider the resultant impact on the electric utility system operations, and do not consider the power systems reliability.

It may be seen from the literature that transactive energy applied through smart thermostat bidding is well-established in the literature as a transactive control method. Despite such transactive control, energy market applications in previous literature have been limited to inclusion in real-time energy markets, which only consider reliability from a power delivery and power outage perspective. Furthermore, the role of the battery energy storage systems in residential prosumers when considering a transactive energy framework has not been fully investigated in the literature. Finally, transactive energy literature has not considered the

effects of transactive control on transformer lifetime degradation, which impacts grid reliability.

2.6 Summary

The emergence of plug-in electric vehicles charging at residential homes with high penetration is expected to result in significant reliability issues. Such reliability impact of plug-in electric vehicle charging is most concerned with the resultant decreased transformer lifetime due to additional system loading. While PV penetration continues to increase, studies have shown that additional generation offered by rooftop solar PV may improve transformer lifetimes, but such improvement is limited due to a mismatch between PEV charging and PV generation peak times. At higher penetration levels however, PV generation may result in reverse power flow causing considerable overvoltage. Given that a number of solution methodologies play a role in voltage regulation, such as on-load tap changing transformers, transformer loss of life mitigation has received minimal attention in literature, despite transformers being one of the most expensive assets in electric power distribution systems.

As transformer lifetime decreases with the addition of plug-in electric vehicle charging, but may also experience decreased lifetime in the case of large reverse power flow in systems with high PV penetration, the ideal solution looks to supply growing plug-in electric vehicle charging demand using the increasing number of PV on the system. Balancing PV generation and plug-in electric vehicle charging is normally impractical however, as PV generation may only occur during sunlight hours, whereas most plug-in electric vehicle charging begins in the evening when plug-in electric vehicle owners are expected to return home. Given that energy storage systems, which store energy for future use, are capable of storing the energy provided

by PV generation for release at a future point in time, the potential exists to store PV generation in ESS during sunlight hours to discharge during evening hours at which plug-in electric charging issues have been found.

Previous studies have briefly investigated the potential to charge ESS during peak sunlight hours using PV generation and discharge during hours of high load demand in the evening. While the results of such studies have been promising, there is a lack of incentive for the ESS owners, whom are expected to use ESS for the benefit of electric utilities, to comply with electric utility control signals. Instead, it has been seen that residential customers install ESS in their homes for their own economic benefit [55], and the opportunity exists for pricing signals to establish a mutually beneficial arrangement between electric utility and ESS owners.

More recently, academic literature and real world projects have begun to assess the potential of employing economic considerations into distribution system control, described as transactive energy. Considering transactive energy is a recently emerging term, formal methodologies on the application of transactive energy to perform distribution system control are not yet defined. Furthermore, a means of quantifying the potential benefits of employing transactive energy control in a distribution system is needed to accurately assess the feasibility of transactive energy control schemes.

3 Emerging Distributed Energy Resources in Active Distribution Systems

3.1 Introduction

In order to employ transactive control within the distribution system, an active distribution system is required. An active distribution system extends upon the traditional distribution system definition to consider systems which may control distributed energy resources, distributed energy resources of which constitute generation, loads, and storage [73]. Battery energy storage systems, distributed generation, plug-in electric vehicle charging loads, and rooftop solar PV generation constitute distributed energy resources which have recently begun to penetrate the electric power distribution system and particularly in the residential sector.

3.2 Energy Storage System

An electrical energy storage system constitutes any medium capable of storing and releasing electric energy on the power system, which have only recently become large enough in size to be viable additions to the distribution system [74]. Through selectively storing and releasing electric energy, energy storage systems are capable of resolving the generation-demand mismatch by transferring energy through time. In this respect, an energy storage system may charge during off-peak hours and resultantly release stored energy during peak hours, to reduce strain on the power system.

While pumped storage hydropower (PSH) and compressed air energy storage (CAES) are the most common forms of bulk electric storage today [75], these technologies have low energy density making the more energy-dense battery storage medium preferred in distribution system environments [76]. Lithium-ion battery energy storage, which represents 85.6% of

cumulative energy storage power capacity installed in 2015 [77], naturally operates using direct current (DC) whereas the distribution system uses alternating current (AC). In order to provide power to the distribution system, battery energy storage systems require an additional DC to AC inverter with typical storage protection devices as depicted in Fig. 3.1 [78].

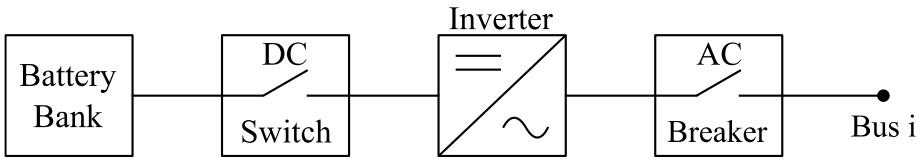

Fig. 3.1: Battery Energy Storage System Schematic

As most storage systems do not have reactive power capabilities [79], electric utilities may employ storage within the distribution system using active power control to perform functions such as: electric service reliability, renewables capacity firming, and energy cost management [80].

Energy storage system in the distribution load flow model is considerable as a combination of a positive charging load $P_{e,t}^{Ch}$ and negative discharging load $P_{e,t}^{Dis}$, assuming no reactive power, and subject to energy storage system power and energy constraints (3.1)-(3.5) [81].

$$0 \le P_{e,t}^{Ch} \le P_e^{Ch,\max} \tag{3.1}$$

$$0 \le P_{e,t}^{Dis} \le P_e^{Dis,\max} \tag{3.2}$$

$$E_{e,t} = E_{e,t-1} + P_{e,t}^{Ch} \cdot \eta_e - P_{e,t}^{Dis} \big/ \eta_e \tag{3.3}$$

$$E_e^{\min} \le E_{e,t} \le E_e^{\max} \tag{3.4}$$

$$E_{e,0} = E_e^{ini} = E_{e,T} \tag{3.5}$$

Where $P_{e,t}^{Ch}$ and $P_{e,t}^{Dis}$ are the charging and discharging powers of energy storage system e at time t, $P_e^{Ch,max}$ and $P_e^{Dis,max}$ are the maximum charging and discharging powers of the storage system, $E_{e,t}$ is the energy of storage system e at time t, E_e^{min} and E_e^{max} denote the minimum and maximum allowable energy limits of the storage system, E_e^{ini} denotes the initial energy stored, η_e is the charging efficiency of storage system e, and T is the final time period t.

In this respect, constraint (3.1) and (3.2) provide maximum limitations on the rate of charging and discharging by the energy storage system. Constraint (3.3) considers the efficiency of charging and discharging the energy storage medium due to losses in the power conversion system. Storage system energy constraints and maximum depth of discharge are bounded in (3.4). Finally, constraint (3.5) requires the energy storage system to begin and end with a fixed amount of energy stored to ensure the initial storage system state is deterministic at any given day.

3.3 Distributed Generation

Distributed generation is the concept of providing generation resources locally within the distribution system. Furthermore, these generators typically range between 1kW to 50MW in capacity, and are largely dispersed within the distribution system itself [82]. The inclusion of distributed generators directly reduce the amount of power to be imported through the transmission system, ultimately reducing line losses and line congestion, and further offers operational benefits such as increased system reliability and power quality [83]. Distributed generators may be owned by either the electric utility or by private investors as a means of generating revenue.

Distributed generators generate power through one of many sources, such as: coal, natural gas, biomass, water, wind, and solar. While non-renewable generation resources such as coal and natural gas may output emissions during power generation, unlike renewable generation sources such as wind and solar, these fuel-powered generators allow control over the generators output, allowing the distribution system operator to schedule generation to meet changing grid needs. Conversely, distributed generators of renewable energy sources provide power without significant environmental emissions, however reliance and intermittency of uncontrollable sources such as solar generation create significant uncertainty on the output, which varies significantly over time. Furthermore, renewable sources such as photovoltaic solar panels suffer from chronological coincidence, such that all solar panels on the system output power simultaneously during sunlight hours as opposed to an even distribution throughout the day. Such combined generation events may lead to reverse power flow conditions on the distribution system, potentially disrupting protection devices [15]. Given that distributed generation penetration is growing rapidly, DG additions are expected to match bulk generation additions by 2020 [84], the majority of which is solar PV [85]. While the significant increase in solar generation plays a large role in reducing environmental emissions, the electric utility is tasked with the responsibility of effectively managing the distribution system under these changing conditions.

In terms of modeling, controllable distributed generators act as a negative PQ load (3.6) on the distribution system, with active and reactive powers specified as control variables.

$$I_{i,d}^{\rho} = \left(\frac{S_{i,d}^{\rho}}{V_i^{\rho}} \right)^* \tag{3.6}$$

Where $I_{i,d}{}^{\rho}$ is the current injected by DG d into phase ρ of bus i, considering apparent power $S_{i,d}{}^{\rho}$ and bus voltage $V_i{}^{\rho}$.

3.4 Plug-in Electric Vehicle Charging

Undergoing a recent paradigm shift from conventional fossil fueled vehicles to vehicles powered by electrical energy, electric vehicles represent personal transportation vehicles which generate propulsion through powering an electric motor using energy stored in the vehicle's battery. Furthermore, the subset of electric vehicles classified as plug-in electric vehicles (PEV) have the capability to charge the on-board battery using a plug-in connection to the distribution system. Plug-in electric vehicles may also be categorized into plug-in battery electric vehicles (PBEV) and plug-in hybrid electric vehicles (PHEV), the latter of which offer the ability to power the engine with fossil fuel as a back-up source in the case of low battery charge. Furthermore, plug-in hybrid electric vehicles differ from regular hybrid electric vehicles (HEV). While both PHEV and HEV may use both gas and stored electrical energy as power propulsion mediums, HEV battery charging does not occur through a connection to the power system. For example, the Toyota Prius HEV charges the electric battery through a combination of the gas engine during acceleration and regenerative braking techniques [86].

Following Ontario's Long Term Energy Plan (LTEP) which aims to promote less environmental emissions [2], the Government of Ontario has established a "Smart Grid Fund" which scope includes, but is not limited to, the encouragement of plug-in electric vehicles penetration [3]. Realization of this Smart Grid Fund comes in the form of financial incentives towards the purchase or lease of new plug-in electric vehicles [4] using programs such as Ontario's Electric Vehicles (OEV) or Green License Plates [87]. Due to these incentives, and

similar PEV incentives around the world, the global PEV market expects significant growth over the next decade as seen in Fig. 3.2, including doubling the number of PEV sales over the next 2 years [88]. Such increased sales further expect PEV to represent 2.2% of all light duty vehicles on the road by 2035 [89].

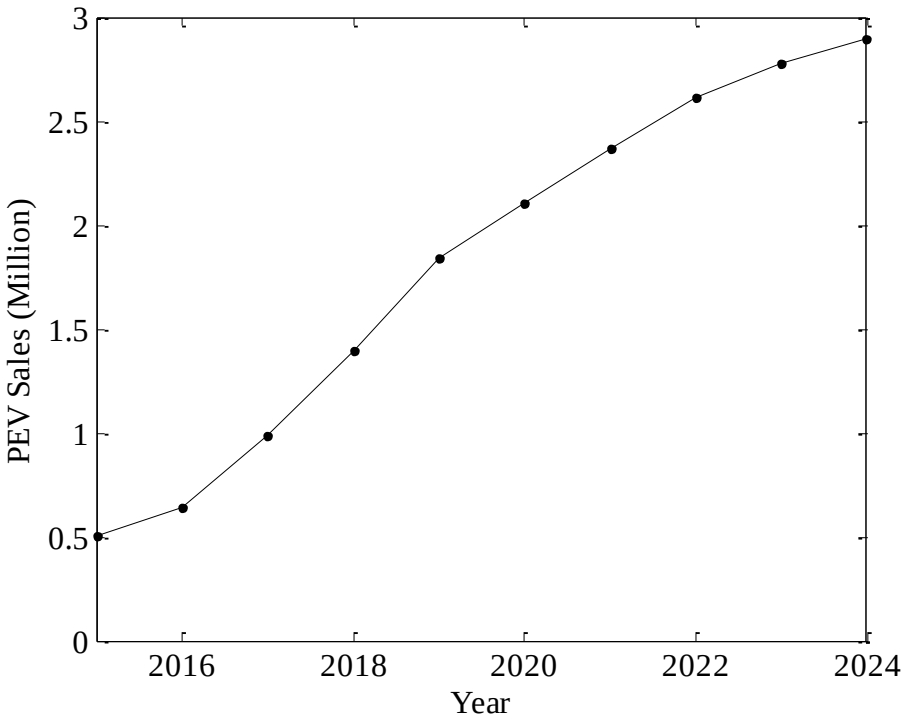

Fig. 3.2: PEV Sales Forecast Across the World [88]

While significant growth of PEV reduces direct emissions of fossil fuels, as PEV emissions are based on the source of generation used for plug-in electric vehicle charging, the resultant addition of plug-in electric vehicle charging load on the distribution system becomes a concern. Studies [7, 17, 90, 91] have investigated the impact of PEV charging on distribution systems and have found that the increased charging from PEV are capable of causing abnormal

grid operation, including problems such as increased transformer loss of life, voltage violations, and neutral overload.

In determination of a PEV charging model for distribution load flow, each PEV is representable as a battery load, with a specified energy required to fully charge at an efficiency based on the vehicle charger [30]. Assuming the PEV owner begins with a full state of charge (SOC), the battery energy depletes at an assumed linear rate based on the driving distance of the vehicle (3.7), according to the vehicles specific energy γ_v (kWh/mile) (3.8).

$$E_v = \frac{\max\left\{\delta_v \times \gamma_v, E_v^{\max}\right\}}{\eta_v} \tag{3.7}$$

$$c_v = \frac{E_v^{tot}}{r_v^{tot}} \tag{3.8}$$

Where δ_v is the driving distance travelled by vehicle v in miles, c_v is the energy consumption of vehicle v in kWh/mile, E_v^{max} is the largest amount of energy the vehicle may absorb based on minimum SOC (3.9), η_v is the charger efficiency, E_v^{tot} is the battery capacity of the PEV, and r_v^{tot} is the maximum driving range of the PEV.

$$E_v^{\max} = E_v^{tot} \times SOC_{\min} \tag{3.9}$$

Where SOC_{min} is the minimum allowable state of charge of the PEV, based on whether the vehicle is a PBEV or PHEV, and is outlined in Table 3.1 using values obtained from [17]. Assuming all plug-in electric vehicles are Nissan Leaf, taken as the plug-in electric vehicle with the largest cumulative annual sales reported in 2014 [92], the resultant PEV parameters are outlined in Table 3.2 [93]. Furthermore, plug-in electric vehicle driving distances have been sampled from the Canadian Plug-in Electric Vehicle Survey (CPEVS) 2015 [94], with cumulative distribution function (CDF) given in Fig. 3.3.

Table 3.1 PEV Minimum State of Charge

Hour of Day	Percent of Peak Load
PBEV	5%
PHEV	30%

Table 3.2 Vehicle and Charger Parameters for Nissan Leaf

Parameter	Value
c_v	0.15 kWh/mi
E_v^{tot}	24 kWh
SOC_{min}	5%
η_v	90%

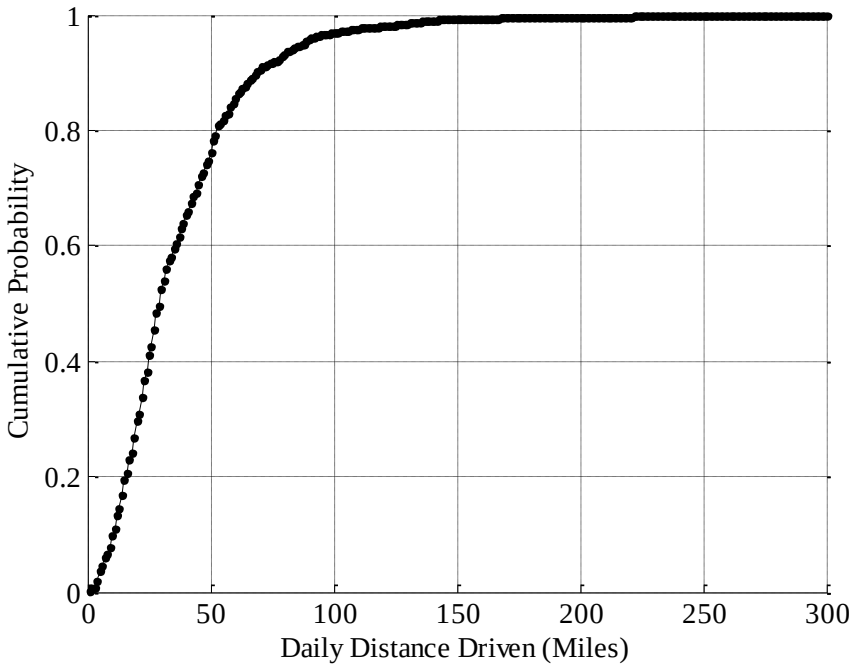

Fig. 3.3: Daily Driving Distance for PEV Based on CPEVS 2015 Survey

When connecting PEV to the distribution system to charge, PEV charging on the system traditionally acts as a constant power load, at a charging rate specified by the charger used, which draws power at rated load until the PEV battery is fully charged. Common charging levels and powers associated with PEV charging at residential homes are outlined in Table 3.3. Given the hourly resolution of the simulation, if an instance occurs whereby the charging power for one hour is greater than the energy required by the vehicle, the vehicle is assumed to reduce charging to a rate equal with the energy required by the battery.

Table 3.3 Common PEV Charging Levels and Powers

Charging Level	Power Rating (kW)
1	1.4
2	3.7
2	6.6
2	10.0
2	20.0

Plug-in electric vehicles are assumed to charge at home, which constitutes the vast majority of surveyed PEV charging events [32]. Furthermore, the vast majority of PEV charging events begin when the PEV returns home from the final trip of the day [32], denoted as the home arrival time (HAT). Plug-in electric vehicle home arrival times are sampled from the CPEVS 2015 [94], with the cumulative distribution function of the HAT displayed in Fig. 3.4.

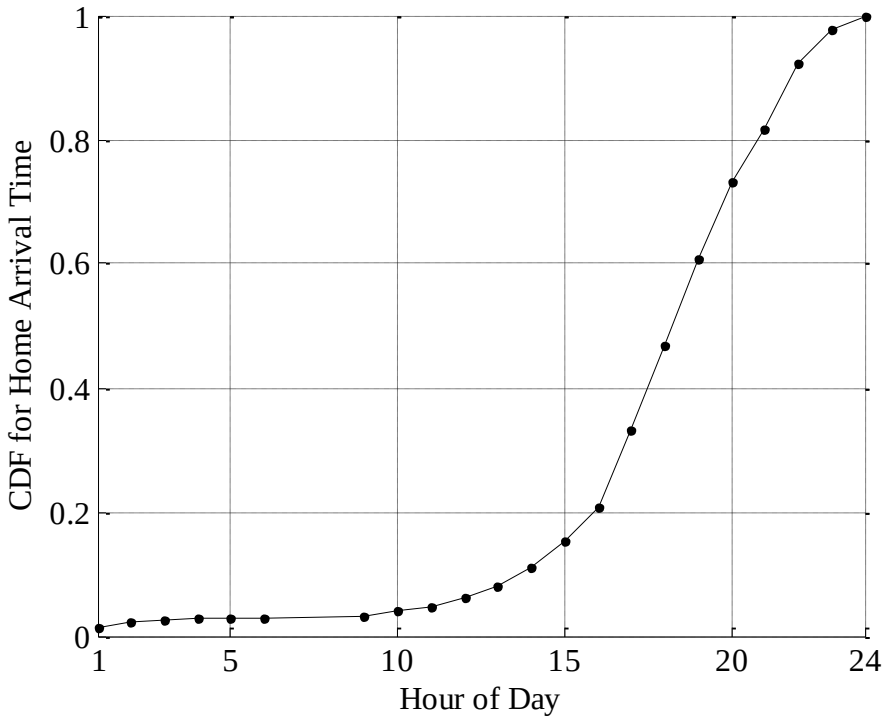

Fig. 3.4: Home Arrival Time for PEV Based on CPEVS 2015 Survey

Lastly, PEV owners are capable of charging the vehicle only when connected to the system, and after the PEV owner leaves the residence, PEV charging can no longer occur. In order to accommodate this constraint in the PEV charging model, each PEV is sampled for the connection duration as outlined in Fig. 3.5 [32]. Based on the duration of the physical connection, the PEV charging model on the system may be formulated as a set of constraints in (3.10)-(3.12). In the case a plug-in electric vehicle is not able to fully charge in the given connection duration, the PEV charges at full power on the system until removal.

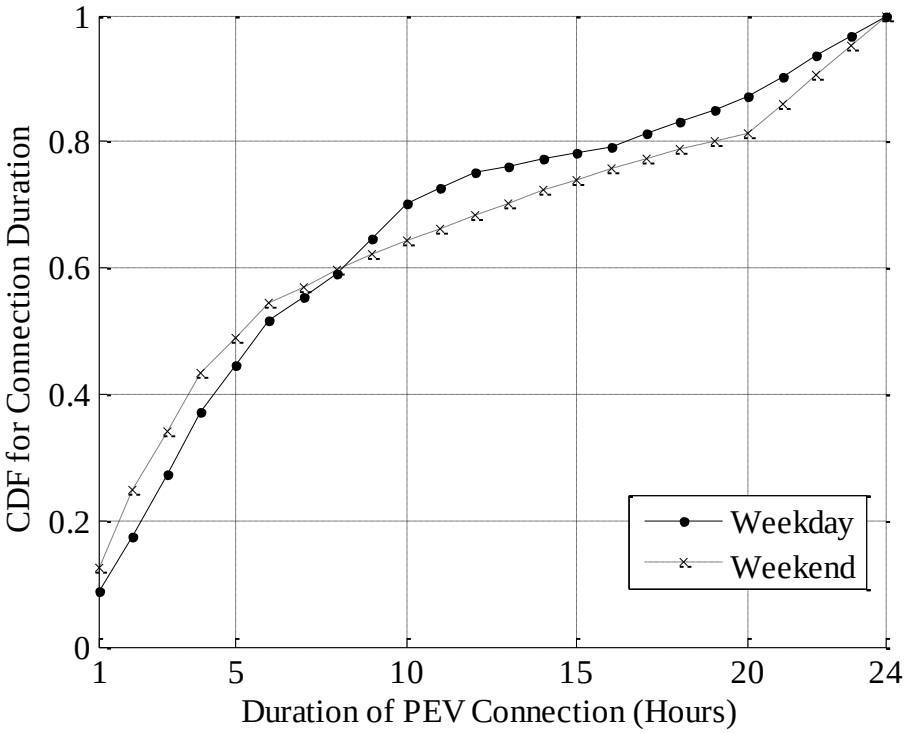

Fig. 3.5: Connection Duration for PEV Based on CPEVS 2015 Survey

$$0 \le P_{v,t} \le P_v^{\max} \tag{3.10}$$

$$P_{v,t} = 0, \forall t \in \Xi \tag{3.11}$$

$$\sum_{t \in T} P_{v,t} \cdot \eta_v = E_v \tag{3.12}$$

Where $P_{v,t}$ is the charging power of PEV v at time t, P_v^{max} is the maximum power rating of the PEV based on charger power rating, Ξ is the set of all hours the PEV is disconnected as a subset of the set of all hours of the day T.

3.5 Rooftop Solar Panel Generation

Rooftop solar photovoltaics (PV) represent one of the largest changes to the distribution system infrastructure under the Smart Grid paradigm. Through converting solar energy to

electrical energy, the addition of solar panels at residential customers' homes allow homeowners to generate power delivered back to the grid, changing traditional residential power consumers to power prosumers. Furthermore, as rooftop PV power produces electric energy through harnessing solar energy, the electricity generation of rooftop PV is without environmental emissions, thus aligning with Ontario's LTEP [2]. In recognition of these environmental benefits, the Government of Ontario has introduced the micro feed-in-tariff (microFIT) program [5] to provide financial incentive for home owners to install up to 10kW of generation. Taking advantage of such offers, the microFIT program has seen a cumulative amount of 20MW of installed PV capacity throughout Ontario as of the end of 2015 [95].

Rooftop solar panels are capable of delivering power to the grid through the process depicted in Fig. 3.6. The solar PV generation process begins with direct current power generation at the solar array, which generates power controlled by the charge controller using maximum power point tracking (MPPT), given as a percentage of the solar arrays rated power based on the irradiance and temperature (3.13). For solar arrays with grid connectivity, the power draw of the charge controller is considered negligible in comparison to the solar array output.

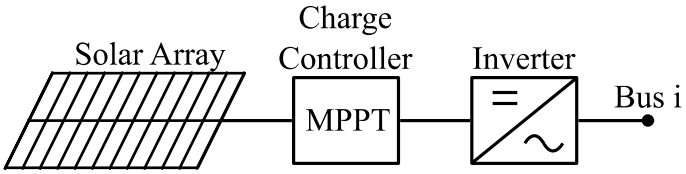

Fig. 3.6: Rooftop Solar PV Architecture

$$P_{p,array} = P_p^{rated} \times IRR_t \times F_T\left(T_t\right) \tag{3.13}$$

Where $P_{p,array}$ is the power output of solar array p, P_p^{rated} is the nameplate rating of the solar array, IRR_t and T_t are the irradiance (kW/m²) and ambient temperature (°C), and $F_T(T_t)$ is a temperature factor calculated through linear interpolation of Table 3.4 [96].

Table 3.4 Temperature Factor for Solar Array Output

T(°C)	$F_T(T)$
0	1.2
25	1.0
75	0.8
100	0.6

In order to convert the direct current (DC) power generated by the solar panel to the alternating current (AC) distribution system, the solar panel system includes an inverter, with AC power output to the distribution system based on the inverter's efficiency defined in (3.14).

$$P_{p,out} = P_{p,array} \times F_{Inv}\left(P_{p,pu}\right) \tag{3.14}$$

$$P_{p,pu} = \frac{P_{p,array}}{P_p^{rated}} \tag{3.15}$$

Where $P_{p,out}$ is the output power of the PV system to the distribution system, $F_{Inv}(P_{p,pu})$ is the inverter efficiency based on per unit power generation of the panel $P_{p,pu}$ (3.15) based on Table 3.5 [96].

Table 3.5 Inverter Efficiency Factor

$P_{p,pu}$	$F_{Inv}(P_{p,pu})$
0.1	0.86
0.2	0.90
0.4	0.93
1.0	0.97

Climatological data of hourly temperature and irradiance for the region of Sacramento, California was taken from the National Renewable Energy Laboratory (NREL) National Solar Radiation Database (NSRDB) for the year of 2009, representing the most recent year available which did not contain erroneous values of -9900 according to the NSRDB User's Manual [97].

3.6 Summary

Active distribution systems are distribution systems which allow for the control of distributed energy resources, which consist of generation, loading, and storage devices. Through predictive modeling, the electric utility may determine control actions in order to improve grid reliability and efficiency during the operation of the distribution system. This work considers the modeling of active distribution system resources including: energy storage systems, distributed generators, plug-in electric vehicles, and rooftop solar photovoltaics.

Energy storage systems are capable of storing energy through charging from the distribution system. Energy stored in an energy storage system may later be discharged back into the system, providing generational resources based on the energy stored within the storage medium itself. This work considers the usage of lithium ion battery energy storage, which constitutes the largest installed energy storage capacity installed in 2015, and provides a detailed model to determine the effects seen on the distribution system.

Distributed generators are small scale generation units connected at the distribution system level, and may be rated up to 50MW in generation capacity. Through providing generational resources close to the loading, the line losses are reduced and therefore the distribution system operates at a higher efficiency. In the case distributed generator operates on natural gas, the distribution system operator may schedule the output of the distributed

generation, to provide efficient control of the distribution system, which has been modeled in this chapter.

Plug-in electric vehicles are beginning to increase in market penetration, as vehicle drivers begin to replace conventional fossil fueled vehicles which vehicles which provide propulsion through consumption of electrical energy. In order to charge the battery storage of electric vehicles, plug-in electric vehicles directly connect at the distribution system, typically at residential homes, to charge the plug-in electric vehicles battery through drawing grid power. This chapter provides a model used to determine the charging power and energy drawn by plug-in electric vehicles through the consideration of vehicles' driving distance and time at which the vehicle returns home.

Rooftop solar photovoltaic generation is also gaining significant increase in market penetration at residential homes. Through converting solar energy to electrical energy, residential homeowners may not only consume electrical power, but also produce power using rooftop solar photovoltaics during sunlight hours. In order to forecast the amount of generation supplied by residential customers with rooftop solar photovoltaics, this chapter further detailed a model for rooftop solar generation, considering the temperature and irradiance climatological conditions.

Having considered models of active distribution system components, the distribution system operator is capable of estimating the operation of the distribution system in advance, and must consider the economics of the distribution system operation to ensure the distribution system operation is performed economically. The following chapter provides a detailed look into the calculation of distribution system operational economics, such that the electric utility may consider the operation of the distribution system from an economical perspective.

4 Economics of Distribution System Operation

4.1 Introduction

In determining distribution system economics considering transactive control on residential ESS owners, economics must be considered for both the electric utility and the residential ESS owners independently. The electric utility is tasked with procurement of generational resources to meet the load demand of all customers within the distribution system. In order to procure energy, the electric utility may import power from the bulk power system through the day-ahead energy market, schedule generation from distributed generation resources, and purchase rooftop solar PV power generated at residential customers. Residential customers alternatively must consider their load demand, which they are charged for energy consumption based on either time-of-use pricing or real-time pricing techniques through distribution locational marginal pricing.

4.2 Day-Ahead Scheduling and Energy Market

The traditional power system model is separated into three distinct sections: generation, transmission, and distribution. While the generation section is tasked with the bulk generation of power, the energy is not immediately sold by the generation system to end-use consumers. The transmission system, which handles the transmission of bulk power, purchases power from the bulk generation sector, for sale to distribution electric utilities at the wholesale price. The power purchased by distribution electric utilities is used to deliver power to end-use industrial, commercial, and residential customers at the retail price. In this respect, purchase of energy is split into the retail market, which consists of end use customer purchase for consumption, and

the wholesale market, where bulk quantities of power are purchased to be resold to end-use consumers [98].

Distribution system operators, which act on behalf of electric utilities, aim to meet load demand by procuring energy through: generational facilities owned by the distribution electric utility, bilateral contracts established with distributed generators within the system, or through the purchase of electricity in the wholesale market.

The wholesale day-ahead energy market acts as an auction for electricity performed one day in advance. In the day-ahead energy market, generation facilities bid on the cost and supply of power available to meet the forecasted load required by the system throughout the following day. Once all bids have been received by the deadline, expected loading is paired to the generation bids based on increasing costs until a price is determined in which supply matches demand. At this point, the wholesale day-ahead energy market is said to be cleared, and the cost for purchasing energy by a transmission system operator in the day-ahead market is set, however this price does not immediately reflect the cost to the distribution system operator (DSO).

In scheduling and economic operations, the wholesale power purchased by the transmission system operator incurs economic losses in delivering power to the distribution system. Considering the transmission system incurs power losses and potential line congestion, the transmission system operator (TSO) applies a unique locational marginal price (LMP) to each bus on the system. Through locational marginal pricing, the wholesale cost of power is increased individually on each node according to the potential line losses, congestion, and

energy procurement costs that would be incurred by supplying the additional loading at each particular node [99].

Following locational marginal pricing, the distribution system operator (DSO) is then able to purchase energy from the transmission system for a cost based on the locational marginal price at the point of connection between transmission and distribution systems. The distribution system operator schedules the power to be purchased in the day-ahead market based on the forecasted load and generation within the distribution system, expressible in (4.1). The DSO aims to minimize the forecasted error in day-ahead scheduling, as additional costs are incurred for compensating mismatch of supply and demand in operation during real-time power delivery, which is purchased through the real-time market.

$$c_t^{\mathrm{Im}\,port} = c_t^{DAM} \cdot P_t^{sub} \tag{4.1}$$

Where c_t^{Import} is the cost to the DSO to import P_t^{sub} active power at the substation at time step t, considering import costs from the transmission system given as c_t^{DAM}.

Following recommendation of the Reactive Power Task Force, reactive power transmission is not chargeable in the wholesale market, providing reactive power generation does not exceed the reactive power which may be supplied by the generator at 0.95 power factor under rated power conditions [100]. This constraint may be imposed on the distribution system, applied to the reactive power imported at the substation with respect to the substation

transformers rating. In the case reactive power exceeds the limit, the transmission system may charge for reactive power at a rate of $1.893/MVAR-hour based on [100].

4.3 Distributed Generation Costs

Distributed generators may be owned by either the distribution electric utility or by private entities, each of which exhibit a different set of economic considerations. Assuming large distributed generators are typically fuel-based and may be controlled or scheduled, electric utility owned distributed generators are controllable by the distribution system operator at will. The drawback of such controllability for electric utility owned distributed generation is that the electric utility must invest in the capital costs, operations and maintenance costs, and costs of fuel usage in order to build and use the distributed generator. Distributed generators which are private or investor owned do not require the utility to pay large capital costs up front, and do not incur direct operations and maintenance costs. The drawback of private owned distributed generators for the electric utility however, is that the electric utility must enter into a contractual arrangement to acquire generation from the private owner, which may limit the available output of the DG unit, and the costs of power generation are expectedly higher than those of electric utility owned distributed generators, as the private investor aims to profit from such a transaction.

The costs associated with electric utility owned distributed generators are well established according to the DG's rating and operating schedule using Table 4.1 [101]. All DG in this work are assumed electric utility owned gas turbine units, taken as the dispatchable distributed generation source with the largest installed energy capacity in Ontario [102], with

operating and maintenance costs equal to the average value of the range in Table 4.1 ($0.007/kWh) [101].

Table 4.1 Distributed Generator Cost Parameters [101]

Cost Parameter	Internal Combustion DG	Gas Turbine DG	Microturbine DG	Fuel Cell DG
Capital Cost ($/kW)	300-900	300-1,000	700-1,100	2,800-4,700
Operating and maintenance costs ($/kWh)	0.007-0.015	0.004-0.010	0.005-0.016	0.005-0.010

4.4 Residential Prosumer Economic Considerations

Electricity consumers in the distribution system typically consists of residential and small commercial customers, each of which are metered and charged for energy usage. Both commercial and residential customers alike are assumed to be charged for energy based on the time-of-use rates in Ontario, Canada, given as the most prominent consumer pricing scheme in Ontario [103] and is summarized in Table 4.2 [104]. Alternatively, residential customers may be charged for electricity consumption based on distribution locational marginal pricing (DLMP) as outlined in Section 4.5.

Residential customers furthermore may additionally generate power through rooftop solar photovoltaic installation. In the case a residential customer has installed rooftop solar panels, the solar generation is metered separately from the customers' house load meter, and is compensable at the microFIT schedule pricing under a fixed rate of 29.4 ¢/kWh throughout

the entire day based on the 2016 price schedule for rooftop solar PV rated between 6kW-10kW [105].

Table 4.2 Time of Use Pricing Guidelines [104]

Time Interval	Summer	Weekend/Holiday	Winter
7pm-7am	Off-Peak (8.7 ¢/kWh)	Off-Peak (8.7 ¢/kWh)	Off-Peak (8.7 ¢/kWh)
7am-11am	Mid-Peak (13.2 ¢/kWh)	Off-Peak (8.7 ¢/kWh)	On-Peak (18.0 ¢/kWh)
11am-5pm	On-Peak (18.0 ¢/kWh)	Off-Peak (8.7 ¢/kWh)	Mid-Peak (13.2 ¢/kWh)
5pm-7pm	Mid-Peak (13.2 ¢/kWh)	Off-Peak (8.7 ¢/kWh)	On-Peak (18.0 ¢/kWh)

4.5 Distributed Locational Marginal Pricing

Distribution locational marginal pricing (DLMP) is an extension of the traditional locational marginal pricing (LMP) method employed on the transmission system, and is used to establish the marginal costs associated with supplying increased power for each node on the system [106]. The concept of DLMP looks to extend LMP to the distribution system, by providing unique price signals at each node, which may be used as an economic control signal [107].

As DLMP looks to calculate the exact distributed locational marginal price ($DLMP_i$) of supplying one additional kW of power at node i (4.2) [108].

$$DLMP_i = \frac{C_{DSO}\left(x^{i'}\right) - C_{DSO}\left(x\right)}{\sum_{x \in L}\left(x^{i'} - x\right)} \tag{4.2}$$

Where $C_{DSO(x)}$ is the cost of the distribution system operator to procure generation to meet load demand under system load set x, $x^{i'}$ is the load set given an increase of 1kW loading on bus i, and L is the set of all loads on the system.

In order to exemplify DLMP pricing, the following scenario is given, considering the IEEE 4 Bus Test Distribution System depicted in Fig. 4.1 [109] which has been modified to include a three-phase DG at node 3, with cost and capacity parameters for each source given in Table 4.3. In the example, the cost of importing power at the infinite bus is taken as the average LMP for the area of Houston, Texas over the 2010 year, with the cost of DG generation taken as the average operation and maintenance costs to operate a gas turbine DG defined in Table 4.1. For simplicity, the example system model is considered lossless and neglects reactive power. Furthermore, for demonstration purposes, line 1 is assumed to have a carrying capacity of 2MW.

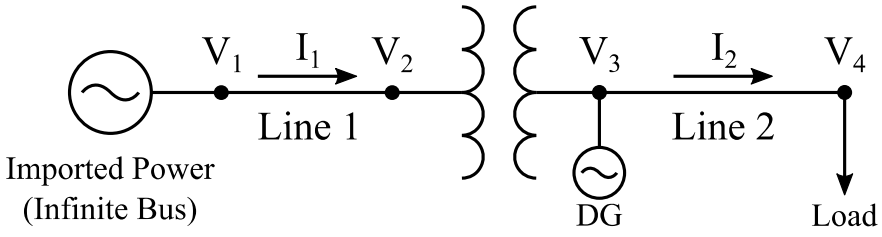

Fig. 4.1: IEEE 4 Bus Test Distribution System with DG at Node 3

Table 4.3 Cost and Capacity Parameters for Test System Sources

Source	Cost	Capacity
Infinite Bus	$0.0392/kWh	Assumed infinite
DG	$0.08/kWh	2MW

In the case the initial load is 1MW, the load is most economically served by the infinite bus at a cost of $0.0392/kWh, for a total of cost of $39.20. For an additional loading of 1kW at the load node, the load may still be served by the infinite bus at the cheaper rate of $0.0392/kWh, therefore the DLMP at node 4 in this scenario is $0.0392/kWh.

In a separate case, if the load is 2MW initially, the generation required to serve the 2MW load may be provided entirely by the infinite bus at the rate of $0.0392/kWh, for a total cost of $78.40. In order to calculate the DLMP price however, an additional kW of loading at node 4 must be served by the less economical DG at a rate of $0.08/kWh, due to the capacity restriction placed on line 1, and the DLMP consequently becomes $0.08/kWh. Such DLMP examples presented reflect the marginal energy costs of locational pricing, however the addition of line losses may further increase DLMP above basic energy costs alone and must be taken into consideration.

In order to provide a numerical example to calculate the distribution locational marginal price under the effects of losses, a second sample calculation is performed on the Y-Y step down balanced IEEE 4 Bus Test Distribution Feeder, with line segment data, transformer data, and load data outlined in Table 4.4, Table 4.5, and Table 4.6 respectively, with line impedance further detailed. For this example, the locational marginal price of importing power at the substation of $0.0392/kWh, representing the average hourly LMP for the area of Houston, Texas over the 2010 year [110].

Table 4.4 Line Segment Data

Node A	Node B	Length (ft.)	Config.
1	2	2,000	1
3	4	2,500	1

Table 4.5 IEEE 4 Bus Transformer Data

Connection	kVA	kVLL – High	kVLL – Low	R(%)	X(%)
Step-Down	6,000	12.47	4.16	1.0	6.0

Table 4.6 IEEE 4 Bus Load Data

Node	kW	Power Factor
4	5,400	0.9 lagging

Line Configuration 1:

$$z = \begin{bmatrix} 0.4576 + j1.0780 & 0.1559 + j0.5017 & 0.1535 + j0.3849 \\ & 0.4666 + j1.0482 & 0.1580 + j0.4236 \\ & & 0.4615 + j1.0651 \end{bmatrix} \Omega / mile$$

As the system in this example does not have DG, the electric utility must procure all generational resources from the infinite bus. In the case with normal load value set *x*, the cost to the distribution system operator may be expressible as the power imported to the system through the infinite bus in order to satisfy the load and losses in the system (4.3)

$$C_{DSO}(x) = P_{Source} \cdot c_{Source} \tag{4.3}$$

Where P_{Source} is the power imported at the source (infinite bus), and c_{Source} is the locational marginal price of importing power at the infinite bus given as \$0.0392/kWh in the example.

Under the provided loading *x*, the resultant real power imported from the infinite bus is 5,959.7kW and costs the DSO C_{DSO} \$233.62024 assuming a time interval of one hour in length. The distributed locational marginal pricing at the load node (node 4, $DLMP_4$) is the incremental cost $C_{DSO}(x^{4'})$ of adding 1kW of load more to node 4. In this respect, the load at Node 4 experiences additional loading of 1kW (5,401 + j2,615.34 kVA), constituting the modified load set $x^{4'}$, and the real power imported at the infinite bus solved using power flow is 5,960.9kW which costs the DSO $C_{DSO}(x^{4'})$ \$233.66728. The resultant change in cost to the DSO to increase load at node 4 by 1kW is given in (4.4), and results in a DLMP price at node 4 is \$0.04704/kWh, or 4.704 ¢/kWh.

$$DLMP_4 = \frac{\$233.66728 - \$233.62024}{(5{,}401\ kW + j\,2{,}615.34\ kVAR) - (5{,}400\ kW + j\,2{,}615.34\ kVAR)} \qquad (4.4)$$

4.6 Summary

The material given in Chapter 4 provides detailing into the two economic entities involved in transactive control using residential energy storage systems. The first economic entity is the distribution system operator, whose major concern is the procurement of

generational resources to meet the expected load demand. The second economic entity consist of residential customers whom have installed residential energy storage systems.

The distribution system operator is tasked with the procurement of generational resources for a 24-hour interval at an hourly resolution, one day in advance of systems operation, known as the day-ahead energy market. Through scheduling generation resources such as: distributed generation, energy storage connected to the primary system, and procuring power from the transmission substation through the substation transformer; the distribution system operator purchases energy in advance to meet the expected load demand at minimum cost, while adhering to system constraints.

Residential energy storage system owners are charged for energy usage by the electric utility whom transports power to meet the customers energy needs, referred to as the retail market. Given that residential energy storage system owners have the capability to control their residential energy storage system charging and discharging, it is expected that residential energy storage system owners will control their energy storage system to maximize their electricity bill savings. Based on the pricing scheme applied to residential customers, these residential customers may be charged based on either time-of-use pricing, which sets a fixed pricing schedule to residential customers in advance, or distributed locational marginal pricing, which reflects the cost of providing power to the customer, and is only known 24 hours in advance due to the day-ahead electricity market.

Given that residential energy storage system owners are interested in energy storage system control to maximize their own personal economic gain, this objective may ultimately

incur increased transformer loss of life, which conflicts with the distribution system operator's grid reliability objective. Chapter 5 looks to detail the methodology by which an interaction is performed between distribution system operator and residential energy storage system owners, to mutual benefit.

5 Transactive Energy Framework Applied to Day-Ahead Scheduling

5.1 Introduction

In this work, transactive control is applied to residential ESS to mitigate transformer loss of life violations in day-ahead operation. In order to determine transformer loss of life, the estimated state of the system must be determined prior to the actual operation of the system using power flow, which requires estimates of residential demand. After establishing the expected behavior of the distribution system over the day-ahead time interval, transactive control may be applied by the electric utility through requesting residential ESS to reschedule their charging and discharging profiles, the new residential ESS profiles of which may be determined using optimization techniques. Since both electric utility and residential ESS owner are competing to maximize their own economic benefit, game theory is applied to determine a method the electric utility may use to place a value on the cost of residential ESS rescheduling.

5.2 Power Flow Algorithm

In order to estimate the state of the power system at any given time, an algorithm is required to estimate the voltage and current at every node and line in the system. After having solved the system for voltages and currents, parameters such as power and losses may be further derived from the initial voltage and current results. The class of algorithms which determine the systems state under given load and generation input are referred to as power flow algorithms [111].

Traditionally in the transmission system, the Newton-Raphson iterative method is commonly used to perform power flow, which relies on partial derivatives of developed power

flow equations [112]. While this algorithm results in rapid convergence to solve the power flow problem, this algorithm excels only in the transmission system environment due to balanced loading conditions with low resistance to reactance (R/X) ratios.

The distribution system, which delivers power to end-use residential customers, differs in architecture from the transmission system in many respects. While the transmission system experiences highly balanced loading and low R/X ratios, the relatively large spacing between conductors in the distribution system may result in ill-conditioning of the Jacobian matrix in Newton-Raphson [113], ultimately resulting in slow or even no solution convergence. Furthermore, distribution systems are typically radial or weakly meshed, making them much more naturally suited to iterative ladder theory [111].

The system shown in Fig. 5.1 exemplifies a simple radial distribution system, consisting of as a series of line segments which provide power to loads on the system. As based on the theory in [111], a forward/backward iterative sweep method is employed, which iterates between solving forward (forward sweep) for node voltages, and solving backwards (backward sweep) to determine line currents.

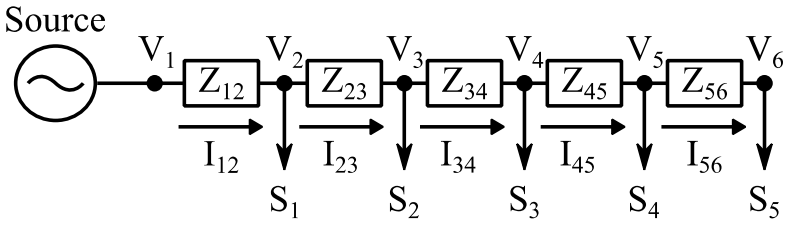

Fig. 5.1: Ladder System Diagram

In order to perform forward/backward sweep power flow, each distribution system component (e.g. lines or transformers) are modeled as a set of A, B, C, and D transfer matrices

as represented in Fig. 5.2, where VLN_{abc} is a vector of the line to neutral voltages for phases *a*, *b*, and *c*, and I_{abc} is a vector of the *a*, *b*, and *c* phase currents. Having modeled each feeder and transformer in the form of A, B, C, and D transfer matrices, the voltage at node *m* given the voltage at node *n* may be determined using forward sweep equation (5.1), which uses voltage phasing and voltage drop transfer matrices A and B respectively. Similarly, backward sweep equation (5.2) may be used to determine $[I_{abc}]_n$ given $[I_{abc}]_m$ using the current phasing and current drop transfer matrices C and D respectively.

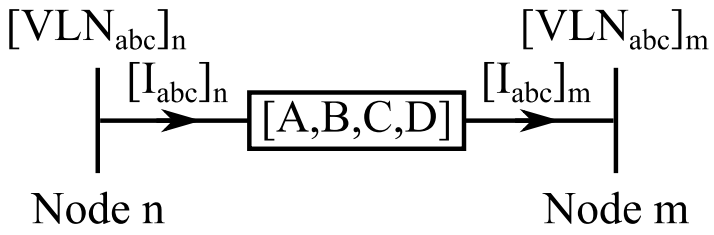

Fig. 5.2: Transfer Matrix Representation of Distribution System Component

$$[VLN_{abc}]_m = [A]\cdot[VLN_{abc}]_n - [B]\cdot[I_{abc}]_n \tag{5.1}$$

$$[I_{abc}]_n = [C]\cdot[VLN_{abc}]_m + [D]\cdot[I_{abc}]_n \tag{5.2}$$

In order to accommodate the split-phase secondary distribution system, equations (5.1) and (5.2) may easily be reformulated in terms of two-phase components as given in (5.3) and (5.4). The interested reader may refer to [111] for more detail on the formulation of A, B, C, and D matrices in both primary and secondary distribution system components.

$$[VLN_{ab}]_m = [A]\cdot[VLN_{ab}]_n - [B]\cdot[I_{ab}]_n \tag{5.3}$$

$$[I_{ab}]_n = [C]\cdot[VLN_{ab}]_m + [D]\cdot[I_{ab}]_n \tag{5.4}$$

Following the iterative procedure outlined in [111], the forward/backward sweep power flow is repeated until convergence equations (5.5) and (5.6) are satisfied.

$$Error_i = \frac{\left\| V_{new,i} \right| - \left| V_{old,i} \right\|}{V_{nom,i}} \tag{5.5}$$

$$Max\{Error\} \leq Tolerance \tag{5.6}$$

Where $V_{new,i}$ and $V_{old,i}$ represent the voltage at node *i* before and after the current iteration, $V_{nom,i}$ is the nominal voltage of node *i*, and Tolerance is the specified maximum change in voltage between iterations to consider the power flow solution as converged, given as 0.001 [114]. The resultant complete power flow algorithm is as depicted in Fig. 5.3.

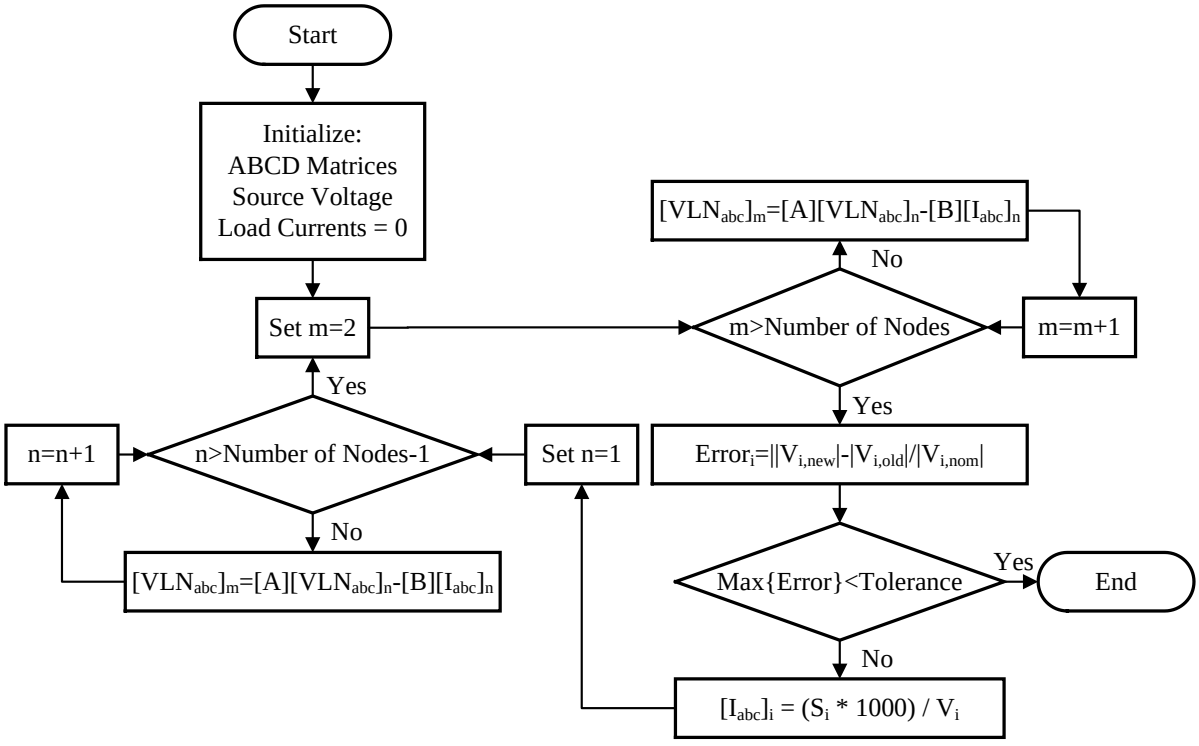

Fig. 5.3: Forward/Backward Sweep Power Flow

5.3 Transformer's Life Time Estimation

Distribution system transformers experience increased heating as power flowing through the transformer increases, which is calculated using a procedure standardized by IEEE C57.91-2011 [31]. Assuming a normal transformer insulation life of 180,000 hours, the percentage loss of life of any transformer's winding insulation is expressible in (5.7).

$$LoL(\%) = \frac{F_{EQA} \times T \times 100}{Normal \quad Insulation \quad Life} \tag{5.7}$$

Where T is the total time period considered, and F_{EQA} is the average equivalent aging factor of the transformer determined in (5.8), considering accelerated aging factor $F_{AA,t}$ (5.9) and time interval Δt.

$$F_{EQA} = \frac{\sum_{t=1}^{T} F_{AA,t} \Delta t}{\sum_{t=1}^{T} \Delta t} \tag{5.8}$$

$$F_{AA} = e^{\left[\frac{15000}{383} - \frac{15000}{\theta_H + 273}\right]} \tag{5.9}$$

The accelerated aging factor of the transformer for any time step t depends on the transformers hottest-spot temperature θ_H, which varies with time according to (5.10).

$$\theta_H = \theta_A + \Delta\theta_{TO} + \Delta\theta_H \tag{5.10}$$

Considering θ_A the ambient temperature over the time period considered, $\Delta\theta_{TO}$ the temperature increase due to top-oil rise, and hottest-spot temperature increase due to the winding $\Delta\theta_{TO}$. Consideration of the thermal model is given in Fig. 5.4, which shows the respective measures calculated in (5.10) for calculation of the hottest-spot temperature in a substation distribution transformer with oil natural air natural (ONAN) cooling [115].

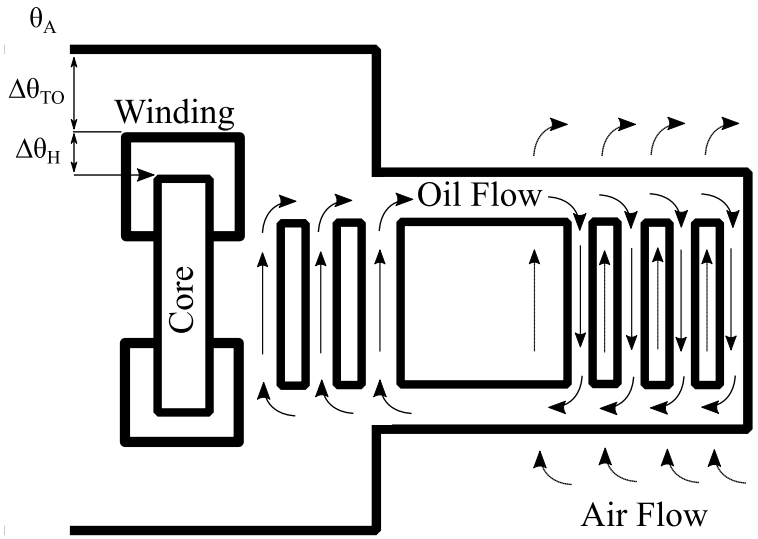

Fig. 5.4: Cross Sectional View of Substation Transformer

Top-oil rise temperature is expressible in (5.11) considering stable top-oil temperature $\Delta\theta_{TO,S}$ and initial increase in temperature due to top-oil $\Delta\theta_{TO,i}$. Top-oil temperature rise is dampened by thermal time constant τ_{TO}, which limits the rate of change of temperature and denotes the time required for 63.2% of total temperature change to occur.

$$\Delta\theta_{TO} = \left(\Delta\theta_{TO,S} - \Delta\theta_{TO,i}\right)\cdot\left(1 - e^{-\frac{t}{\tau_{TO}}}\right) + \Delta\theta_{TO,i} \tag{5.11}$$

Initial top-oil rise $\Delta\theta_{TO,i}$ is calculated considering the top-oil rise increase above ambient temperature at rated load conditions $\Delta\theta_{TO,R}$ and the per unit ratio of initial to rated load K_i (5.12). Furthermore, constant n represents an empirically derived constant which models a correlation between the change in temperature variation given a change in the load, and R quantifies the ratio of rated load losses to no load losses.

$$\Delta\theta_{TO,i} = \Delta\theta_{TO,R}\left[\frac{K_i^2 R + 1}{R + 1}\right]^n \tag{5.12}$$

Lastly, the stable top-oil rise $\Delta\theta_{TO,S}$ is similarly calculated in (5.13) considering the per unit ratio of stable to rated load K_S.

$$\Delta\theta_{TO,S} = \Delta\theta_{TO,R}\left[\frac{K_S^2 R+1}{R+1}\right]^n \tag{5.13}$$

Hottest-spot temperature rise (5.14)-(5.16) follows similar formulation as in top-oil rise, considering stable and initial hottest-spot temperatures $\Delta\theta_{H,S}$ and $\Delta\theta_{H,i}$ respectively, and is thermally dampened according to the winding time constant τ_w.

$$\Delta\theta_H = \left(\Delta\theta_{H,S} - \Delta\theta_{H,i}\right)\cdot\left(1-e^{-\frac{t}{\tau_w}}\right) + \Delta\theta_{H,i} \tag{5.14}$$

$$\Delta\theta_{H,i} = \Delta\theta_{H,R}\cdot K_i^{2\cdot m} \tag{5.15}$$

$$\Delta\theta_{H,S} = \Delta\theta_{H,R}\cdot K_S^{2\cdot m} \tag{5.16}$$

Where m is an empirical constant used to model the windings change in variation given a change in loading.

Typical values for both substation transformer and distribution transformers with respect to the loss of life calculations are given in Table 5.1 [116].

Finally, as substation transformers consist of three separate windings, and distribution transformers have two split-phase windings, the loss of life of each transformer is taken as the winding which incurred the largest loss of life degradation. In this case, K_S and K_i may be calculated for each individual phase in (5.17) and (5.18) assuming the power rating of each winding is equally divided amongst the number of windings in the transformer. Such calculation of the transformer loss of life given multiple windings for the three-phase substation transformer is exemplified in Algorithm 1 [31]. Considering normal insulation life

of 180,000 hours for each transformer, it is equivalently considerable as a transformer loss of life of 0.013% per day or 4.87% per year.

Table 5.1 Transformer Loss of Life Parameters

Parameter	25kVA Transformer Value	50kVA Transformer Value	5,000kVA Transformer Value
$\Delta\theta_{H,R}$	20.3°C	27.0°C	35.0°C
$\Delta\theta_{TO,R}$	38.8°C	53.0°C	55.0°C
τ_{TO}	2.50 hours	6.86 hours	3.00 hours
τ_w	0.08 hours	0.08 hours	0.08 hours
m	0.8	0.8	0.8
n	0.8	0.8	0.8
R	5.65	4.87	3.20

Algorithm 1. Estimation of Transformer Loss of Life Considering Multiple Phase

Connections

1: **Start**

2: **For** each transformer phase ρ in set of all phases P

3: $K_S^{\rho} = S_{txf}^{\rho}/(S_{txf}^{rated}/3)$ (5.17)

4: $K_i^{\rho} = S_{txf,i}^{\rho}/(S_{txf}^{rated}/3)$ (5.18)

5: Calculate loss of life for transformer phase ρ (LoL_{ρ}) using (5.7)

6: **End for**

7: Transformer loss of life is the maximum loss of life experienced by any transformer phase

$LoL_{txf} = \max(LoL_P)$ (5.19)

8: **End**

5.4 Residential House Load Profile Forecasting

In order to accurately predict future load demand in the distribution system, the distribution system operator employs load forecasting. Load forecasting is a technique which draws from regression methods, and uses prior loading data and temperature predictor variables to predict the future load demand over a time horizon [117]. Load forecasting models have been developed in this work based on artificial neural networks (ANNs), as these methods may construct a load forecasting model without predefined variable relationships and are able to consider more complex relationships between predictor and target variables than traditional regression techniques [118].

5.4.1 Artificial Neural Network

Artificial neural networks (ANNs) are a branch of artificial intelligence techniques primarily used in decision making or predictive models featuring a large number of input variables and/or involve complex interactions which may not be well suited to traditional computing methods. Through modeling the process used in biological nervous systems for decision making, a predictive model for a set of output variables ν_o may be represented as a network of node-based interactions on input variable set ν_i seen in Fig. 5.5.

Following the artificial neural network in Fig. 5.5, each node in the network may be modeled as seen in Fig. 5.6, represented as having a value equal to the weighted summation of all given inputs, using weighting values w obtained through training the ANN model. The value of the node is then applied to a transfer function used to map the resultant node value to a corresponding output value.

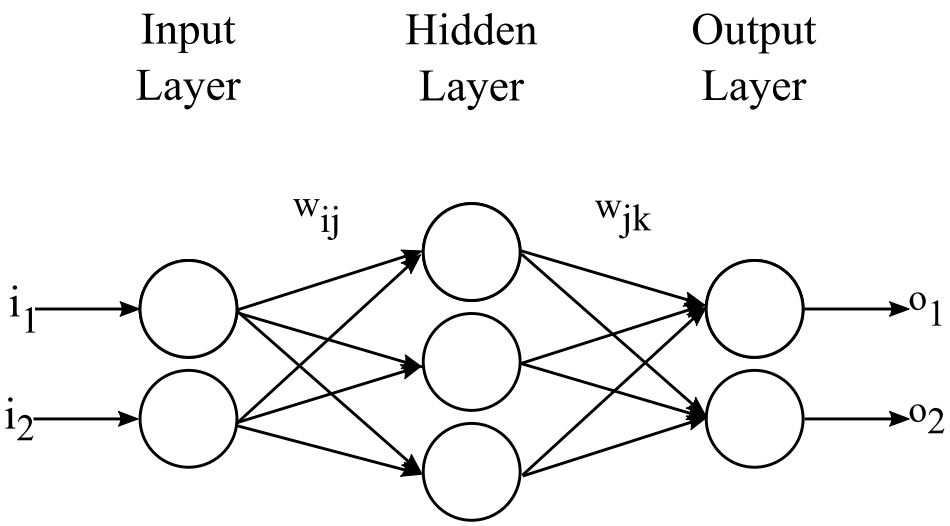

Fig. 5.5: Artificial Neural Network Model

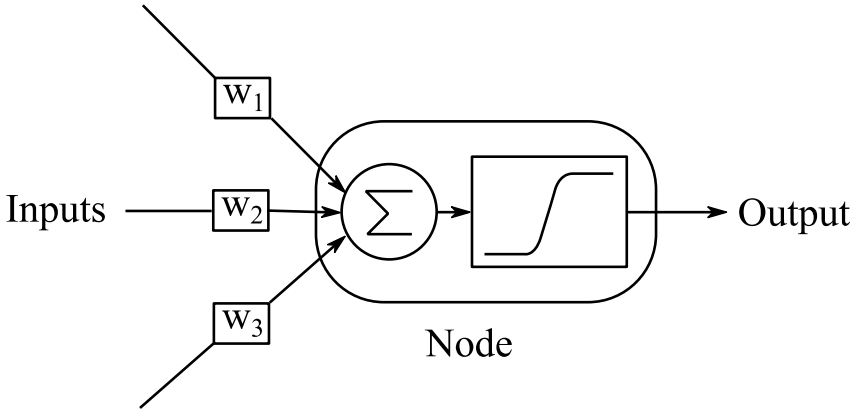

Fig. 5.6: Artificial Neural Network Node Model

The method of constructing an artificial neural network forecasting model is given in Fig. 5.7 [119], consisting of both calibration and forecasting stages. Through calibration of the artificial neural network model using historical data, the artificial neural network load forecasting model is established and may be used to predict future load conditions.

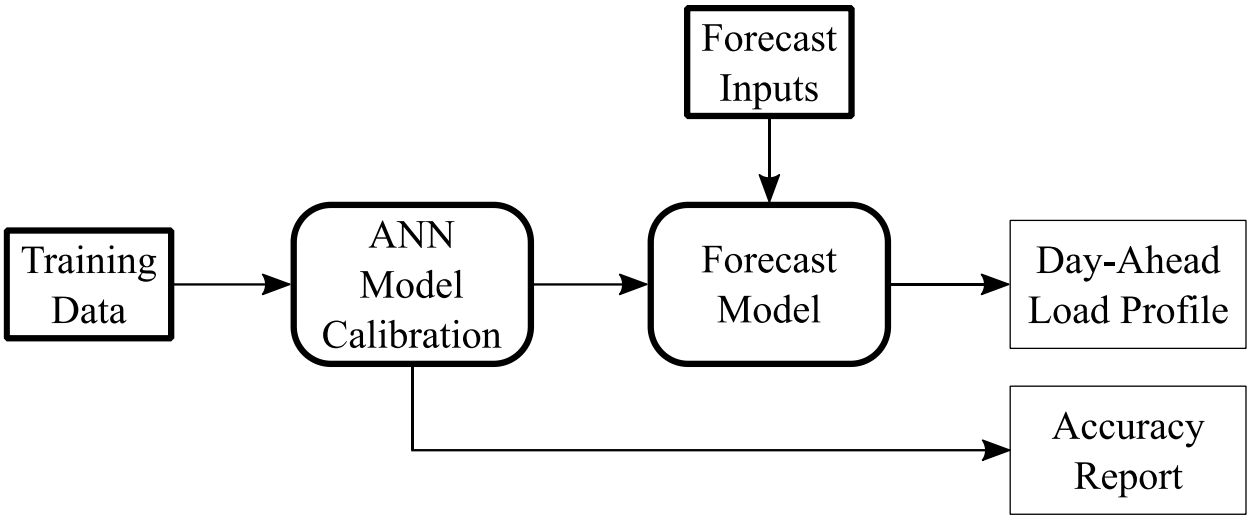

Fig. 5.7: Model Architecture of Load Forecasting

5.4.2 Calibration Stage

Artificial neural network models are considered a supervised learning algorithm, requiring training (commonly referred to as calibration) to evaluate the weighting values in the network. Through employing a feedback loop as shown in Fig. 5.8, weighting values of the ANN model are adjusted until a given stopping criterion is reached. With respect to the stopping criteria used for training, training of the artificial neural network is complete when either the number of iterations (denoted as the epoch) reaches the maximum allowed number, or alternatively if the number of validation checks (successive iterations which do not see an improvement in performance) reach a given threshold. For this work, the maximum number of iterations and validation checks was given as 1,000 and 6 respectively as recommended in [119].

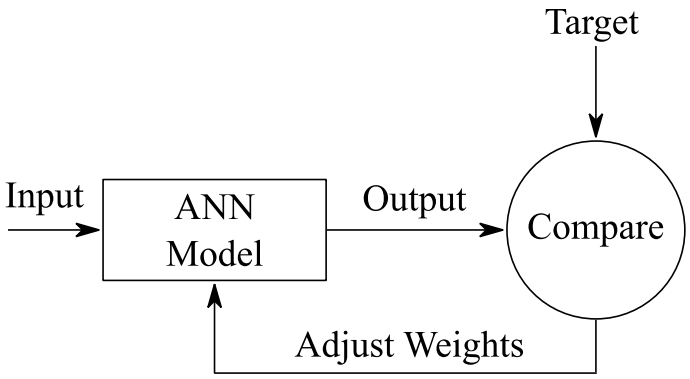

Fig. 5.8: Neural Network Calibration

5.4.3 Forecasting Stage

Having calibrated the artificial neural network model, the resultant ANN may be used to perform load forecasting. In order to forecast load conditions for a future time period, the set of input data (otherwise known as predictors) must be given, which corresponds to the same set of inputs used to train the ANN model. Given a set of historical data, the data is split into two groups, one for training, and one for testing. Typically in load forecasting, the testing set constitutes the most recent year of historical data, whereas the training set contains all the historical data prior to the testing period. Given the neural network model calibrated using the training data, the forecasting model is used to generate predicted loads for the time period used for testing, and is compared with the test set for forecasting accuracy.

In evaluation of the accuracy of the forecasting algorithm, three different accuracy functions are considered, including: mean absolute percent error (MAPE) (5.20), mean absolute error (MAE) (5.21), and the average daily peak MAPE (5.22).

$$MAPE = \frac{\sum_{t=1}^{T} \frac{\left| S_t^M - S_t^F \right|}{S_t^M} \times 100}{T} \tag{5.20}$$

$$MAE = \frac{\sum_{t=1}^{T} \left| S_t^M - S_t^F \right|}{T} \tag{5.21}$$

$$MAPE_{ADP} = \frac{\sum_{d=1}^{D} \max\left(\frac{\left| S_{d,h}^M - S_{d,h}^F \right|}{S_{d,h}^M} \times 100 \right)}{D} \tag{5.22}$$

5.4.4 Test Bed

In developing the load forecasting model, a combination of data regarding temperature conditions, seasonality, and the load conditions were used as predictors. Specifically, the input data includes:

1) Dry Bulb Temperature (continuous value in °F): The dry bulb temperature is the measured ambient air temperature , which is typical in thermodynamic models and consequently plays a significant role in predicting load conditions.

2) Dew Point Temperature (continuous value in °F): The dew point is a calculated temperature point which denotes the temperature at which moisture in the air becomes precipitation. As the dew point generally denotes the humidity of any given day, inclusion of the dew point alongside the dry bulb temperature constitute the inclusion of weather related factors into the forecasting model.

3) Hour of the Day (integer between 1-24): The system load seen is highly dependent on the time of day, and is given as an integer between 1-24 to represent the hourly resolution of the load flow distribution system model.

4) Day of the Week (integer between 1-7): The day of the week, representable as Sunday: 1, Monday: 2, Tuesday: 3, Wednesday: 4, Thursday: 5, Friday: 6, and Saturday: 7, reflects the

observation that power consumption habits follow patterns particular to a specific day of the week.

5) Is Working Day (binary value): The "Is Working Day" flag denotes whether or not the forecasted day in question is a working day, with a value of 1 if yes or 0 if not. Such information has large baring on residential consumption patterns and as such, plays a significant role in forecasting.

6) Previous Week Same Hour Load: Load forecasting makes use of previous load information in predicting future loading, including the load seen for the previous week at the same hour to be predicted. For example, prediction of the load seen at week 3 hour 6 benefits from knowledge of the load seen at week 2 hour 6.

7) Previous Day Same Hour Load: Similarly to input parameter 6, prediction of load for hour h of a given day d of week w requires the loading seen for hour h of day d-1 of week w.

8) Previous 24 Hour Average Load: The last standard prediction measure in forecasting includes usage of the average load demand seen across the previous day.

For each set of input data (predictors), ANN load forecasting models were trained considering 20 hidden layer nodes, with stopping criterion based on the first reaching of 1,000 epochs or 6 validation checks based on [119]. The resultant output consisted of 1 output node for each ANN load forecasting model, which constitutes the predicted load value for hour *h* of day *d* in week *w*, with data organized in years. Transfer functions for hidden layers consisted of the hyperbolic tangent sigmoid function (5.23) based on node value ς, with output node function linear (5.24). Model performance was evaluated in calibration using mean absolute error (5.21), with resultant accuracy measures for each model performed over the 2010 year given in Table 5.2.

$$\tan sig(\varsigma) = \frac{2}{\left(1 + e^{-2\varsigma}\right)} - 1 \tag{5.23}$$

$$purelin(\varsigma) = \varsigma \tag{5.24}$$

Table 5.2 Artificial Neural Network Model Accuracy Indices

ANN House Model	MAPE	MAE	$MAPE_{ADP}$
1	2.91%	0.11MWh	2.28%
2	1.66%	0.08MWh	1.32%
3	2.35%	0.11MWh	2.07%
4	6.20%	0.14MWh	3.64%
5	4.97%	0.11MWh	3.34%
6	5.10%	0.12MWh	2.96%

5.5 Transactive Control of Energy Storage Systems in Day-Ahead Scheduling

5.5.1 Transactive Energy Exchanges

Typically in Ontario, Canada, residential customers are subject to time-variant pricing schemes such as time-of-use pricing [104]. Under these circumstances, residential ESS owners may control their ESS to charge energy during off-peak or low pricing hours, and discharge energy during peak hours, effectively performing energy arbitrage. In this respect, it may be assumed that residential ESS charging/discharging profiles are assumed controlled to maximize savings on their energy bill (5.25), which is dependent on the cost of electricity to the consumer c_t over time series t; subject to power (5.26) and energy (5.27) constraints.

$$\max f = \sum_{t=1}^{T} c_t \cdot P_t^e \cdot \Delta T \tag{5.25}$$

$$P^{e}_{\min} \le P^{e}_{t} \le P^{e}_{\max} \tag{5.26}$$

$$E^{e}_{\min} \le E^{e}_{t} \le E^{e}_{\max} \tag{5.27}$$

Where P_t^e is the charging/discharging power of ESS e, and ΔT is the length of each time interval. In the event that the electric utility recognizes a violation of transformer loss of life, the electric utility may opt to reschedule residential customer ESS charging/discharging profiles as a means of applying load shifting without adversely affecting the customers' ability to use appliances. The proposed architecture of ESS scheduling control is depicted in Fig. 5.9, which outlines the communicating entities that impact the distribution systems operation. As seen in Fig. 5.9, the distribution system operator (DSO) has complete control of utility owned DG within the primary distribution system; and consequently requests generational resources from the DG or from the transmission system operator (TSO) through a substation connection to the transmission system. In the case these resources do not adequately meet transformer loss of life limits, the DSO may then resort to rescheduling of residential customer ESS.

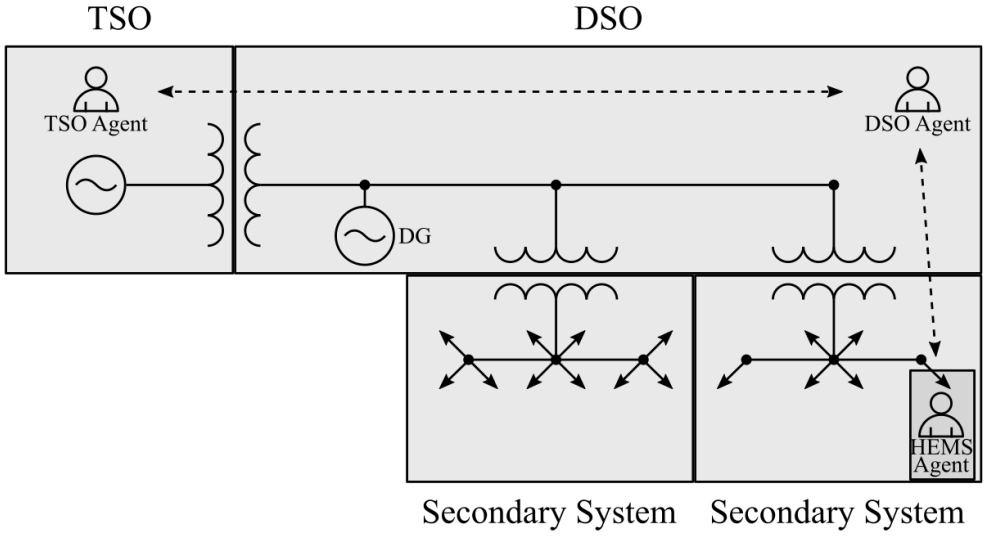

Fig. 5.9: Proposed Communication Scheme for Residential ESS Rescheduling

In order to reschedule residential customer ESS, the DSO must bid to home energy management systems (HEMS), which are assumed to control the residential ESS at each home, a request to change the residential ESS charging/discharging profile for the 24 hour day-ahead interval. As the home energy management system acts on behalf of the residential homeowners interests, the DSO must offer to the HEMS an economic benefit equal to or greater than that which the HEMS would have achieved by residential ESS charging/discharging for maximum savings.

To highlight the transformer lifetime improvement capabilities of this proposed method, the DSO agent may perform peak-to-average power reduction at distribution transformers feeding secondary systems (5.28). Using a greedy method, the DSO considers the forecasted transformer loading based on (5.29) using forecasted profiles of: house loads S_H^t (Section 5.4.1), plug-in electric vehicle charging loads P_V^t (Section 3.4), rooftop solar PV generation P_{PV}^t (Section 3.5), and ESS charging/discharging profiles P_{ESS}^t (Section 5.5.1). In this respect the energy storage charging and discharging profiles P^t_{ESS} have been separated from household demand as this separates the controllable energy storage device within the residential system from the uncontrollable remaining house loading.

Based on greedy optimization, the optimal charging/discharging profile for each ESS is solved one at a time, with procedure outlined in Fig. 5.10, until all residential ESS in the secondary system are assigned charging/discharging profiles to minimize PAPR at the transformer.

$$PAPR = \frac{\max\left\{P_{Txf}^{t}\right\}}{\sum_{t=1}^{T} P_{Txf}^{t}} \tag{5.28}$$

$$P_{Txf}^{t} = P_{H}^{t} + P_{V}^{t} - P_{PV}^{t} + P_{ESS}^{t} \tag{5.29}$$

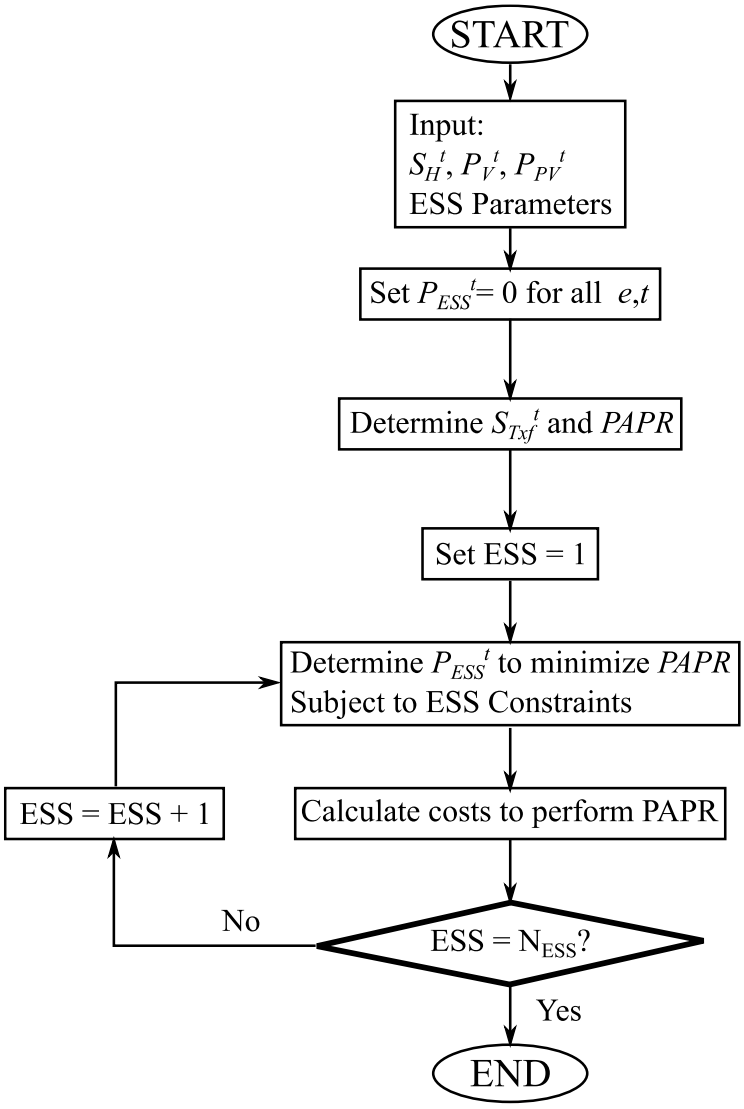

Fig. 5.10: Algorithm used by DSO to Perform PAPR in Secondary System

In order for the electric utility to change the ESS profile of a residential customer, it is assumed that the electric utility places a bid to the home energy management system of each

residential customer that must adjust their ESS charging/discharging profile based on PAPR optimization. The bid made by the electric utility to each residential ESS owner's HEMS will include a desired ESS charging/discharging profile (based on PAPR reduction) and an associated economic value to be gained by the residential customer for agreeing to perform the ESS charging/discharging profile outlined. Given that the ESS owner and the DSO agent are both financially competing entities, which receive compensation based on their control strategies, an economic game is formed to determine what economic value the electric utility should bid to ensure the home energy management system accepts the bid, which may be solved using game theory.

5.5.2 Game Theory and Ultimatum Offer Solution

Game theory deals with the analysis and determination of an optimal playing strategy in a game, which has been defined by Gardner as, "any rule-governed situation with a well-defined outcome, characterized by strategic interdependence" [120]. Game theory looks to provide a solution traditionally in the field of business and economics, and has significant applications to economic negotiations and bargaining.

Through considering each player in the game as having a strategy (a means of determining valid moves in the game), the focus of game theory is to determine the optimal playing strategy for each player. By numerically representing the benefit of performing a given strategy to each player as a utility function, which is commonly taken as economic profit, each player employs a strategy to maximize their own personal gain.

A common problem in game theory is referred to as an ultimatum game, in which one player provides an offer to another player as a "take it or leave it" offer. Under such constraints, it is assumed that the player receiving the offer will accept the offer if the value to the player by accepting the offer is greater than or equal to the value the player would receive if the offer were rejected. As the DSO is concerned about transformer loss of life mitigation, it is the DSO which will offer an ultimatum offer to each residential ESS owner to reschedule their charging/discharging profile at a compensable value. To match the savings that would have been obtained by the residential ESS owner for rejecting the offer, the DSO must bid a compensable value equal to the amount of economic loss the residential ESS owner occurs due to ESS rescheduling. The number of ultimatum offers made by the DSO is equal to the number of HEMS with ESS which must reschedule their charging/discharging profiles based on the results of PAPR minimization algorithm previously outlined in Fig. 5.10.

For example, consider the case of a residential homeowner having a Tesla Powerwall battery energy storage system rated 3.2kW and 6.4kWh [121] and is subject to time of use pricing rates for the summer detailed in Table 4.2. Assuming negligible losses, the home energy management system of the residential ESS owner, having knowledge of the time of use rates for the following day, would schedule a full charge of 6.4kWh during off-peak periods when energy cost is at a minimum, and discharge all 6.4kWh during on-peak rates. In this situation, the cost of charging the ESS is 8.7¢/kWh × 6.4kWh, for a cumulative energy cost of 55.68¢. Similarly, by discharging 6.4kWh stored in the ESS during on-peak pricing hours, the ESS owner has saved 18.0¢/kWh × 6.4kWh, for a cumulative reduction in costs by 115.20¢. Due to the prior cost of 55.68¢ used to charge the ESS, the home energy management system

may consider this ESS charging/discharging profile to have a value of 59.52¢, or $0.5952, representing the total savings achieved on the residential ESS owner's energy bill due to the ESS charging/discharging profile.

If the electric utility were to estimate the loss of life of the distribution transformer which feeds the exemplified residential ESS were to be in violation, the electric utility would attempt to reschedule the residential ESS within the system based on PAPR (5.28). In this case, the results of PAPR by the electric utility may find the residential ESS must shift the intended on-peak discharging instead to mid-peak times. Under this scenario, the electric utility would request the example residential ESS to charge 6.4kWh at the off-peak rate of 8.7¢/kWh and discharge 6.4kWh at a rate of 13.2¢/kWh during mid-peak times, resulting in a charging cost of 55.68¢ and discharging savings of 84.48¢. Given that the proposed residential ESS charging/discharging schedule only provides the homeowner with a total savings of 28.8¢, or $0.2880, the cost to the residential ESS owner for changing their ESS charging/discharging profile is $0.3072, representing the reduction in energy bill savings due to the ESS charging/discharging profile proposed by the electric utility. In order to convince the home energy management system of the residential ESS owner to accept the ultimatum and consequently reschedule ESS charging/discharging based on the proposed profile by the electric utility, the electric utility must bid to the residential ESS owner at least $0.3072 to perform the requested charging/discharging profile. If the bid placed by the DSO does not meet or exceed the savings normally achievable by the original residential ESS charging/discharging profile, the residential ESS owner rejects the offer made by the DSO as the offer would result in economic loss to the homeowner. For further reading, a detailed scenario of residential ESS

payment calculations for residential ESS charging/discharging profile rescheduling may be seen in Appendix A.

Under the ultimatum solution determined using game theory, the electric utility may compensate each residential customer for their lost energy bill savings C_{Cust} by rescheduling the charging and discharging times of their residential ESS based on the new charging/discharging profile proposed by the electric utility (5.30). The bid placed by the electric utility to each residential ESS owner may be calculated as the change in residential customer profit when the ESS charging/discharging profile is set based on maximum savings *Profit(MS)* versus the savings obtained using the residential ESS charging/discharging profile requested by the electric utility as determined through PAPR control *Profit(PAPR)* (5.31).

$$C_{Utility} = \sum_{c \in C} C_{Cust} \tag{5.30}$$

$$C_{Cust} = Profit(MS) - Profit(PAPR) \tag{5.31}$$

Where C is the set of all residential customers c.

5.5.3 MultiAgent Systems

5.5.3.1 Single Agent Systems

While the term "agent" used in software carries different traits depending on the application it is being developed for, Wooldridge and Jennings broadly classify an agent as being "a computer system that is situated in some environment, and that is capable of autonomous action in this environment in order to meet its design objectives" [122]. In this respect, an agent may form a closed loop with the environment, in which the agent

continuously senses the environment, performs processing to determine control actions, and consequently applies the control actions to the environment in an attempt to change the environments state.

For example, an agent may be embedded in an intelligent electronic device (IED) which acts as a relay feeding power to a low priority load. This IED may sample the frequency of the voltage using voltage transformers (VT) at the point on the system the IED is connected. In the case the frequency is in danger of experiencing underfrequency conditions, the IED may attempt to prevent the issue through disconnecting the low priority load using the relay device.

While this example is a simple application of an agent, it demonstrates an agent's ability to be reactive (responding to changes in an environment) and proactive (taking initiative to prevent problems). Another major capability required by intelligent agents is social ability [122], in which a group of agents may socialize and negotiate with each other in order to achieve more complex tasks. In computing very highly distributed or larger scale tasks, it is often more computationally efficient to apply a system of agents versus a single computing entity to resolve a problem. In such cases, the environment may be described as a multi-agent system.

5.5.3.2 Multi-Agent Systems

A multi-agent system (MAS) is an environment which hosts a group of agents that interact with each other. Depending on the objectives and goals of each individual agent, the agents may either be working cooperatively or even competitively, in the case one agent's goal conflicts with that of another agent.

An example of a MAS with both competitive and cooperative elements is the application of demand response, with one agent representing the electric utility and another agent representing a customer with controllable loads. In this example, both the electric utility and customer agents share the objective of maintaining high reliability of power delivered to the customer. These agents have conflicting interests however, as the electric utility may need the customer to reduce their loading to retain the lifetime of the distribution transformer. While the customer is interested in system reliability, the loading reduction to extend the distribution transformer's lifetime may sacrifice the customer's comfortability or may temporarily interrupt power delivery to the household. In this respect, the intelligent agents must negotiate to come to an agreeance between how much load the customer is willing to reduce, and possibly how much financial compensation the electric utility will provide the customer to support such load reduction. After a mutually beneficial agreement is reached, the customer agent will control the customer's house environment to reduce loading to the value negotiated between customer and electric utility agents.

This example of initiating demand response between the electric utility and customer not only demonstrates the social ability of agents, but also reveals the intricacy of the interactions between agents, as the electric utility did not have direct control over the customers actions. While the electric utility could not directly control the customer, the electric utility instead negotiated with the customer agent to perform the actions the electric utility required. Consequently, the customer agent may be assumed located within the customers household and, unless informed through the electric utility agent, has no knowledge of the grids operating conditions. Furthermore, since the goal of customer agents is to maximize savings, which may

conflict with the electric utility agent's goal of prolonging transformer's lifetimes, the electric utility agent must bid an offer to the customer agent to change their energy storage profile. As the customer ultimately has control over their residential ESS unit, the electric utility must negotiate with the customer to establish a deal which is mutually beneficial to both parties. In this respect, a transactive market is formed, with a clearing price set by the ultimatum game detailed in Section 5.5.2.

5.5.3.3 Multi-Agent Communications

As agents are located in different devices in different geographic locations, a communication protocol must be established such that agents can properly send and receive messages for discussion and negotiations. As agents are software entities that may be embedded in any processing device, agent-to-agent communication standards are only specified at the application layer of the OSI model [123].

Agent communication at the application layer has been standardized by the Foundation for Intelligent Physical Agents (FIPA) [124], which establishes communications between agents through a series of communicative acts. When one agent wishes to communicate with another agent, the communicating agent must send to the receiving agent a standardized communicative act, listed in Table 5.3, which describes the purpose or intent of the sending agent to the receiving agent. For example, an agent which would like another agent to perform an action would send a message using the "Request" communicative act.

As multiagent environments may be characterized as having a large number of agents with many messages circulating simultaneously, FIPA has developed a set of message

parameters in [125] which are embedded in the message envelope to identify the sender, receiver, and time stamp.

Table 5.3 Communicative Acts Recognized by FIPA [126]

Numeric Identifier	Communicative Act	Numeric Identifier	Communicative Act
1	Accept Proposal	12	Propagate
2	Agree	13	Propose
3	Cancel	14	Proxy
4	Call for Proposal	15	Query If
5	Confirm	16	Query Ref
6	Disconfirm	17	Refuse
7	Failure	18	Reject Proposal
8	Inform	19	Request
9	Inform If	20	Request When
10	Inform Ref	21	Request Whenever
11	Not Understood	22	Subscribe

An example of coordinated agent communication may be the bidding process of the DSO agent attempting to reschedule the residential ESS charging/discharging profiles within a secondary distribution system as controllable through the residential home energy management system agents. In this example, the DSO agent (the initiator) has sensed a transformer loss of life violation and initiates a resolution by sending a bid to each residential HEMS agent containing a requested ESS charging/discharging profile and economic incentive to be received upon accepting the offer. The recipient home energy management system agents each receive their proposal by the DSO agent, and resultantly respond to the DSO agent with either a refuse (in the case the economic benefit bid by the DSO results in overall economic loss) or accept request.

The DSO agent, which may exist as part of the SCADA system used by the electric utility, upon receiving all responses, will establish contracts with each accepting home energy

management system agent that has accepted the electric utilities offer. Home energy management system agents which have accepted the bid have effectively formed a contract with the DSO agent, and will charge and discharge their residential ESS to the schedule provided in bid originally made by the DSO agent the home energy management system agent.

5.6 Energy Management and Optimization

Energy management is the field of applying control actions to determine the best means of performing a given energy related objective. While such objectives largely focus on the reduction of energy usage or increasing energy efficiency, energy management is characterized as having a large number of potential control actions. Given many different control actions exist on the system, and considering significant complexities of the power systems operation, the ability to determine the most appropriate control actions is best handled by optimization methods.

Mathematical optimization is the branch of mathematics devoted to obtaining the best values for a control set in a mathematically defined system. A subset of optimization which aims to provide good solutions through trial and error based learning algorithms within reasonable time when the systems complexity is large or mathematically undefined is known as metaheuristics. In this work, mathematical optimization is considered, as the control actions taken by energy storage systems and distributed generators constitute convex optimization problems, and therefore may take on mathematical optimization solutions as opposed to stochastic optimization techniques typically seen in metaheuristic optimization.

5.6.1 Optimization of Energy Storage System Operation in Primary Distribution Systems

Energy storage systems have the potential to play a large number of roles in the distribution system, each of which determines control actions through various means. In this work, the energy storage systems owned by the electric utility and directly connected to the primary distribution system act as energy arbitrage units, specifically through the charging and discharging of electric power imported at the substation. As the distribution electric utility incurs costs for drawing power from the transmission system based on the locational marginal price (LMP), the distribution system operator may charge energy storage systems during low pricing periods, to be discharged during high pricing periods, consequently minimizing the cost of importing power to the distribution system (5.32).

$$\min f = \sum_{t=1}^{T} c_t \cdot \left(\sum_{e=1}^{E} P_t^{e,Ch} - P_t^{e,Dis} \right) \cdot \Delta T \tag{5.32}$$

Where c_t is the cost to the distribution system operator for the import of energy at the substation transformer in \$/kWh at time interval t in set of time intervals over the day T, $P_t^{e,Ch}$ and $P_t^{e,Dis}$ are the power absorbed and released respectively in energy storage system e of the set of all energy storage systems E, and ΔT is the duration of time intervals.

The resultant objective function is further constrained due to battery charging limitations (5.33) and (5.34), battery charging efficiency (5.35), and energy constraint (5.36). Further energy constraint (5.37) is assumed to restrict the energy storage system to start and end with the same energy, thus allowing independence between daily simulations.

$$0 \le P_{e,t}^{Ch} \le P_e^{Ch,\max} \tag{5.33}$$

$$0 \le P_{e,t}^{Dis} \le P_e^{Dis,\max} \tag{5.34}$$

$$E_{e,t} = E_{e,t-1} + P_{e,t}^{Ch} \cdot \eta_e - P_{e,t}^{Dis} \big/ \eta_e \tag{5.35}$$

$$E_e^{\min} \le E_{e,t} \le E_e^{\max} \tag{5.36}$$

$$E_{e,0} = E_e^{ini} = E_{e,T} \tag{5.37}$$

Where $P_{max}^{e,Ch}$ and $P_{max}^{e,Dis}$ are the charging and discharging limits of the energy storage system, η_e is the charging and discharging efficiency. Given the objective function and constraints in the optimization problem are linear, the resultant system of equations is solved using linear programming [127], through application of the interior point algorithm [128].

5.6.2 Optimization of Distributed Generation Units in the Primary Distribution System

Unlike energy storage systems, distributed generators are capable of generating electric power as opposed to drawing power from a stored energy medium. In order to properly determine the optimal control actions for distributed generation, assuming the distributed generator is capable of scheduling generation, a power flow algorithm must be used in determining the system states, to ensure the power generated by DG units do not result in substation transformer loss of life violation. Furthermore, the day-ahead scheduling nature of the problem places a time constraint on the optimization algorithm, and requires a solution to be determined quickly in real-time. For such reasons the sequential quadratic programming method has been performed, as employed using the interior-point 'FMINCON' method in MATLAB, based on the recommendation in [108] and previously employed for DG optimization in unbalanced distribution systems in [129].

Sequential quadratic programming (SQP) methods are a deterministic means of approaching a solution which may be applied to smooth, nonlinear functions with constraints. Based on Quasi-Newton computational methods [130], optimization is performed iteratively based on Hessian approximations of the Lagrangian function [131], with bounded constraints folded into the objective function using established Karush-Kuhn-Tucker (KKT) equations through the procedure detailed in [127].

In order to determine optimal power flow, DG active power dispatch for DG units owned and operated by the electric utility for the 24-hour period was determined to minimize costs of power procurement to the electric utility (5.38).

$$\min C_{DSO} = \sum_{t=1}^{T} \left(c_t^{Sub} \cdot P_t^{Sub} + \sum_{g \in G} c_t^g \cdot P_t^g \right) \tag{5.38}$$

Where C_{DSO} is the cost to the electric utility to procure generation to meet load demand, c_t^{Sub} is the locational marginal price to the utility to buy power from the transmission system, P_t^{Sub} is the power through the substation transformer which constitutes power import from the transmission system, c_t^g is the operational cost of running generator g, and P_t^g is the power output of generator g at time step t. Considering DG are subject to maximum power generation based on their nameplate rating $P^g{}_{max}$ (5.39), the results of optimization look to find a minimum cost solution which retains the loss of life of the substation transformer within loss of life limits (5.40) affected by the demand-supply balance constraint (5.41) affecting substation power drawn to feed all loads l and losses within the system.

$$P_t^g \leq P_{\max}^g \tag{5.39}$$

$$LoL_T \leq LoL_T{}^{max} \tag{5.40}$$

$$P_t^{Sub} + \sum_{g \in G} P_t^g = \sum_{l \in L} P_t^l + P_t^{Loss} \tag{5.41}$$

where LoL_T is the substation transformer loss of life, and LoL_T^{max} is the loss of life limit on substation transformer set by IEEE C57.91 [31].

5.6.3 Transactive Energy Control in Day-Ahead Scheduling

Many system operators look to increase grid reliability and reduce economic risk through the procurement of resources one day in advance, referred to as day-ahead scheduling [132]. Through forecasting the expected demand on the system in advance, electric utilities have time to procure and dispatch resources for optimal power systems operation. Some electric utilities further opt to establish a real-time market, in which power and energy are estimated and contracts are established with generational and load resources for a 5-minute period in advance. Given that ESS are energy based resources which must first store energy to be later released, ESS scheduling and dispatch is more naturally suited to day-ahead scheduling. In order to effectively integrate ESS control within the day-ahead scheduling problem, the proposed procedure is detailed in Algorithm 2.

As seen in Algorithm 2, day-ahead dispatch is completed upon determining the optimal DG dispatch schedules after all forecasted load and generation profiles are determined. In order to retain high reliability of the distribution system, this work proposes the DSO evaluate the expected transformer loss of life in the day-ahead scheduling problem for both distribution transformers and substation transformers. In the event a distribution transformer is found to exceed loss of life limits, the electric utility may perform peak-to-average power reduction (PAPR) to reduce loss of life within the distribution transformer. After all predicted

distribution transformer loss of life violations have been resolved, the DSO must ensure that the substation transformer loss of life is retained within applicable limits.

Algorithm 2. Transactive Energy Operational Framework

1: **Start**

2: **Input:**

Day-ahead pricing information climatological data given in Section 6.1.5

House load forecast models defined in Section 5.4

EV driving distance and home arrival time data given in Section 3.4

3: **Forecast:**

House load profiles based on Section 5.4

EV profiles based on Section 3.4

PV profiles based on Section 3.5

4: Determine DLMP pricing based on Section 4.5

5: Determine profiles of primary connected ESS based on Section 5.6.1

6: Determine ESS profile for maximum savings for each residential home using (5.25)

7: Schedule optimal DG dispatch according to Section 5.6.2

8: Perform power flow given in Section 5.2

9: Evaluate loss of life for each transformer according to Section 5.3

10: **For** each distribution transformer experiencing loss of life above the limit

11: Perform PAPR (5.28) and use game theory (Section 5.5.2) to determine DSO bid to each ESS owner in the secondary system of the distribution transformer experiencing loss of life violation

12: **End for**

13: **While** substation transformer loss of life violates the allowable limit

14: Perform PAPR (5.28) and use game theory (Section 5.5.2) to determine DSO bid to each ESS owner in the secondary system of the distribution transformer with the largest initial PAPR

15: Perform PAPR (5.28) on each electric utility owned ESS directed connected to the primary distribution system

16: **End While**

17: Reschedule optimal DG dispatch based on Section 5.6.2

18: Run power flow (Section 5.2) to determine system state

19: Update loss of life for each transformer (Section 5.3)

20: **End**

Substation transformers typically act as energy import nodes, connecting the transmission system and the distribution system, with power profile determined by the load and generational resources within the primary and secondary systems. As the substation transformers power profile is thus dependent on all resources within the primary and secondary systems, the DSO may opt to resolve substation transformer loss of life through both residential ESS, electric utility-owned energy storage systems directly connected to the primary distribution system, and primary DG units. As residential ESS control is advantageous over DG control in the sense that residential ESS control also effectively reduces distribution transformer loss of life simultaneously, it is assumed the DSO will benefit from acting on residential ESS control before attempting to reschedule DG or primary system connected ESS in substation transformer loss of life mitigation. In this respect, the DSO will successively

perform PAPR from the distribution transformer with the highest peak-to-average ratio until the substation transformer loss of life is determined to be reduced below the 0.01333% daily limit based on IEEE standards [31].

After the substation transformer is relieved of loss of life violation, the DSO must re-determine the optimal dispatch of DG resources to accommodate the change in system state due to rescheduling of residential ESS profiles, at which point the day-ahead scheduling problem is solved and the electric utility may establish bilateral contracts for scheduled resources.

5.7 Summary

The work outlined in this Chapter provides the detailed methodology by which the distribution system operator may predict and respond to transformer loss of life violations in the day-ahead energy market, using transactive control. Through forecasting expected generation and loading on the system, the distribution system operator may perform power flow to identify transformers exceeding the daily loss of life limit within the system. Having identified transformers exceeding the daily loss of life limit, the distribution system operator may then consider the rescheduling of residential energy storage systems to perform peak-to-average power reduction, with an associated financial incentive to ensure residential customer participation. After rescheduling residential energy storage system resources to mitigate transformer loss of life violations, the distribution system operator may then recalculate transformer loss of life using updated power flow results, to validate successful mitigation of transformer loss of life violations.

Load forecasting of residential house loads may be determined through the developed artificial neural network methodology. Through initial training of the load forecasting neural network model, considering climatological and historical house loading data, the distribution system operator may use forecasted climate conditions as a means of forecasting house loading in the day-ahead interval.

A power flow algorithm has been employed in this work to determine the state of the distribution system. Due to the large number of single phase loads, and ill-conditioning of transmission system power flow algorithms, the forward-backward sweep method has been employed to solve for the unbalanced, three-phase distribution system. The results of performing power flow allow the distribution system operator to know the voltage, current, and power throughout the entirety of the distribution system, which may be used to ensure transformers do not exceed loss of life limits.

The profile of power demand at each transformer in the distribution system is given from power flow, and may be used to estimate the loss of life at each transformer in the system. Through comparing the loss of life of each transformer with the limitations set by IEEE standards, the distribution system operator may estimate which transformers may violate loss of life limits, and therefore take corrective action to mitigate loss of life in day-ahead scheduling.

Finally, the distribution system operator may employ optimization to perform peak-to-average power reduction for transformers exceeding loss of life violation. Through rescheduling the residential energy storage systems fed by a transformer in violation of loss of

life limits, peak-to-average power reduction looks to determine the best method of charging and discharging residential energy storage systems to minimize transformer loss of life. After obtaining a solution which minimizes peak-to-average power, the distribution system operator then places a bid to all residential energy storage system owners which are to be rescheduled, including the requested charging and discharging ESS profile, as well as an economic incentive to ensure the residential customers' acceptance of the profile. The distribution system operator may use game theory in order to determine the appropriate bid price at which the consumer will accept a change to their intended residential energy storage charging and discharging profile.

Finally, the distribution system operator after rescheduling residential energy storage systems may again run power flow, and calculate estimated transformer loss of life, to validate that all loss of life violations are resolved within the system.

6 Evaluation of Transactive Energy Framework on Test Case System

6.1 System Description

6.1.1 Primary Distribution System

The distribution system used in this work consists of a primary distribution system extended to include secondary distribution networks. The primary distribution system is modeled based on the IEEE 123 Bus Test Distribution System specifications [109], with detailed specifications given in Appendix B, and has been modified to include secondary distribution circuits. In order to include secondary circuits, all single phase spot loads on the IEEE 123 Bus Test Distribution System rated 44.72kVA and 22.36kVA have been removed and replaced with 50kVA and 25kVA center-tapped distribution transformers (TXFCT) respectively. Center-tapped distribution transformers are used to feed secondary circuits as designed according to Section 6.1.3, and the overall primary distribution system diagram is seen in Fig. 6.1 based on the original test system diagram given in [109]. Remaining loads on the primary system which have not been removed are considered commercial loads, with peak value taken as the rated value in the IEEE 123 Bus Test Distribution System documentation, and load profiles as outlined in Section 6.1.2.

The IEEE 123 Bus Test Distribution System has been further modified to include ESS and DG both connected to the primary distribution system; with ratings specified in Table 6.1 [133] and Table 6.2 [134] respectively.

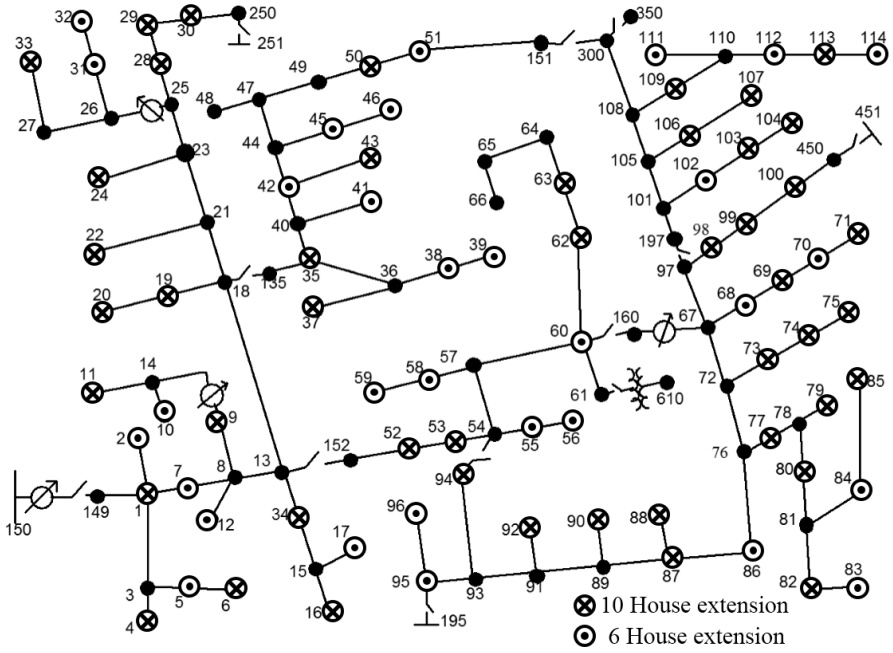

Fig. 6.1: IEEE 123 Bus Test Distribution System with Marked Extension Nodes

Table 6.1 Siting and Sizing Parameters for Primary ESS [133]

Node	kW Rating
20	150
42	200
90	60
97	150

Table 6.2 Siting and Sizing Parameters for DG [134]

Node	kW Rating
67	1,080
72	1,320
47	540

6.1.2 Primary Distribution System Loads

The IEEE 123 Bus Test Distribution System [109] defines 91 single-phase spot load connections. Of the 91 single-phase spot load connections, 47 connections are rated 44.72kVA

and have been removed and replaced with 50kVA distribution transformers feeding 10 house secondary circuits. Moreover, 31 single-phase spot loads are rated 22.36kVA and have been removed and replaced with 25kVA distribution transformers feeding 6 houses respectively. The remaining 13 single-phase spot loads are assumed commercial loads [7] with peak load values specified in the IEEE 123 Bus Test Distribution System [109] as given in Appendix B. Given that commercial loads have low variability [135], all commercial loads in the system may be represented using a single load profile. The resultant load profile applied to all commercial loads within the system is given in Table 6.3 [136].

Table 6.3 Representative Commercial Load Profile

Hour of Day	Percent of Peak Load	Hour of Day	Percent of Peak Load
1	20.8	13	80.0
2	19.2	14	80.0
3	17.6	15	80.0
4	17.6	16	78.4
5	17.6	17	78.4
6	17.6	18	75.2
7	19.2	19	65.6
8	27.2	20	54.4
9	51.2	21	44.8
10	72.0	22	36.8
11	78.4	23	30.4
12	80.0	24	27.2

6.1.3 Secondary Distribution System

Secondary distribution circuits extend from the 50kVA and 25kVA distribution transformers, with distribution transformer placement determined in Section 6.1.1. In this respect, 50kVA distribution transformers extend 10 house secondary circuits as shown in Fig. 6.2, with labels n_{H1}-n_{H10} representing residential house loads 1-10 respectively in the secondary

circuit. Similarly, 25kVA distribution transformers extend 6 house secondary circuits given in Fig. 6.3, with n_{H1}-n_{H6} representing residential homes 1-6 respectively. Secondary circuit layout was determined based on the secondary design archetypes outlined in [137], with secondary line and service drop parameters defined in [138] as detailed in Appendix C.

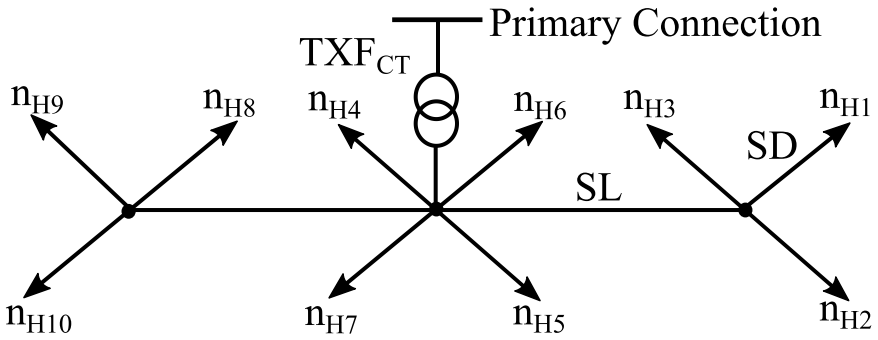

Fig. 6.2: 10 House Secondary Circuit

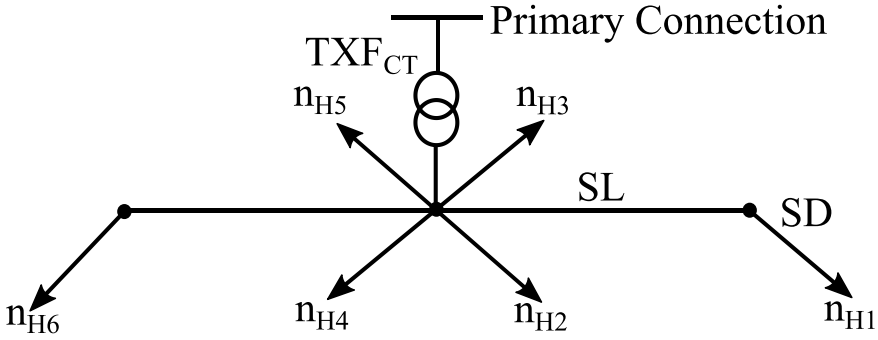

Fig. 6.3: 6 House Secondary Circuit

6.1.4 Residential Homes

The load profile for residential households in this work are determined as the basic house load consisting of a combination of appliances and lighting loads, which may be further extended to include: plug-in electric vehicle charging, rooftop solar PV generation, and energy storage system profiles. Inclusion of PEV, PV, and ESS are based on the simulation scenario.

Basic residential house loading is assumed 6.64kVA at each house [139], with load profile determined using the artificial neural network load forecasting method detailed in Section 5.4 and has been applied to the Baltimore Gas and Electric (BG&E) profile historical data given in [140]. The BG&E load profile data includes hourly load profiles for 6 distinct residential load classes in Baltimore, Maryland, with load class definitions provided in [141]. Plug-in electric vehicle charging and rooftop solar PV profiles are assumed to be estimated by the home energy management system and provided to the DSO agent, through the methods determined based on Section 3.4 and Section 3.5 respectively. Residential ESS at all homes are assumed Tesla Powerwall [121] rated 3.2kW and 6.4kWh.

6.1.5 Climatological Data and Day-Ahead Profiles

Forecasted climatological data corresponding to dry bulb temperature, dew point temperature, and irradiance were given as measured data from the NSRDB [142]. Day-ahead market prices corresponding to the cost of importing/exporting power at the substation were taken from the Electric Reliability Council of Texas (ERCOT) 2010 historical data [110].

6.2 Results

In order to show the effectiveness of transactive energy control applied in the day-ahead energy market, the results first outline the procedure defined in Algorithm 2, applied to a single day of the year. The representative day has been taken as September 1, 2010, which has been found to require transactive control to mitigate loss of life violations on both 25kVA and 50kVA distribution transformers. The representative day considers penetration rates of 1 PEV/House and 10kW rooftop solar PV generation per house. After analysis of a single day-

ahead scenario, the results of applying such day-ahead transactive energy control will be evaluated at an annual time frame.

6.2.1 Transactive Energy Control for Day-Ahead Scheduling

6.2.1.1 Transactive Energy Control for Day-Ahead Scheduling Considering DLMP Pricing

The results observed in Fig. 6.4 show the day-ahead hourly nodal prices for the secondary systems which extend from IEEE 123 Bus Test Distribution System node 16 and node 104, as compared with the locational marginal price (LMP). Given that the operating and maintenance costs of the gas turbine is assumed 0.008$/kWh, which is less expensive than the LMP prices at all hours of the day seen on inspection of Fig. 6.4, all DG in the system are found to output maximum rated power throughout the day, resulting in reverse power flow at hours midnight-6pm and 11pm-midnight, with forward power flow between the hours of 6pm-11pm.

As seen in Fig. 6.4, the locational marginal price for the distribution system operator to import power is higher than the distributed locational marginal price of power paid by residential customers during the hours of reverse power flow. Given that power flow is in the reverse direction, the addition of loading during these hours reduces the losses in the system, and therefore additional loading reduces the cost of operation to the distribution system operator. For example, at noon under the effects of reverse power flow, the LMP is $0.0355/kWh, whereas at node 16 the DLMP is $0.0343/kWh, and at node 104 the DLMP is $0.0330/kWh. It may also be seen from this example that the DLMP at node 104 is less than that of node 16. Given that all DG's are outputting maximum power, additional loading may

only be supplied through an increase in power at the source node, which has larger impact on losses at the further node in the system, such as node 104 when compared to node 16.

Considering LMP pricing in the system, profiles of the ESS directly connected to the primary distribution system may be optimized for the electric utility according to the method outlined in Section 5.6.1, with resultant charging and discharging profiles seen in Table 6.4. A similar method may be used considering optimal residential ESS charging and discharging profiles using (5.25) as described in Section 5.5.1, which is outlined in more detail in Appendix A.

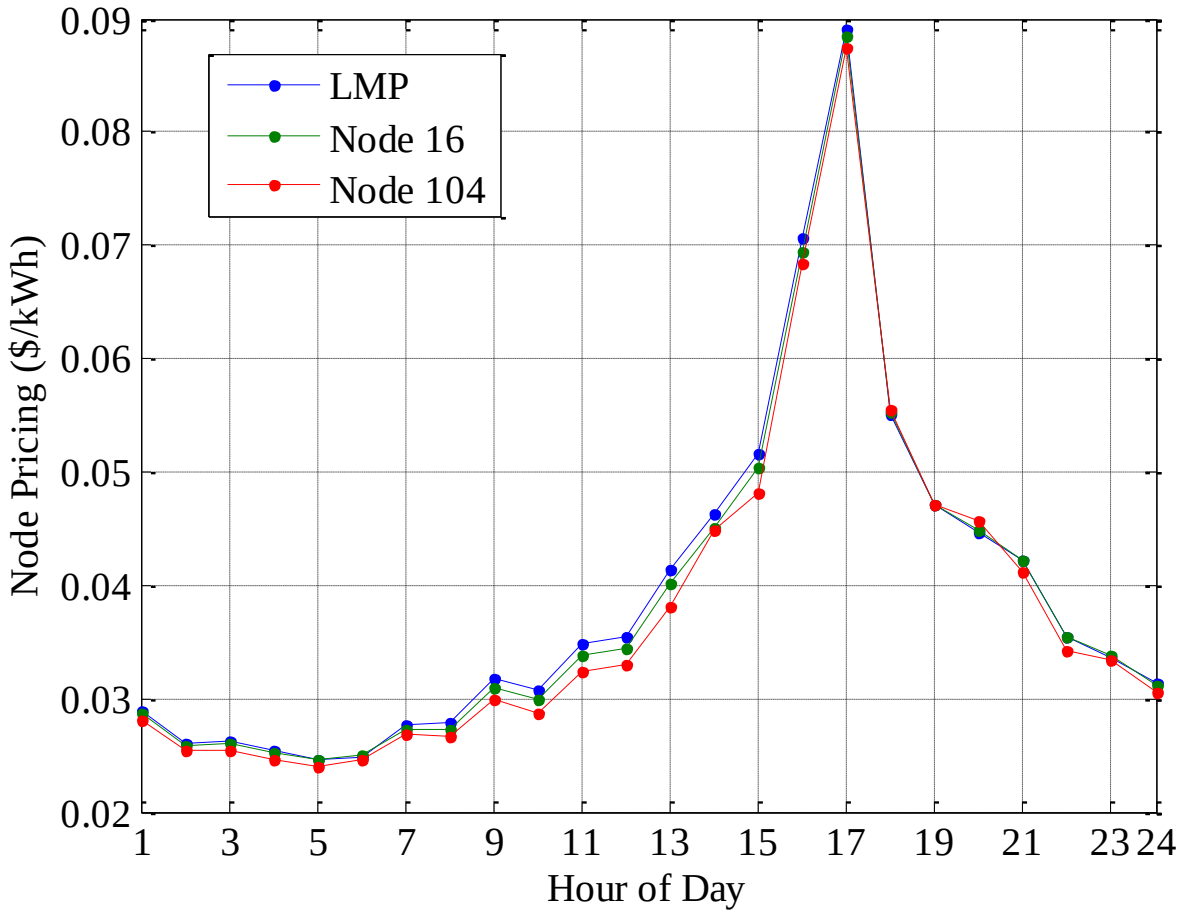

Fig. 6.4: DLMP Prices for Sample Secondary Systems

From Table 6.4 it may be seen that ESS connected to the primary distribution system need only alternate between charging and discharging once over the 24 hour period specified.

After having optimized all residential ESS charging/discharging profiles and solving for power flow, the daily loss of life of the substation transformer was found to be 0.0025%, which did not violate the daily loss of life limit of 0.0133%, and therefore DG optimal dispatch remains unchanged prior to transactive energy control.

Having solved power flow to determine the expected operation of the distribution system in the day-ahead scenario, the cumulative active power losses in the system are found to be 2.44MWh, with resultant daily loss of life of all 25kVA distribution transformers and all 50kVA distribution transformers seen in Table 6.5 and Table 6.6 respectively.

Inspection of Table 6.5 and Table 6.6 reveal a median distribution transformer loss of life of 0.0084% and 0.0048% for 25kVA and 50kVA distribution transformers respectively. Given 25kVA distribution transformers feed secondary systems containing 6 houses, the ratio of distribution transformer kVA rating to the number of homes fed by the distribution transformer is 4.17. Similarly, 50kVA distribution transformers feeding 10 homes have a ratio of 5kVA/home. Since the 25kVA distribution transformers feed systems which are proportionally larger than 50kVA distribution transformers, it is expected that 25kVA distribution transformers experience more loss of life. Furthermore, on comparison with the loss of life limit of 0.0133% per day, it is seen from Table 6.5 and Table 6.6 that a total of six different 25kVA distribution transformers and only one 50kVA distribution transformer exceed loss of

life limits, which must be resolved by the distribution system operator using the transactive control methodology, as exemplified in Appendix A.

Table 6.4 Primary ESS Profiles for Maximum DSO Savings[a]

Hour of Day	Hourly LMP ($/kWh)	ESS 1 (kW)	ESS 2 (kW)	ESS 3 (kW)	ESS 4 (kW)
1	0.0289	0.00	0.00	0.00	0.00
2	0.0261	0.00	0.00	0.00	0.00
3	0.0263	0.00	0.00	0.00	0.00
4	0.0254	-16.67	-7.41	-6.66	-5.56
5	0.0246	-75.00	-33.33	-29.99	-25.00
6	0.0249	-74.97	-33.32	-30.01	-24.99
7	0.0277	0.00	0.00	0.00	0.00
8	0.0279	0.00	0.00	0.00	0.00
9	0.0318	0.00	0.00	0.00	0.00
10	0.0308	0.00	0.00	0.00	0.00
11	0.0349	0.00	0.00	0.00	0.00
12	0.0355	0.00	0.00	0.00	0.00
13	0.0414	0.00	0.00	0.00	0.00
14	0.0463	0.00	0.00	0.00	0.00
15	0.0517	0.00	0.00	0.00	0.00
16	0.0707	60.00	26.67	24.00	20.00
17	0.0891	75.00	33.33	30.00	25.00
18	0.0552	0.00	0.00	0.00	0.00
19	0.0471	0.00	0.00	0.00	0.00
20	0.0447	0.00	0.00	0.00	0.00
21	0.0422	0.00	0.00	0.00	0.00
22	0.0354	0.00	0.00	0.00	0.00
23	0.0337	0.00	0.00	0.00	0.00
24	0.0313	0.00	0.00	0.00	0.00

[a] Negative values are considered discharging and positive values are charging

Having applied the PAPR scheme (5.28) to determine the optimal rescheduling of residential ESS charging/discharging profiles, and applying game theory in Section 5.5.2 to determine the resultant cost the electric utility must bid to ensure the rescheduling will be accepted by the residential ESS owner, the resultant summary of transactive control for September 1, 2010 is given in Table 6.7.

Table 6.5 Loss of Life of 25kVA Distribution Transformer before Applying Transactive Energy

Primary Node	Dist. Txf. LoL (%)	Primary Node	Dist. Txf. LoL (%)	Primary Node	Dist. Txf. LoL (%)
2	0.0066	42	0.0047	83	0.0120
5	0.0059	45	0.0092	84	0.0085
7	0.0084	46	0.0097	86	0.0081
10	0.0105	51	0.0132	95	0.0042
12	0.0054	55	0.0122	96	0.0107
17	0.0072	56	0.0155	102	0.0057
31	0.0232	58	0.0053	111	0.0164
32	0.0220	59	0.0065	112	0.0088
38	0.0075	60	0.0050	114	0.0218
39	0.0040	68	0.0071		
41	0.0161	70	0.0070		

Table 6.6 Loss of Life of 50kVA Distribution Transformer before Applying Transactive Energy

Primary Node	Dist. Txf. LoL (%)	Primary Node	Dist. Txf. LoL (%)	Primary Node	Dist. Txf. LoL (%)
1	0.0075	37	0.0058	85	0.0061
4	0.0040	43	0.0027	87	0.0052
6	0.0035	50	0.0046	88	0.0059
9	0.0047	52	0.0033	90	0.0025
11	0.0048	53	0.0060	92	0.0091
16	0.0059	62	0.0047	94	0.0038
19	0.0057	63	0.0062	98	0.0048
20	0.0036	69	0.0036	99	0.0069
22	0.0118	71	0.0091	100	0.0043
24	0.0058	73	0.0040	103	0.0041
28	0.0048	74	0.0031	104	0.0158
29	0.0081	75	0.0056	106	0.0038
30	0.0078	77	0.0059	107	0.0038
33	0.0046	79	0.0079	109	0.0089
34	0.0046	80	0.0047	113	0.0037
35	0.0060	82	0.0043		

Table 6.7 Distribution Transformer Loss of Life Reduction Due to Transactive Energy

Primary Node	Txf Rating (kVA)	LoL Before TE (%)	LoL After TE (%)	Cost to Utility ($)
31	25	0.0232	0.0003	1.68
32	25	0.0220	0.0003	1.55
41	25	0.0161	0.0002	1.78
56	25	0.0155	0.0004	1.63
111	25	0.0164	0.0002	1.59
114	25	0.0218	0.0003	1.67
104	50	0.0158	0.0005	2.76

It may be seen on inspection of Table 6.7 that the cost to the electric utility to perform PAPR through rescheduling of residential ESS charging/discharging profiles is higher in the case of secondary systems extending from 50kVA distribution transformers versus secondary systems which extend from 25kVA distribution transformers. As the number of residential homes fed from a 50kVA distribution transformer is larger than the number of homes fed by a 25kVA distribution transformer, the electric utility may adjust more residential ESS charging/discharging profiles in PAPR on secondary systems extending from 50kVA distribution transformers, and therefore more bids to residential ESS owners are placed. Furthermore, it may be seen from inspection of Table 6.7 that the proposed transactive energy scheme is capable of resolving all distribution transformer loss of life issues for September 1, 2010, at a cumulative cost of $12.66 as the sum of all bids to residential ESS owners for PAPR optimization. Finally, upon performing the transactive energy scheme, the resultant system losses have reduced from an original 2.44MWh down to 2.35MWh, a reduction in active power losses of 3.69%, and as such has improved the systems operating efficiency.

6.2.1.2 Transactive Energy Control for Day-Ahead Scheduling Considering TOU Pricing

Inspection of Fig. 6.5 outlines the day-ahead hourly nodal prices, which are applied equally to all residential customers under time-of-use pricing, as compared with the locational marginal price (LMP). Considering the LMP in both DLMP and TOU cases is independent of the residential customer pricing scheme, the operating and maintenance costs of the gas turbine is less expensive than the LMP pricing at all hours of the day, resulting in maximum output of all DG units as previously described for DLMP residential customer pricing in 6.2.1.1.

Furthermore, as the LMP profile is equal in both TOU and DLMP residential customer pricing schemes, the charging and discharging profiles of the ESS directly connected to the primary distribution system remain as given in Table 6.4.

After having optimized all residential ESS charging/discharging profiles in the case of TOU residential customer pricing, and solving for power flow, the loss of life of the substation transformer was found to be 0.0031%. While the loss of life of the substation transformer under TOU residential customer pricing was not found to violate the daily loss of life limit of 0.0133%, the substation transformer was found to experience more loss of life under TOU residential customer pricing than the DLMP case, with loss of life in the DLMP case reported as 0.0025%. The reason for an increase in loss of life is due to the significant magnitude of reverse power flow which occurs during hours 13 and 15, as a combination of rooftop solar PV generation, distributed generation, and cumulative residential energy storage system discharging.

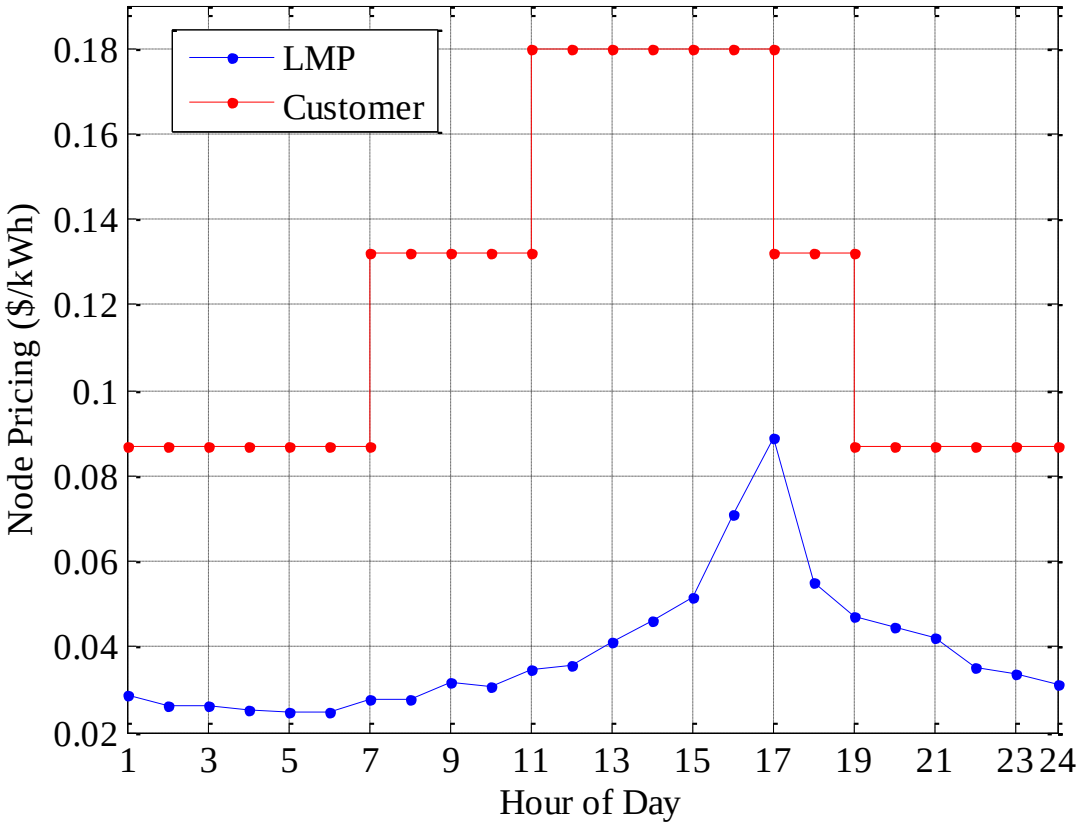

Fig. 6.5: TOU Prices for Secondary Systems

For the case of TOU residential customer pricing, cumulative active power losses in the system are found to be 2.22MWh, which is 0.22MWh less than the cumulative active power losses seen in DLMP residential customer pricing. Moreover, the resultant loss of life of all 25kVA distribution transformers and all 50kVA distribution transformers for the TOU residential customer pricing case may be seen in Table 6.8 and Table 6.9 respectively.

Table 6.8 Loss of Life of 25kVA Distribution Transformers before Applying Transactive Energy

Primary Node	Dist. Txf. LoL (%)	Primary Node	Dist. Txf. LoL (%)	Primary Node	Dist. Txf. LoL (%)
2	0.0070	42	0.0052	83	0.0128
5	0.0067	45	0.0096	84	0.0104
7	0.0089	46	0.0105	86	0.0087
10	0.0109	51	0.0143	95	0.0047
12	0.0060	55	0.0148	96	0.0127
17	0.0079	56	0.0178	102	0.0061
31	0.0248	58	0.0056	111	0.0177
32	0.0262	59	0.0076	112	0.0099
38	0.0092	60	0.0059	114	0.0231
39	0.0051	68	0.0077		
41	0.0178	70	0.0074		

Table 6.9 Loss of Life of 50kVA Distribution Transformers before Applying Transactive Energy

Primary Node	Dist. Txf. LoL (%)	Primary Node	Dist. Txf. LoL (%)	Primary Node	Dist. Txf. LoL (%)
1	0.0071	37	0.0054	85	0.0059
4	0.0041	43	0.0025	87	0.0054
6	0.0037	50	0.0045	88	0.0056
9	0.0043	52	0.0030	90	0.0025
11	0.0045	53	0.0054	92	0.0091
16	0.0069	62	0.0045	94	0.0034
19	0.0049	63	0.0061	98	0.0046
20	0.0029	69	0.0036	99	0.0068
22	0.0120	71	0.0092	100	0.0044
24	0.0060	73	0.0041	103	0.0040
28	0.0045	74	0.0029	104	0.0166
29	0.0076	75	0.0052	106	0.0044
30	0.0093	77	0.0063	107	0.0040
33	0.0043	79	0.0078	109	0.0078
34	0.0048	80	0.0045	113	0.0036
35	0.0056	82	0.0038		

A comparison of the median 25kVA distribution transformer loss of life considering TOU pricing in Table 6.8, and DLMP pricing in Table 6.5, shows a median 25kVA distribution transformer loss of life of 0.0084% for DLMP and 0.0092% for TOU respectively. The increase in loss of life seen in TOU pricing versus that of DLMP pricing may be attributed to the overlap between residential ESS discharge hours and rooftop solar PV generation hours, which results in significant reverse power flow on distribution transformers. Such reverse power flow is not as significant in the case of 50kVA distribution transformers however, as comparison of Table 6.9 and Table 6.6 provides a median value of 50kVA distribution transformer loss of life of 0.0046% and 0.0048% for TOU and DLMP residential customer pricing schemes respectively.

After having applied PAPR, similarly as given for Table 6.7; the resultant summary of transactive control for September 1, 2010 under TOU residential customer pricing is given in Table 6.10.

Table 6.10 Distribution Transformer Loss of Life Reduction Due to Transactive Energy

Primary Node	Txf Rating (kVA)	LoL Before TE (%)	LoL After TE (%)	Cost to Utility ($)
31	25	0.0248	0.0003	0.57
32	25	0.0262	0.0003	0.39
41	25	0.0178	0.0002	0.29
56	25	0.0178	0.0004	0.19
111	25	0.0177	0.0002	0.23
114	25	0.0231	0.0003	0.19
104	50	0.0166	0.0005	0.33

A comparison of the bids placed under transactive control to mitigate loss of life violations shows that the electric utility must place higher bids in the case of DLMP pricing versus that of TOU pricing to resolve a distribution transformer experiencing loss of life violation. For example, the cost to mitigate transformer loss of life on the 50kVA distribution transformer extending from primary node 104 is $0.33 in TOU pricing (Table 6.10) versus $2.76 in DLMP pricing (Table 6.7). Such increased bid costs are the result of more charging and discharging in DLMP pricing, versus that of TOU, which has been exemplified in Appendix A.

Finally, upon performing the transactive energy scheme, the resultant system active power losses have reduced from an original 2.22MWh down to 2.14MWh, resulting in a reduction in active power losses of 3.60%.

6.2.2 Transactive Energy Control for Day-Ahead Scheduling for One Year

Day-ahead scheduling was performed at an hourly resolution for each day over the 365 days in the 2010 year. Transformer loss of life was considered annually, based on the summation of the expected loss of life for each day throughout the year (6.1). Four different PEV and PV penetration scenarios were considered to investigate the annual results of day-ahead scheduling applied to each day of the year, under the proposed transactive energy control scheme outlined in Algorithm 2. The complete scenario listing is as given in Table 6.11, and has been performed for both DLMP and TOU residential customer pricing schemes. In this respect, DLMP pricing is analogous to real-time pricing, in which residential customers are charged for energy based on the DLMP pricing scheme defined in Section 4.5, and TOU pricing refers to typical time-of-use pricing rates in Ontario, Canada, outlined in Table 4.2.

$$LoL_{Txf}^{Year} = \sum_{d=1}^{365} LoL_{Txf}^{d} \quad (6.1)$$

Where LoL_{Txf}^{Year} is the annual loss of life of the transformer, as a summation of the daily loss of life for each day *d* throughout the year's duration.

Table 6.11 Studied Scenarios

Scenario	PEV Penetration	PV Penetration
1	0 PEV/House	0 kW/House
2	0 PEV/House	10 kW/House
3	1 PEV/House	0 kW/House
4	1 PEV/House	10 kW/House

6.2.2.1 Transactive Energy Control for Day-Ahead Scheduling for One Year Considering DLMP Pricing

Having applied day-ahead scheduling to each day of the 2010 year, Table 6.12 and Table 6.13 reveal statistical results of the annual transformer loss of life for 25kVA and 50kVA distribution transformers respectively, when transactive energy control has not been applied to the system.

Table 6.12 25kVA Distribution Transformer Annual LoL without Transactive Control

Scenario	Minimum LoL	Median LoL	Maximum LoL
1	0.3224%	0.3310%	0.3449%
2	0.2559%	0.2732%	0.2805%
3	0.4463%	0.9090%	1.9749%
4	0.3567%	0.7329%	1.6275%

Table 6.13 50kVA Distribution Transformer Annual LoL without Transactive Control

Scenario	Minimum LoL	Median LoL	Maximum LoL
1	0.3013%	0.3254%	0.4998%
2	0.1841%	0.2312%	0.2776%
3	0.5025%	0.8335%	2.4452%
4	0.2689%	0.4704%	1.5932%

Initial inspection of scenario 4 shows a median annual loss of life value of 0.7329% for 25kVA distribution transformers in Table 6.12 and 0.4704% for 50kVA distribution transformers in Table 6.13, which aligns with the observation that 25kVA distribution transformers experience more loss of life than 50kVA distribution transformers previously described in Section 6.2.1.1. A comparison of scenarios 1-4 in Table 6.12 reveals median annual 25kVA distribution transformer loss of life is least in the case of scenario 2, and highest in the case of scenario 3. As scenario 2 considers the case without PEV charging and with rooftop solar PV generation, it is expected that rooftop solar PV generation reduces the demand on the distribution transformers and therefore reduces loss of life. Consequently, as scenario 3 includes PEV charging but lacks rooftop solar PV generation, it is also expected that the increased load demand results in more distribution transformer loading and therefore higher loss of life.

Table 6.14 and Table 6.15 detail the loss of life of 25kVA and 50kVA distribution transformers respectively, with the application of transactive energy control. A comparison of the 25kVA distribution transformer loss of life in scenario 3 without transactive control (Table 6.12) shows a median value of 0.9090% which decreases to 0.5197% with transactive control (Table 6.14). The reduction in median LoL of 0.3893% due to the addition of transactive

control is the largest reduction amongst all scenarios considered in Table 6.11, as the inclusion of plug-in electric vehicle charging results in more transformer loss of life violations, and therefore requires more residential ESS rescheduling for PAPR. A comparison of scenario 2 for Table 6.12 and Table 6.14 shows the least reduction in median 25kVA distribution transformer loss of life, with a reduction in median LoL value due to the addition of transactive control by 0.0167%. Given that the inclusion of rooftop solar PV generation reduces transformer LoL, less transformer loss of life violations occur and therefore the DSO does not need to perform PAPR as frequently as in the other scenarios considered. Furthermore, a comparison of scenario 2 for 50kVA distribution transformers without transactive control (Table 6.13) and with transactive control (Table 6.15) shows nearly identical distribution transformer loss of life results. Given that 50kVA distribution transformers experience less loss of life than 25kVA distribution transformers, and rooftop solar PV further reduces transformer loss of life, 50kVA distribution transformer loss of life violation seldom occurs and therefore minimal transactive control corrective action is taken.

Table 6.14 25kVA Distribution Transformer Annual LoL with Transactive Control

Scenario	Minimum LoL	Median LoL	Maximum LoL
1	0.2762%	0.2844%	0.2958%
2	0.2390%	0.2565%	0.2636%
3	0.3498%	0.5197%	0.7473%
4	0.3017%	0.4382%	0.6484%

Table 6.15 50kVA Distribution Transformer Annual LoL with Transactive Control

Scenario	Minimum LoL	Median LoL	Maximum LoL
1	0.2712%	0.2981%	0.4428%
2	0.1840%	0.2312%	0.2776%
3	0.4096%	0.5338%	0.8457%
4	0.2690%	0.4193%	0.6848%

Economic considerations may be seen in Table 6.16, which outlines the cumulative annual costs to the distribution system operator for transactive control, as the sum of all bids made to residential ESS owners throughout the year for PAPR optimization. A comparison of scenario 1 and scenario 2 in Table 6.16 reveals that the cumulative amount of bids made by the DSO to residential ESS owners is less in the case of rooftop solar PV (scenario 2) than without rooftop solar PV inclusion (scenario 1). As rooftop solar PV was found to reduce the number of transformer loss of life violations, the DSO requires less corrective action through PAPR and therefore does not place as many bids to residential ESS owners. In the case of plug-in electric vehicle charging on the system however, the cumulative annual bids placed by the DSO raises from $177.03 in scenario 1 to $1,273.17 in scenario 3 respectively. Given that the median annual transformer loss of life for 25kVA distribution transformers before transactive control is 0.3310% and 0.9090% in scenario 1 and 3 respectively, with an increase of 0.3254% to 0.8335% in 50kVA distribution transformers, the DSO experiences more loss of life violations in the case of PEV, and therefore accumulate larger annual costs.

Table 6.16 Annual Costs of Transactive Control for DLMP Pricing

Scenario	Cumulative Annual Costs of DSO Bids to Residential ESS Owners ($)
1	177.03
2	50.26
3	1,273.17
4	1,193.20

Finally, Table 6.17 summarizes the resultant effects of transactive control in the reduction of annual active power losses in the system. Consideration of Table 6.17 shows an increase of annual losses from 626MWh in scenario 1 without transactive control (TC) and 792MWh in

scenario 2. While under typical circumstances rooftop solar PV generation acts to reduce system losses, an excess of solar generation, combined with DG output, results in significant reverse power flow magnitude and therefore the active losses in the system are found to increase.

Table 6.17 Annual Active Power Losses for DLMP Pricing

Scenario	Annual Losses Without TE (MWh)	Annual Losses With TE (MWh)	Reduction in Annual Losses Due to TE (%)
1	626	624	0.23
2	792	791	0.03
3	657	645	1.71
4	807	799	1.08

A comparison of annual active power losses without transactive control versus transactive control shows that the addition of transactive control results in less system losses for each scenario, with the least reduction in scenario 2 and most reduction in scenario 3. Considering scenario 2 has the least transformer loss of life violations, and scenario 3 has most transformer loss of life violations, the amount of corrective action taken, and therefore the reduction in losses due to PAPR, is smallest and largest in scenario 2 and 3 respectively.

6.2.2.2 Transactive Energy Control for Day-Ahead Scheduling for One Year Considering TOU Pricing

The results of Table 6.18 and Table 6.19 provide the median 25kVA and 50kVA distribution transformer annual loss of life under TOU residential customer pricing, as comparable with Table 6.12 and Table 6.13 for DLMP residential customer pricing.

Table 6.18 25kVA Distribution Transformer Annual LoL without Transactive Control

Scenario	Minimum LoL	Median LoL	Maximum LoL
1	0.2180%	0.2190%	0.2203%
2	0.1704%	0.1713%	0.1723%
3	0.3356%	0.6740%	1.6586%
4	0.2359%	0.4264%	1.2719%

Table 6.19 50kVA Distribution Transformer Annual LoL without Transactive Control

Scenario	Minimum LoL	Median LoL	Maximum LoL
1	0.1543%	0.1557%	0.2271%
2	0.1041%	0.1229%	0.1373%
3	0.2638%	0.4510%	1.3513%
4	0.1389%	0.2575%	0.8137%

A comparison of 25kVA distribution transformer annual loss of life for TOU pricing in Table 6.18 and DLMP pricing in Table 6.12 outlines 0.4264% and 0.7329% median annual 25kVA distribution transformer loss of life in scenario 4 under TOU pricing and DLMP pricing respectively. Considering TOU pricing results in one on-peak and one off-peak cycle throughout each day, the opportunity exists for residential ESS owners to charge and discharge once per day to maximize savings. As detailed further in Appendix A, DLMP profiles may result in more than one cycle of charging and discharging residential ESS profiles, resulting in higher transformer loss of life with respect to residential customers under DLMP pricing.

Table 6.20 and Table 6.21 detail the loss of life of 25kVA and 50kVA distribution transformers after transactive energy control is applied, in comparison to the cases without transactive control in Table 6.18 and Table 6.19 respectively. Upon consideration of scenario 3, it may been that a comparison of the median 25kVA distribution transformer loss of life

reduces from 0.6740% in Table 6.18 to 0.3914% in Table 6.20. As previously seen in the DLMP residential customer pricing, distribution transformer loss of life violations are mitigated through transactive energy control, ultimately reducing the transformers loss of life. Moreover, it may be seen that distribution transformer loss of life does not change in scenario 2 for 25kVA distribution transformers (Table 6.20 and Table 6.18) as well as 50kVA distribution transformers (Table 6.21 and Table 6.19). As scenario 2 under TOU residential customer pricing was not found to experience transformer loss of life violations, transactive control did not require residential ESS rescheduling and therefore no bids were made by the DSO.

Table 6.20 25kVA Distribution Transformer Annual LoL with Transactive Control

Scenario	Minimum LoL	Median LoL	Maximum LoL
1	0.1880%	0.1888%	0.1898%
2	0.1704%	0.1713%	0.1723%
3	0.2612%	0.3914%	0.5393%
4	0.2051%	0.3328%	0.4342%

Table 6.21 50kVA Distribution Transformer Annual LoL with Transactive Control

Scenario	Minimum LoL	Median LoL	Maximum LoL
1	0.1432%	0.1455%	0.2041%
2	0.1041%	0.1229%	0.1373%
3	0.2225%	0.3586%	0.5760%
4	0.1391%	0.2288%	0.4484%

The cumulative annual costs of bids made by the DSO to residential owners to resolve transformer loss of life violations under TOU pricing is seen in Table 6.22. From Table 6.22 it may be seen that the cumulative annual costs of bids made by the DSO is $0 under scenario 2. Given that scenario 2 does not experience transformer loss of life violations, it is expected that the DSO will not need to perform PAPR to resolve loss of life issues, and therefore no bids to

residential ESS owners are made. A comparison of the cumulative annual costs of DSO bids in scenario 4 reveals an increase in the cumulative annual cost of bids from $1,193.20 in DLMP pricing (Table 6.16) to $2,888.95 in TOU pricing (Table 6.22). Despite DLMP pricing having larger distribution transformer loss of life values than given in TOU pricing, the difference in price between on-peak and off-peak times under TOU pricing is typically larger than the price differences in DLMP pricing. Due to larger price differences in TOU pricing, residential ESS owners may require significantly larger bid prices by the DSO to perform residential ESS rescheduling in TOU residential customer pricing versus that in DLMP pricing.

Table 6.22 Annual Costs of Transactive Control for TOU Pricing

Scenario	Cumulative Annual Costs of DSO Bids to Residential ESS Owners ($)
1	321.84
2	0.00
3	2,384.07
4	2,888.95

Finally, Table 6.23 summarizes the resultant effects of transactive control in the reduction of annual active power losses in the system for the case of TOU pricing. A comparison of Table 6.23 and Table 6.17 reveals annual active power losses in scenario 4 of 658MWh under TOU pricing, and 807MWh under DLMP pricing. In a similar manner to increased distribution transformer loss of life, the increased activity of residential ESS charging and discharging under DLMP pricing schemes results in larger losses on the system. Furthermore, it is also seen that the reduction in annual losses due to transactive energy control for scenario 4 is 0.54% in TOU pricing and 1.08% in DLMP pricing respectively.

Given that more distribution transformer loss of life violations occur under DLMP pricing, a larger number of secondary systems are subject to residential ESS rescheduling for PAPR, and therefore the system experiences a reduced amount of losses.

Table 6.23 Annual Active Power Losses for TOU Pricing

Scenario	Annual Losses Without TE (MWh)	Annual Losses With TE (MWh)	Reduction in Annual Losses Due to TE (%)
1	471	471	0.09
2	639	639	0.00
3	503	501	0.58
4	658	654	0.54

7 Conclusions and Recommendations

7.1 Summary and Conclusions

The work outlined in this dissertation presents a detailed methodology to employ transactive energy control through residential energy storage system rescheduling at a secondary system level in order to resolve transformer loss of life violations in both distribution and substation transformers. This work has considered the technical and economic effects of the proposed transactive energy scheme under varying plug-in electric vehicle and rooftop solar photovoltaic penetrations for each day of the day-ahead energy market throughout the duration of a year.

In order to mitigate loss of life violations in distribution transformers at the secondary distribution system, the electric utility may reschedule the charging and discharging operations of residential energy storage systems, the cost of which is imposed on the electric utility to pay the residential energy storage system owner for lost energy bill savings. Such control techniques are also available to the electric utility to reduce substation transformer loss of life, with additional availability of the electric utility to schedule distributed generator operations or energy storage systems connected to the primary distribution system as alternative forms of control.

Results of the simulation without transactive control have revealed that the 25kVA and 50kVA distribution transformers experience 1.5 times larger annual loss of life when residential customers charge energy storage systems subject to DLMP versus TOU residential

customer pricing. Furthermore, distribution transformer loss of life is found to triple in the case without rooftop solar photovoltaic generation with the addition of plug-in electric vehicles, which requires increased usage of residential peak-to-average power reduction to mitigate transformer loss of life violations.

The addition of transactive energy control into the system is capable of significantly reducing the median annual loss of life of distribution transformers, up to 40% in the case of plug-in electric vehicles without rooftop solar PV generation. The transactive control methodology was found to be more effective in the case of DLMP residential customer pricing than TOU pricing, with median 25kVA distribution transformer annual loss of life reduced by up to 42.83% in DLMP and 41.93% in TOU residential customer pricing methods for cases with plug-in electric vehicle charging without rooftop solar PV generation respectively. As DLMP customer pricing experienced more distribution transformer loss of life violations than in the case of TOU residential customer pricing, scenarios considering DLMP customer pricing took more corrective PAPR action to reduce distribution transformer loss of life. Such results are more prevalent in the case of 50kVA distribution transformers, which experience 35.96% median annual loss of life reduction in DLMP residential customer pricing versus 20.49% under TOU residential customer pricing respectively. The effectiveness of transactive energy control is least significant in the case of rooftop solar PV generation without plug-in electric vehicles, which expects the lowest distribution transformer loss of life, and therefore requires the least corrective residential energy storage system rescheduling.

Moreover, it was determined that the proposed transactive control scheme is capable of increasing grid efficiency through active power loss reduction. In the case of DLMP residential

customer pricing, a maximum reduction of 1.71% cumulative active power losses annually in the case with plug-in electric vehicle charging was found, versus a maximum active power loss reduction of 0.58% under TOU residential customer pricing. The system was found to experience larger losses under DLMP residential customer pricing due to increased number of charging/discharging cycles of residential ESS versus the TOU residential customer pricing case. As DLMP residential customer pricing also resulted in more distribution transformer loss of life violations versus TOU residential customer pricing, more residential ESS rescheduling occurred in the case of DLMP residential customer pricing and therefore a higher reduction in annual active power losses was achieved.

Furthermore, the bids placed by the distribution system operator to perform PAPR in mitigation of transformer loss of life violations was found to be larger when residential customers were billed for energy based on TOU pricing than DLMP pricing, resulting in approximately 1.8 times more cumulative annual costs of bidding. Despite a higher number of distribution transformer loss of life violations seen to occur when residential customers are charged based on DLMP pricing, residential customers typically acquire larger energy savings under the TOU residential customer pricing scheme, and therefore the cost to the electric utility to perform residential energy storage system rescheduling is larger under TOU residential customer pricing than DLMP residential customer pricing.

Finally, it was determined that DLMP residential customer pricing was found to experience larger distribution transformer loss of life and more annual active power losses than in the case of TOU residential customer pricing. Given that DLMP residential customer pricing experienced more distribution transformer loss of life violations than in TOU residential

customer pricing, the electric utility performed more corrective PAPR action in DLMP residential customer pricing and therefore a higher reduction in distribution transformer loss of life and annual active power losses was found when transactive control was applied to the system. While DLMP residential customer pricing performed more residential ESS charging/discharging profile rescheduling, the cumulative annual costs of placing bids by the was found to cost nearly half as much to the electric utility under DLMP residential customer pricing than TOU residential customer pricing. As the electric utility places bids to residential customers for ESS rescheduling based on the energy savings of the residential customer, the lower savings to residential customers under DLMP residential customer pricing resulted in less economic cost to the electric utility than under TOU residential customer pricing.

7.2 Contributions

The work performed in this paper has extended the application of transactive energy to include the capability of considering a transactive market applied to the day-ahead energy market, as a means of integrating residential ESS control through a transactive market. Through consideration of the day-ahead energy market, a 24-hour duration for ESS scheduling has been considered, which provides opportunity to schedule ESS charging and discharging in advance. In order to apply the ideals of transactive energy, the ESS transactive control scheme was used to: increase grid reliability through mitigating transformer loss of life violations, and increase grid efficiency in terms of reduced system losses. In pursuit of this work, the following contributions are outlined as follows:

1. Established a methodology to quantify transformer loss of life in the day-ahead scheduling problem, considering distributed energy resources at residential households including: PEV, PV, and ESS
2. Developed a transactive energy framework which allows for distribution utility control over residential energy storage systems, applied to perform peak-to-average power reduction of distribution transformers, consequently resulting in decreased transformer loss of life
3. Developed a game theoretic solution to determine the minimum cost to distribution utilities to perform residential energy storage control on residential energy storage system devices
4. A test case system was established to evaluate the reduction in transformer loss of life and active power losses through the proposed transactive energy control methodology, applied for each day of a single year, considering varying plug-in battery electric vehicle and rooftop solar photovoltaic penetration
5. The effectiveness of the proposed transactive energy control scheme was considered under both time of use (TOU) pricing and distribution locational marginal pricing (DLMP) residential customer pricing schemes

7.3 Recommendations

The results of this work have shown that the potential exists for both the electric utility and residential customer to mutually benefit from establishing a transactive energy control methodology. From the residential energy storage system owner's perspective, the energy storage provides economic benefit in the form of reduced energy bills due to the pre-purchase

of energy at low cost hours to be dispatched at higher cost hours. While this provides an opportunity for the electric utility to economically control the energy storage system, the electric utility may further benefit from rescheduling residential energy storage systems as necessary to alleviate grid operational issues. Through employing the transactive control scheme formulated in this work, which establishes a means of the allowing electric utility to reschedule the charging/discharging profiles of residential energy storage systems, the electric utility may reduce the rate at which transformer lifetimes degrade within pre-specified limitations. The result of applying the proposed transactive control methodology ultimately defers the need to upgrade or replace transformers in both the primary and secondary distribution system which experience accelerated lifetime degradation under increasing plug-in electric vehicle and rooftop solar photovoltaic penetrations.

7.4 Future Work

In order for the electric utility to gain further economic benefit from the usage of transactive energy control on residential energy storage systems, a number of extensions to this work may be performed. From the perspective of distribution systems operation, the transactive energy scheme may further aim to limit voltage and current violations on the system, to retain high power quality in operation. The electric utility may also choose to broaden the scope of the proposed transactive energy control methodology to include other customer or private investor owned devices capable of performing control action which constitute generation, storage, or loading within the distribution system. From an economical perspective, the electric utility may instead look to employ secondary energy storage system control when the cost of the residential energy storage system rescheduling action results in

overall economic benefit to the electric utility, as opposed to performing residential energy storage system rescheduling only in the case of transformer loss of life violation. Furthermore, such transactive control methodology may be employed in impact studies to evaluate the capability of the control methodology to extend the PEV penetration capacity within the system, including the consideration of different vehicle compositions and robustness of the solution methodology. Moreover, due to the limitations of the proposed transactive energy control methodology acting in the day-ahead energy market, the opportunity exists for any forecasting errors to be absorbed through the usage of real-time energy market transactive energy control techniques. Lastly, residential energy storage rescheduling performed by the electric utility may seek to expand the operational functionality to accommodate additional control actions, such as residential energy storage system rescheduling to maximize overall electric utility profit considering the payout to the residential energy storage system owners.

8 References

[1] U.S. Department of Energy. (Sept. 5, 2016). *Smart Grid*. Available: http://energy.gov/oe/services/technology-development/smart-grid

[2] Ontario Ministry of Energy, "Achieving Balance: Ontario's Long-Term Energy Plan," Toronto, Ontario, Dec. 2013.

[3] Ontario Ministry of Energy, "Smart Grid Fund Guidelines," Toronto, Ontario, Sept. 2015.

[4] Ontario Ministry of Transportation, "Electric Vehicle Incentive Program (EVIP) Guide," Feb. 2016.

[5] IESO. (Jan. 2016, Jan. 7 2016). *MicroFIT Program*. Available: http://microfit.powerauthority.on.ca/about-microfit

[6] M.K. Gray and W. G. Morsi, "Probabilistic quantification of voltage unbalance and neutral current in secondary distribution systems due to plug-in battery electric vehicle charging," *Elect. Power Energy Syst.*, vol. 133, pp. 249-256, Apr. 2016.

[7] M.K. Gray and W.G. Morsi, "Power quality assessment in distribution systems embedded with plug-in hybrid and battery electric vehicles," *IEEE Trans. Power Syst.*, vol. 30, pp. 663-671, Mar. 2015.

[8] M.K. Gray and W. G. Morsi, "Economic assessment of phase reconfiguration to mitigate the unbalance due to plug-in electric vehicles charging," *Elect. Power Energy Syst.*, vol. 140, pp. 329-336, Nov. 2016.

[9] M.K. Gray and W. G. Morsi, "On the role of prosumers owning rooftop solar photovoltaic in reducing the impact on transformer's aging due to plug-in electric vehicles," *Elect. Power Energy Syst.*, vol. PP, pp. 1-10, 2017.

[10] R. Massiello. (May/Jun. 2016) Transactive energy: the hot topic in the industry. *IEEE Power & Energy Magazine*.

[11] GridWise Architecture Council, "GridWise Transactive Energy Framework Version 1.0," GWAC, Report PNNL-22946, Jan. 2015.

[12] Plug'n Drive, "Electric Vehicles: Reducing Ontario's Greenhouse Gas Emissions," May 2015.

[13] National Energy Board, "Canada's Energy Future 2016: Energy Supply and Demand Projections to 2040," Canada, 2016.

[14] A. Eller and A. Dehamna, "Residential Energy Storage: Advanced Lead-Acid, Flow, and Lithium Ion Battery Systems for Residential Applications: Global Market Analysis and Forecasts," Navigant Research, Q2, 2016.

[15] S.F. Abdelsamad, W.G. Morsi, and T. S. Sidhu, "Probabilistic impact of transportation electrification on the loss-of-life of distribution transformers in the presence of rooftop solar photovoltaic," *IEEE Trans. Sustain. Energy*, vol. 6, pp. 1565-1573, Oct. 2015.

[16] Z. Jiao, X. Wang, and H. Gong, "Wide area measurement/wide area information-based control strategy to fast relieve overloads in a self-healing power grid," *IET Generation, Transmission & Distribution*, vol. 8, pp. 1168-1176, May 2013.

[17] M.S. ElNozahy and M.M.A. Salama, "A comprehensive study of the impacts of PHEVs on residential distribution networks," *IEEE Trans. Sustain. Energy*, vol. 5, pp. 332-342, Jan. 2014.

[18] Y.O. Assolami and W.G. Morsi, "Impact of second-generation plug-in battery electric vehicles on the aging of distribution transformers considering TOU prices," *IEEE Trans. Sustain. Energy*, vol. 6, pp. 1606-1614, Oct. 2015.
[19] Independent Electricity System Operator, "Feed-in Tariff MicroFIT Contract: Version 4.0," Jun. 2016.
[20] Electric Power Research Institute, "Estimating the Costs and Benefits of the Smart Grid: A Preliminary Estimate of the Investment Requirements and the Resultant Benefits of a Fully Functioning Smart Grid," EPRI Report 1022519, California, USA, Mar. 2011.
[21] R. Lordan, "Power Delivery System of the Future: A Preliminary Estimate of Costs and Benefits," EPRI Report 1011001, California, USA, Jul. 2004.
[22] R. James, "The Power to Reduce CO2 Emissions: The Full Portfolio," EPRI Report 1020389, California, USA, Oct. 2009.
[23] A. Masoum, S. Deilami, P. Moses, and A. Abu-Siada, "Impact of plug-in electrical vehicles on voltage profile and losses of residential system," in *Proc. Australasian Universities Power Engineering Conference (AUPEC)*, 2010, pp. 1-6.
[24] F. Shahnia, A. Ghosh, G. Ledwich, and F. Zare, "Voltage unbalance sensitivity analysis of plug-in electric vehicles in distribution networks," in *Proc. Australasian Universities Power Engineering Conferences (AUPEC)*, 2011, pp. 1-6.
[25] P. Moses, S. Deilami, and A. Masoum, "Power quality of smart grids with plug-in electric vehicles considering battery charging profile," in *Proc. Innovative Smart Grid Technologies (ISGT)*, 2010, pp. 1-7.
[26] M. Masoum, P. Moses, and K. Smedley, "Distribution transformer losses and performance in smart grids with residential plug-in electric vehicles," in *Proc. Innovative Smart Grid Technologies (ISGT)*, 2011, pp. 1-7.
[27] S. Shafiee, M. Fotuhi-Firuzabad, and M. Rastegar, "Investigating the impacts of plug-in hybrid electric vehicles on power distribution systems," *IEEE Trans. Smart Grid*, vol. 4, pp. 1351-1360, 2013.
[28] M. Masoum, P. Moses, and S. Hajforoosh, "Distribution transformer stress in smart grid with coordinated charging of plug-in electric vehicles," in *Proc. Innovative Smart Grid Technologies (ISGT)*, 2012, pp. 1-8.
[29] P. Papadopoulos, S. Skarvelis-Kazakos, I. Grau, L. Cipcigan, and N. Jenkins, "Electric vehicles' impact on British distribution networks," *Electrical Systems in Transportation*, vol. 2, pp. 91-102, 2012.
[30] C. Jiang, R. Torquato, D. Salles, and W. Xu, "Method to assess the power-quality impact of plug-in electric vehicles," *IEEE Trans. Power Del.*, vol. 29, pp. 958-965, 2014.
[31] "IEEE Guide for Loading Mineral-Oil-Immersed Transformers and Step-Voltage Regulators," IEEE Std. C57.91-2011, Mar. 2012, New York, NY, USA.
[32] Idaho National Laboratory, "Plug-in Electric Vehicle and Infrastructure Analysis," Sept. 2015.
[33] S. Shao, M. Pipattansomporn, and S. Rahman, "Challenges of PHEV penetration to the residential distribution network," in *Proc. IEEE Power and Energy Society General Meeting*, Calgary, AB, Canada, 2009, pp. 1-6.

[34] A. Dubey and S. Santoso, "Electric vehicle charging on residential distribution systems: impacts and mitigations," *IEEE Access,* vol. 3, pp. 1871-1893, Nov. 2015.
[35] A. Brooks, E. Lu, D. Reicher, C. Spirakis, and B. Weihl. Demand dispatch. *IEEE Power Energy Mag.* vol. 8, no. 3, pp. 20-29, May/Jun. 2010.
[36] P. Siano, "Demand response and smart grids - a survey," *Renew. Sustain. Energy Rev.,* vol. 30, pp. 461-478, Feb. 2014.
[37] V. Aravinthan and W. Jewell, "Controlled electric vehicle charging for mitigating impacts on distribution assets," *IEEE Trans. Smart Grid,* vol. 6, pp. 999-1009, Mar. 2015.
[38] C.K. Wen, J.C. Chen, J.H. Teng, and P. Ting, "Decentralized plug-in electric vehicle charging selection algorithm in power systems," *IEEE Trans. Smart Grid,* vol. 3, pp. 1779-1789, Dec. 2012.
[39] S. Schey, D. Scoffield, and J. Smart, "A first look at the impact of electric vehicle charging on the electric grid in the EV project," in *Proc. EVS26 Int. Battery, Hybrid, Fuel Cell Electr. Vehicle Symp.*, Los Angeles, CA, USA, May 2012, pp. 1-12.
[40] A. Dubey, S. Santoso, M.P. Cloud, and M. Waclawiak, "Determining time-of-use schedules for electric vehicle loads: a practical perspective," *IEEE Power and Energy Technology Systems Journal,* vol. 2, pp. 12-20, Mar. 2015.
[41] F.M. Uriarte, A. Toliyat, A. Kwasinski, and R.E. Hebner, "Consumer-data approach to assess the effect of residential grid-tied photovoltaic systems and electric vehicles on distribution transformers," in *Proc. IEEE 5th Int. Symp. Power Electron. Distrib. Gener. Syst. (PEDG),* Galway, Ireland, Jun. 2014, pp. 1-8.
[42] T.J. Geiles and S. Islam, "Impact of PEV charging and rooftop PV penetration on distribution transformer life," in *Proc. IEEE Power and Energy Society General Meeting (PESGM),* Vancouver, BC, Jul. 21-25, 2013, pp. 1-5.
[43] P. Westacott and C. Candelise, "Assessing the impacts of photovoltaic penetration across an entire low-voltage distribution network containing 1.5 million customers," *IET Renewable Power Gen.,* vol. 10, pp. 460-466, Mar. 2016.
[44] M. Hasheminamin, V.G. Agelidis, V. Salehi, R. Teodorescu, and B. Hredzak, "Index-based assessment of voltage rise and reverse power flow phenomena in a distribution feeder under high PV penetration," *IEEE J. Photovolt.,* vol. 5, pp. 1158-1168, Jul. 2015.
[45] R. Tonkoski, D. Turcotte, and T.H.M. El-Fouly, "Impact of high PV penetration on voltage profiles in residential neighbourhoods," *IEEE Trans. Sustain. Energy,* vol. 3, pp. 518-527, Jul. 2012.
[46] M.S. ElNozahy and M.M.A. Salama, "Studying the feasibility of charging plug-in hybrid electric vehicles using photovoltaic electricity in residential distribution systems," *Elect. Power Syst. Res.,* vol. 110, pp. 133-143, May 2014.
[47] Y. Liu, J. Bebic, B. Kroposki, J. Bedout, and W. Ren, "Distribution system voltage performance analysis for high-penetration PV," in *Proc. IEEE Energy,* Atlanta, GA, Nov. 2008, pp. 1-8.
[48] E. Dall'Anese, S.V. Dhople, and G.B. Giannakis, "Optimal dispatch of photovoltaic inverters in residential distribution systems," *IEEE Trans. Sustain. Energy,* vol. 5, pp. 487-497, Apr. 2014.

[49] R.G. Wandhare and V. Agarwal, "Reactive power capacity enhancement of a PV-grid system to increase PV penetration level in smart grid scenario," *IEEE Trans. Smart Grid,* vol. 5, pp. 1845-1854, Jul. 2014.
[50] E. Yao, P. Samado, V.W.S. Wong, and R. Schober, "Residential demand side management under high penetration of rooftop photovoltaic units," *IEEE Trans. Smart Grid,* vol. 7, pp. 1597-1608, May 2016.
[51] V. Hamidi, F. Li, and F. Robinson, "Demand response in the UK's domestic sector," *Electr. Power Syst. Res.,* vol. 79, pp. 1722-1726, 2009.
[52] P. Grunewald and J. Torriti, "Demand response from the non-domestic sector: early UK experiences and future opportunities," *Energy Policy,* vol. 61, pp. 423-429, 2013.
[53] X. Liu, A. Aichhorn, L. Liu, and H. Li, "Coordinated control of distributed energy storage system with tap changer transformers for voltage rise mitigation under high photovoltaic penetration," *IEEE Trans. Smart Grid,* vol. 3, pp. 897-906, Jun. 2012.
[54] M.J.E. Alam, K.M. Muttaqi, and D. Sutanto, "Distributed energy storage for mitigation of voltage-rise impact caused by rooftop solar PV," in *Proc. IEEE PESGM,* San Diego, CA, Jul. 2012, pp. 1-8.
[55] J. Appen, T. Stetz, M. Braun, and A. Schmiegel, "Local voltage control strategies for PV storage systems in distribution grids," *IEEE Trans. Smart Grid,* vol. 5, pp. 1002-1009, Mar. 2014.
[56] "IEEE Application Guide for IEEE Std 1547, IEEE Standard for Interconnecting Distributed Resources with Electric Power Systems," IEEE Std. 1547.2-2008, 2009.
[57] T. Stetz, J. Appen, F. Niedermeyer, G. Scheibner, R. Sikora, and M. Braun. (Mar/Apr 2015) Twilight of the Grids. *IEEE power & energy magazine*. 50-61.
[58] J.C. Fuller, K.P. Schneider, and D. Chassin, "Analysis of residential demand response and double-auction markets," in *Proc. PESGM*, San Diego, CA, Jul. 2011, pp. 1-7.
[59] D.J. Hammerstrom et. al., "Pacific Northwest GridWise Testbed Demonstration Projects Part I. Olympic Peninsula Project," Richland, Washington, Report PNNL-17167, Oct. 2007.
[60] eMeter Strategic Consulting, "PowerCentsDC Program Final Report," eMeter, Sept. 2010.
[61] AEP Ohio, "GridSMART Demonstration Project - A Community-Based Approach to Leading the Nation in Smart Energy Use," AEP, Ohio, Jun. 2014.
[62] R. Melton, "Pacific Northwest Smart Grid Demonstration Project Technology Performance Report Volumne 1: Technology Performance," PNNL, Richland, Washington, Report PNWD-4438, Jun. 2015.
[63] T. Sahin and D. Shereck, "Renewable energy sources in a transactive energy market," in *Proc. ICSAI*, Shanghai, China, Nov. 2014, pp. 202-208.
[64] D. Jin, X. Zhang, and S. Ghosh, "Simulation models for evaluation of network design and hierarchical transactive control mechanism in smart grids," in *Proc. ISGT*, Washington, DC, Jan. 2012, pp. 1-8.
[65] M.N. Akter and M.A. Mahmud, "Analysis of different scenarios for residential energy management under existing retail market structure," in *Proc. ISGT*, Asia, Bangkok, 2015, pp. 1-6.

[66] N. Zhang, Y. Yan, S. Xu, and W. Su, "Game-theory-based electricity market clearing mechanisms for an open and transactive distribution grid," in *Proc. PESGM*, Denver, CO, Jul. 2015, pp. 1-5.
[67] M. Sandoval and S. Grijalva, "Future grid business model innovation: distributed energy resources services platform for renewable energy integration," in *Proc. APCASE*, Quito, Ecuador, Jul. 2015, pp. 72-77.
[68] S. Widergren, J. Fuller, C. Marinovici, and A. Somani, "Residential transactive control demonstration," in *Proc. ISGT*, Washington, DC, Feb. 2014, pp. 1-5.
[69] S. Behboodi, D.P. Chassin, and C. Crawford, "Electric vehicle participation in transactive power systems using real-time retail prices," in *Proc. HICSS*, Koloa, HI, 2016, pp. 2400-2407.
[70] J. Hu, G. Yang, and H.W. Bindner, "Network constrained transactive control for electric vehicles integration," in *Proc. PESGM*, Denver, CO, Jul. 2015, pp. 1-5.
[71] Y. Chen and M. Hu, "Balancing collective and individual interests in transactive energy management of interconnected micro-grid clusters," *Energy*, vol. 109, pp. 1075-1085, 2016.
[72] S.A. Chandler, J.H. Rinaldi II, R.B. Bass, and L. Beckett, "Smart grid dispatch optimization control techniques for transactive energy systems," in *Proc. SusTech*, Portland, OR, Jul. 2014, pp. 51-54.
[73] C. D'Adamo, S. Jupe, and C. Abbey, "Global survey on planning and operation of active distribution networks," presented at the 20th Internation Conference and Exhibition on Electricity Distribution, Prague, Czech Republic, 2009.
[74] T. Gonen, *Electric Power Distribution Engineering*, London, New York, USA: CRC Press, 2014.
[75] P. Denholm, S.J. Fernandez, D.G. Hall, T. Mai, and S. Tegen, "Energy Storage Technologies, Renewable Electricity Futures Study Volume 2 of 4: Renewable Electricity Generation and Storage Technologies," National Renewable Energy Laboratory, Golden, CO, 2012.
[76] X. Luo, J. Wang, M. Dooner, and J. Clarke, "Overview of current development in electrical energy storage technologies and the application potential in power system operation," *Applied Energy*, vol. 137, pp. 511-536, 2015.
[77] A. Eller and A. Dehamna, "Energy Storage Tracker 1Q16: Market Share Data, Industry Trends, Market Analysis, and Project Tracking by World Region, Technology, Application, and Market Segment," Navigant Research, 2016.
[78] A.A. Akhil, HG. Huff, A.B. Currier, B.C. Kaun, D.M. Rastler, S.B. Chen, *et al.*, "DOE/EPRI 2013 Electricity Storage Handbook in Collaboration with NRECA," Sandia National Laboratories, Albuquerque, New Mexico, Jul. 2013.
[79] J. Eyer and G. Corey, "Energy Storage for the Electric Grid: Benefits and Market Potential Assessment Guide," Sandia National Laboratories, Albuquerque, New Mexico, Feb. 2010.
[80] "IEEE Guide for the Interoperability of Energy Storage Systems Integrated with the Electric Power Infrastructure," IEEE Std. 2030.2-2015, Mar. 2015, New York, NY, USA.

[81] H. Ding, Z. Hu, and Y. Song, "Rolling optimization of wind farm and energy storage system in electricity markets," *IEEE Trans. Power Syst.*, vol. 30, pp. 2676-2684, Sept. 2015.
[82] Epcor, "Distributed Generation," 2002.
[83] U.S. Department of Energy, "The Potential Benefits of Distributed Generation and the Rate Related Issues that May Impede Its Expansion," 2005.
[84] B. Owens, "The Rise of Distributed Power," General Electric, 2014.
[85] P. Silva and ISO New England, "August 2015 Distributed Generation Survey Results," Westborough, MA, Dec. 8, 2015.
[86] Toyota. (2014). *How Hybrids Work: Gas-Electric Hybrids*. Available: http://www.toyota.ca/toyota/en/hybrids/how-hybrids-work
[87] Ontario Ministry of Transportation, "Cars are Evolving," 2013.
[88] S. Shepard and L. Jerram, "Electric Vehicle Market Forecasts: Global Forecasts for Light Duty Hybrid, Plug-In Hybrid, and Battery Electric Vehicle Sales and Vehicles in Use: 2015-2024," Navigant Research, Q4, 2015.
[89] S. Shepard and L. Jerram, "Transportation Forecast: Light Duty Vehicles - Light Duty Stop-Start, Hybrid Electric, Plug-in Hybrid Electric, Battery Electric, Natural Gas, Fuel Cell, Propane Autogas, and Conventional Vehicles: Global Market Forecasts, 2015-2035," Navigant Research, Q2, 2015.
[90] P.S. Moses, M.A.S. Masoum, and S. Hajforoosh, "Overloading of distribution transformers in smart grid due to uncoordinated charging on plug-in electric vehicles," in *Proc. IEEE PES Innovative Smart Grid Technologies (ISGT)*, Washington, DC, Jan. 2012, pp. 1-6.
[91] G.A. Putrus, P. Suwanapingkarl, D. Johnston, E.C. Bentley, and M. Narayana, "Impact of electric vehicles on power distribution networks," in *Proc. IEEE Vehicle Power and Propulsion Conference (VPPC)*, Dearborn, MI, Sep. 2009, pp. 827-831.
[92] (Sept. 14, 2016). *Monthly Plug-in Sales Scorecard*. Available: http://insideevs.com/monthly-plug-in-sales-scorecard/
[93] United States Environmental Protection Agency and United States Department of Energy. *Fuel Economy Estimates*. Available: http://www.fueleconomy.gov/feg/
[94] J. Axsen, H.J. Bailey, and G. Kamiya, "The Canadian plug-in electric vehicle survey (CPEVS 2013): anticipating purchase, use, and grid interactions in British Columbia," Energy and Materials Research Group, Burnaby, B.C., Oct. 31, 2013.
[95] Ontario Power Authority, "Bi-Weekly microFIT Report: Data as of March 18, 2016," 2016.
[96] J.W. Smith, R. Dugan, and W. Sunderman, "Distribution modeling and analysis of high penetration PV," in *Proc. IEEE PESGM*, San Diego, CA, 2011, pp. 1-7.
[97] S. Wilcox, "National Solar Radiation Database 1991-2010 Update: User's Manual," Aug. 2012.
[98] J. Pennsylvani, Maryland Power Pool (PJM). *Market for Electricity*. Available: http://learn.pjm.com/electricity-basics/market-for-electricity.aspx
[99] F. Meng, D. Haughton, B. Chowdhury, M.L. Crow, and G.T. Heydt, "Distributed generation and storage optimal control with state estimation," *IEEE Trans. Smart Grid*, vol. 4, pp. 2266-2273, Dec. 2013.

[100] Reactive Power Task Force, "Payments and Practices Associated with Reactive Power Ancillary Services Provided by Generation Resources," Dec. 12, 2003.
[101] M. Pipattansomporn, M. Willingham, and S. Rahman, "Implications of on-site distributed generation for commercial/industrial facilities," *IEEE Trans. Power Syst.*, vol. 20, pp. 206-212, Feb. 2005.
[102] Independent Electricity System Operator. (Mar. 2016). *Ontario's Supply Mix*. Available: http://www.ieso.ca/Pages/Ontario%27s-Power-System/Supply-Mix/default.aspx
[103] Ontario Energy Board. (May 2015). *Regulated Price Plan (RPP)*. Available: http://www.ontarioenergyboard.ca/oeb/Industry/Regulatory%20Proceedings/Policy%20Initiatives%20and%20Consultations/Regulated%20Price%20Plan
[104] Hydro One. *Time-Of-Use*. Available: http://www.hydroone.com/tou/Pages/Default.aspx
[105] Ontario Power Authority, "FIT/microFIT Price Schedule," 2016.
[106] A.L. Ott, "Experience with PJM market operation, system design, and implementation," *IEEE Trans. Power Syst.*, vol. 18, pp. 528-534, May 2003.
[107] G.T. Heydt, "The next generation of power distribution systems," *IEEE Trans. Smart Grid*, vol. 1, pp. 225-235, Dec. 2010.
[108] N. Steffan, "Applications and Calculation of a Distribution Class Locational Marginal Price," M. Sc, Arizona State University, May 2013.
[109] IEEE Distribution System Analysis Subcommittee. *Distribution Test Feeders*. Available: http://ewh.ieee.org/soc/pes/dsacom/testfeeders/
[110] Electric Reliability Council of Texas (ERCOT). *Market Prices*. Available: http://www.ercot.com/mktinfo/prices
[111] W.H. Kersting, *Distribution System Modeling and Analysis*, 3 ed., CRC Press, 2012.
[112] J.J. Grainger and W.D. Stevenson, *Power System Analysis*, McGraw-Hill, 1994.
[113] S. Talwar, M. Gray, and W.G. Morsi, "Application of directed bacterial foraging optimization for voltage collapse detection," in *Electrical Power and Energy Conference*, London, ON, 2015, pp. 402-407.
[114] S. Khushalani, J.M. Solanki, and N.N. Schulz, "Development of three-phase unbalanced power flow using PV and PQ models for distributed generation and study of the impact of DG models," *IEEE Trans. Power Syst.*, vol. 22, pp. 1019-1025, Aug. 2007.
[115] S.V. Kulkarni and S.A. Khaparde, *Transformer Engineering: Design, Technology, and Diagnostics*, 2 ed., London, New York: CRC Press, 2013.
[116] R. Vicini, O. Micheloud, H. Kumar, and A. Kwasinski, "Transformer and home energy management systems to lessen electrical vehicle impact on the grid," *IET Generation, Transmission & Distribution*, vol. 6, pp. 1202-1208, 2012.
[117] H.S. Hippert, C.E. Pedreira, and R.C. Souza, "Neural networks for short-term load forecasting: a review and evaluation," *IEEE Trans. Power Syst.*, vol. 16, pp. 44-55, Feb. 2001.
[118] D.C. Park, M.A. El-Sharkawi, R.J. Marks II, L.E. Atlas, and M.J. Damborg, "Electric load forecasting using an artificial neural network," *IEEE Trans. Power Syst.*, vol. 6, pp. 442-449, May 1991.

[119] MATLAB. (2010). *Electricity Load and Price Forecasting with MATLAB*. Available: http://www.mathworks.com/videos/electricity-load-and-price-forecasting-with-matlab-81765.html?s_iid=disc_rw_enp_bod
[120] R. Gardner, *Games for Business and Economics*, New York: Wiley, 1995.
[121] Tesla. *Powerwall Energy Storage for a Sustainable Home*. Available: https://www.tesla.com/en_CA/powerwall
[122] M. Wooldridge, *An Introduction to MultiAgent Systems*, England: Wiley, 2002.
[123] F. Perkonigg, D. Brujic, and M. Ristic, "Platform for multiagent application development incorporating accurate communications modeling," *IEEE Trans. Ind. Informat.*, vol. 11, pp. 728-736, Jun. 2015.
[124] F. Bellifemine, G. Caire, and D. Greenwood, *Developing Multi-Agent Systems with JADE*, England: Wiley, 2007.
[125] Foundation for Intelligent Physical Agents. *FIPA Agent Message Transport Envelope Representation in XML Specification*. Available: http://www.fipa.org/specs/fipa00085/SC00085J.html
[126] Foundation for Intelligent Physical Agents. *FIPA Communicative Act Library Specification*. Available: http://www.fipa.org/specs/fipa00037/SC00037J.html
[127] S. Boyd and L. Vandenberghe, *Convex Optimization*, Cambridge University Press, 7 ed., 2009.
[128] MathWorks. *Documentation: linprog*. Available: http://www.mathworks.com/help/optim/ug/linprog.html
[129] S. Bruno, S. Lamonaca, G. Rotondo, U. Stecchi, and M.L. Scala, "Unbalanced three-phase optimal power flow for smart grids," *IEEE Trans. Ind. Electron.*, vol. 58, pp. 4504-4513, Oct. 2011.
[130] C. Brezinski, "A classification of quasi-Newton methods," *Numerical Algorithms*, vol. 33, pp. 123-135, 2003.
[131] MathWorks. *Constrained Nonlinear Optimization Algorithms*. Available: http://www.mathworks.com/help/optim/ug/constrained-nonlinear-optimization-algorithms.html
[132] Independent Electricity System Operator. *Day-Ahead Commitment Process*. Available: http://www.ieso.ca/Pages/Participate/Markets-and-Programs/Day-Ahead-Commitment-Process.aspx
[133] Z. Wang and J. Wang, "Self-healing resilient distribution systems based on sectionalization into Microgrids," *IEEE Trans. Power Syst.*, vol. 30, pp. 3139-3149, Nov. 2015.
[134] S. Dahal and H. Salehfar, "Impact of distributed generators in the power loss and voltage profile of three phase unbalanced distribution network," *Elect. Power Energy Syst.*, vol. 77, pp. 256-262, 2016.
[135] J.A. Jardini, C.M.V. Tahan, M.R. Gouvea, and A. Se Un, "Daily load profiles for residential, commercial and industrial low voltage consumers," *IEEE Trans. Power Del.*, vol. 15, pp. 375-380, 2000.
[136] The Institute of Electrical Engineers of Japan. (2012). *Japanese Power System Models*. Available: http://www2.iee.or.jp/ver2/pes/23-st_model/english/index.html

[137] C.A. Burk, J.L. Bala, and J.Z. Gibson, "Electric secondary distribution system design," in *Proc. North American Power Symposium*, Las Cruces, New Mexico, 2007, pp. 582-588.
[138] J.Z. Gibson, J.L. Bala, and C.A. Burk, "Electric secondary distribution modeling and laod characterization," in *Proc. North American Power Symposium*, Las Cruces, New Mexico, 2007, pp. 575-581.
[139] J. Bishop, "Profiles on Residential Power Consumption," Fire Protection Research Foundation, Quincy, MA, USA, Mar. 2010.
[140] Baltimore Gas and Electric Company. (Sept. 2014). *Load Profiles*. Available: https://supplier.bge.com/electric/load/profiles.asp
[141] Baltimore Gas and Electric Company. (Sept. 2014). *Electric Customer Segmentation*. Available: https://supplier.bge.com/documents/index.asp#all
[142] National Renewable Energy Laboratory. (Aug. 2012). *National Solar Radiation Database (NSRDB)*. Available: https://nsrdb.nrel.gov/

Appendix A Sample Calculation of Payout to Secondary System for ESS Rescheduling

In order to perform peak-to-average power reduction (PAPR), the distribution system operator must request the rescheduling of energy storage system profiles on residential customers with energy storage systems. As residential customers control the charging and discharging of electrical energy to minimize their energy bill by charging during low electricity prices and discharging during high electricity pricing, any rescheduling on behalf of the electric utility results in economic loss to the residential customer. To incentivize the residential customer to accept a request by the DSO to perform energy storage rescheduling, game theory states that the electric utility must offer the residential customer a payment to perform the action which is equal to (or greater than) the economic loss the residential customer would incur through performing the residential ESS rescheduling action.

To exemplify the means of calculating residential customer payouts for ESS rescheduling action, the following scenario is considered. A 6 house secondary system extending from IEEE 123 Bus Test Distribution System node 114 has 100% PEV penetration, 100% PV penetration, and 3.2kW/6.4kWh storage at each house assuming no energy storage efficiency losses for simplicity, with house load profiles given in Table A.1, assuming 0.9 lagging power factor, based on the forecasted load for September 1, 2010 determined in Section 5.4. Similarly, forecasted PEV and PV profiles for the day of September 1, 2010 are outlined in Table A.2 and Table A.3 following the methodology defined in Section 3.4 and Section 3.5 respectively.

Table A.1 Forecasted House Load Profiles for 6 House Secondary System

Hour of Day	House 1 Load (kVA)	House 2 Load (kVA)	House 3 Load (kVA)	House 4 Load (kVA)	House 5 Load (kVA)	House 6 Load (kVA)
1	4.99	1.59	1.84	2.02	3.11	3.44
2	5.04	1.36	1.65	1.79	3.01	3.32
3	4.96	1.28	1.52	1.57	2.89	3.25
4	5.01	1.23	1.45	1.46	2.85	3.30
5	4.99	1.22	1.32	1.54	2.80	3.41
6	5.24	1.36	1.36	1.62	2.93	3.62
7	5.04	1.76	1.49	2.02	3.14	4.07
8	4.79	1.80	1.65	2.42	3.49	4.72
9	4.95	1.82	1.67	2.37	3.85	5.18
10	5.31	1.74	1.91	2.32	4.57	5.49
11	5.76	1.98	2.16	2.60	5.49	5.48
12	6.25	2.27	2.64	2.80	5.87	5.65
13	6.39	2.55	3.14	3.11	6.05	5.63
14	5.92	2.76	3.44	3.15	6.16	5.67
15	5.80	2.87	4.01	3.42	6.18	5.75
16	5.78	3.05	4.34	3.73	6.11	5.74
17	5.87	3.25	4.55	4.05	5.90	5.51
18	5.82	3.71	4.65	4.15	5.48	5.27
19	5.73	3.81	4.38	4.21	5.13	4.98
20	6.09	3.60	4.22	4.23	4.83	4.68
21	6.43	3.49	3.85	4.10	4.49	4.40
22	6.18	3.34	3.61	4.00	4.36	4.24
23	5.78	2.85	3.33	3.51	3.94	3.79
24	5.39	2.29	2.65	2.72	3.42	3.51

Table A.2 Forecasted PEV Charging Profiles for 6 House Secondary System

Hour of Day	House 1 EV Load (kW)	House 2 EV Load (kW)	House 3 EV Load (kW)	House 4 EV Load (kW)	House 5 EV Load (kW)	House 6 EV Load (kW)
1	0.00	0.00	0.00	0.00	0.00	0.00
2	0.00	0.00	0.00	0.00	0.00	0.00
3	0.00	0.00	0.00	0.00	0.00	0.00
4	0.00	0.00	0.00	0.00	0.00	0.00
5	0.00	0.00	0.00	0.00	0.00	0.00
6	0.00	0.00	0.00	0.00	0.00	0.00
7	0.00	0.00	0.00	0.00	0.00	0.00
8	0.00	0.00	0.00	0.00	0.00	0.00
9	0.00	3.40	0.00	0.00	0.00	0.00
10	0.00	0.00	0.00	0.00	0.00	0.00
11	0.00	0.00	0.00	0.00	0.00	0.00
12	0.00	0.00	0.00	0.00	0.00	0.00
13	0.00	0.00	0.00	0.00	0.00	0.00
14	0.00	0.00	0.00	0.00	0.00	0.00
15	0.00	0.00	0.00	0.00	0.00	0.00
16	0.00	0.00	0.00	0.00	0.00	0.00
17	0.00	0.00	0.00	0.00	0.00	0.00
18	0.00	0.00	0.00	0.00	0.00	0.00
19	0.00	0.00	6.60	0.00	0.00	3.23
20	0.00	0.00	4.12	0.00	0.00	0.00
21	6.59	0.00	0.00	0.00	0.00	0.00
22	2.42	0.00	0.00	0.00	6.60	0.00
23	0.00	0.00	0.00	4.42	3.61	0.00
24	0.00	0.00	0.00	0.00	0.00	0.00

Table A.3 Forecasted Rooftop Solar PV Generation Profiles

Hour of Day	House 1 PV Gen. (kW)	House 2 PV Gen. (kW)	House 3 PV Gen. (kW)	House 4 PV Gen. (kW)	House 5 PV Gen. (kW)	House 6 PV Gen. (kW)
1	0.00	0.00	0.00	0.00	0.00	0.00
2	0.00	0.00	0.00	0.00	0.00	0.00
3	0.00	0.00	0.00	0.00	0.00	0.00
4	0.00	0.00	0.00	0.00	0.00	0.00
5	0.00	0.00	0.00	0.00	0.00	0.00
6	0.00	0.00	0.00	0.00	0.00	0.00
7	0.00	0.00	0.00	0.00	0.00	0.00
8	2.29	2.29	2.29	2.29	2.29	2.29
9	3.64	3.64	3.64	3.64	3.64	3.64
10	4.78	4.78	4.78	4.78	4.78	4.78
11	5.57	5.57	5.57	5.57	5.57	5.57
12	5.94	5.94	5.94	5.94	5.94	5.94
13	5.70	5.70	5.70	5.70	5.70	5.70
14	5.32	5.32	5.32	5.32	5.32	5.32
15	4.67	4.67	4.67	4.67	4.67	4.67
16	3.61	3.61	3.61	3.61	3.61	3.61
17	1.88	1.88	1.88	1.88	1.88	1.88
18	0.00	0.00	0.00	0.00	0.00	0.00
19	0.00	0.00	0.00	0.00	0.00	0.00
20	0.00	0.00	0.00	0.00	0.00	0.00
21	0.00	0.00	0.00	0.00	0.00	0.00
22	0.00	0.00	0.00	0.00	0.00	0.00
23	0.00	0.00	0.00	0.00	0.00	0.00
24	0.00	0.00	0.00	0.00	0.00	0.00

Assuming all residential ESS are fully charged initially and in the case residential customers are billed for energy based on time-of-use pricing given in Table A.4, the resultant residential ESS charging/discharging profiles to optimize residential ESS owner savings, as optimized for maximum savings (5.25) outlined in Section 5.5.1, are given in Table A.5, where discharging is given as a positive value and charging values are negative.

Table A.4 Time of Use Pricing for 6 House Secondary System

Hour of Day	Price (¢/kWh)	Hour of Day	Price (¢/kWh)	Hour of Day	Price (¢/kWh)
1	8.70	9	13.20	17	13.20
2	8.70	10	13.20	18	13.20
3	8.70	11	18.00	19	8.70
4	8.70	12	18.00	20	8.70
5	8.70	13	18.00	21	8.70
6	8.70	14	18.00	22	8.70
7	13.20	15	18.00	23	8.70
8	13.20	16	18.00	24	8.70

By calculating the savings on the energy bill for each customer based on (A.1), as a function of the cost of energy c_t at each time interval t and the power charge/discharged by each residential ESS e, it may be seen that each residential customer may expect to find a reduction of 59.52¢.

$$\text{Savings} = \sum_{t=1}^{24} \left(c_t \cdot P_t^e \right) \tag{A.1}$$

After residential home energy management systems communicate the intended residential ESS charging/discharging profiles of Table A.5 to the electric utility, the electric utility then determines loss of life of the secondary transformer, considering an average ambient temperature of 27.60°C, as 0.02315%. As the forecasted transformer loss of life exceeds the daily loss of life limit of 0.01333%, the electric utility must take corrective action using transactive control, to maintain transformer loss of life within the daily limit.

In order to minimize the distribution transformer's loss of life, the electric utility requires residential ESS profiles to charge and discharge according to the results of PAPR optimization (5.28), defined in Section 5.5.1. The resultant charging and discharging profiles for each

residential ESS in the 6 house secondary system is outlined in Table A.6. Given the new residential ESS charging/discharging profiles, the resultant expected distribution transformer loss of life is 0.0003%, which ensures the distribution transformer experiences loss of life below the maximum daily limit.

Table A.5 Residential ESS Profile for Maximum Savings for Sample Day [a]

Hour of Day	House 1 ESS (kW)	House 2 ESS (kW)	House 3 ESS (kW)	House 4 ESS (kW)	House 5 ESS (kW)	House 6 ESS (kW)
1	0.00	0.00	0.00	0.00	0.00	0.00
2	0.00	0.00	0.00	0.00	0.00	0.00
3	0.00	0.00	0.00	0.00	0.00	0.00
4	0.00	0.00	0.00	0.00	0.00	0.00
5	0.00	0.00	0.00	0.00	0.00	0.00
6	0.00	0.00	0.00	0.00	0.00	0.00
7	0.00	0.00	0.00	0.00	0.00	0.00
8	0.00	0.00	0.00	0.00	0.00	0.00
9	0.00	0.00	0.00	0.00	0.00	0.00
10	0.00	0.00	0.00	0.00	0.00	0.00
11	0.00	0.00	0.00	0.00	0.00	0.00
12	0.00	0.00	0.00	0.00	0.00	0.00
13	-3.20	-3.20	-3.20	-3.20	-3.20	-3.20
14	0.00	0.00	0.00	0.00	0.00	0.00
15	-3.20	-3.20	-3.20	-3.20	-3.20	-3.20
16	0.00	0.00	0.00	0.00	0.00	0.00
17	0.00	0.00	0.00	0.00	0.00	0.00
18	0.00	0.00	0.00	0.00	0.00	0.00
19	0.00	0.00	0.00	0.00	0.00	0.00
20	0.00	0.00	0.00	0.00	0.00	0.00
21	0.00	0.00	0.00	0.00	0.00	0.00
22	0.00	0.00	0.00	0.00	0.00	0.00
23	3.20	3.20	3.20	3.20	3.20	3.20
24	3.20	3.20	3.20	3.20	3.20	3.20

[a] Negative values are considered discharging and positive values are charging

Table A.6 Residential ESS Profile for PAPR Minimization for Sample Day [a]

Hour of Day	House 1 ESS (kW)	House 2 ESS (kW)	House 3 ESS (kW)	House 4 ESS (kW)	House 5 ESS (kW)	House 6 ESS (kW)
1	0.00	0.00	0.00	0.00	0.00	0.00
2	0.00	0.00	0.00	0.00	0.00	0.00
3	-0.09	0.00	0.00	0.00	0.00	0.00
4	-0.24	0.00	0.00	0.00	0.00	0.00
5	-0.26	0.00	0.00	0.00	0.00	0.00
6	0.58	0.00	0.00	0.00	0.00	0.00
7	0.00	0.00	0.00	0.00	0.00	0.00
8	0.00	0.00	0.00	0.00	0.00	0.00
9	0.00	0.00	0.00	0.00	0.00	0.00
10	0.00	0.00	-0.06	-1.28	-1.28	-1.28
11	-1.31	-2.01	-1.59	-1.28	-1.28	-1.28
12	-3.12	-2.01	-1.59	-1.28	-1.28	-1.28
13	-1.97	-2.01	-1.59	-1.28	-1.28	-1.28
14	0.00	-0.36	-1.59	-1.28	-1.28	-1.28
15	0.00	0.00	0.00	0.00	0.00	0.00
16	0.00	0.00	0.00	0.00	0.00	0.00
17	0.00	0.00	0.00	0.00	0.00	0.00
18	0.00	0.00	0.00	0.00	0.00	0.00
19	3.20	3.20	1.69	1.28	1.28	1.28
20	-0.46	1.05	1.18	1.28	1.28	1.28
21	1.15	1.05	1.18	1.28	1.28	1.28
22	2.51	1.05	1.18	1.28	1.28	1.28
23	0.00	0.04	1.18	1.28	1.28	1.28
24	0.00	0.00	0.00	0.00	0.00	0.00

[a] Negative values are considered discharging and positive values are charging

Table A.7 shows the resultant energy bill savings for each residential home in the 6 house secondary system, considering both the maximum savings and PAPR residential ESS scheduling profiles. As outlined using the ultimatum offer of game theory, in Section 5.5.2, the electric utility must bid to each residential home a financial offer equivalent to (or greater than) that which would be lost in energy bill savings for the residential customer to operate their ESS under the electric utilities requested profile. As each residential homeowner is offered a value of equal financial worth to their losses, the residential homeowner does not incur financial loss

by accepting the ultimatum, and therefore accepts the electric utilities bid to charge and discharge their ESS based on the electric utilities requested profile provided. For the example outlined in this Appendix, the resultant cost to the electric utility is the sum of all bids paid out to all residential customers, which sums to 18.69¢, or $0.19 for this given scenario, under time of use pricing.

Table A.7 Residential ESS Profile Savings for TOU Pricing

House	Energy Cost Savings for Maximum Savings (¢)	Energy Cost Savings for PAPR (¢)	Electric Utility Bid for Rescheduling (¢)
1	59.52	59.52	0.00
2	59.52	59.52	0.00
3	59.52	59.25	0.27
4	59.52	53.38	6.14
5	59.52	53.38	6.14
6	59.52	53.38	6.14
Total	357.12	338.43	18.69

In a similar scenario, retaining the house load profile values, PEV charging values, and rooftop solar PV generation profiles in Table A.1, Table A.2, and Table A.3 respectively, the resultant DLMP pricing for September 1 2010 is given in Table A.8.

Assuming all residential ESS are fully charged, the resultant residential ESS charging/discharging profiles to optimize residential ESS owner savings for the DLMP profile in Table A.8 based on maximum savings (5.25) outlined in Section 5.5.1, are given in Table A.9, where discharging is given as a positive value and charging negative.

Table A.8 DLMP for 6 House Secondary System

Hour of Day	Price (¢/kWh)	Hour of Day	Price (¢/kWh)	Hour of Day	Price (¢/kWh)
1	2.89	9	2.99	17	9.02
2	2.60	10	2.74	18	5.68
3	2.61	11	3.34	19	4.82
4	2.52	12	3.32	20	4.73
5	2.46	13	3.83	21	4.48
6	2.51	14	4.45	22	3.53
7	2.76	15	4.90	23	3.50
8	2.68	16	6.92	24	3.17

Similarly to the time-of-use pricing case, energy bill savings for each customer may be calculated using (A.1), such that for the example scenario each residential customer may expect to find a reduction of 32.49¢. Upon calculation of the distribution transformer loss of life, with ambient temperature of 27.60°C, it is found that the distribution transformer exceeds loss of life limits, with a value of 0.0218%.

Following PAPR optimization (5.28), defined in Section 5.5.1, the resultant charging and discharging profiles for each residential ESS in the 6 house secondary system considering DLMP energy billing rates is outlined in Table A.10. A comparison of Table A.6 and A.10 reveals identical ESS profiles for PAPR under both time-of-use and DLMP pricing schemes. As the formula for peak-to-average power reduction does not include economic considerations, it is expected that the electric utility may minimize peak-to-average power in both TOU and DLMP examples using the same optimal profiles.

Table A.9 Residential ESS Profile for Maximum Savings[a]

Hour of Day	House 1 ESS (kW)	House 2 ESS (kW)	House 3 ESS (kW)	House 4 ESS (kW)	House 5 ESS (kW)	House 6 ESS (kW)
1	-3.20	-3.20	-3.20	-3.20	-3.20	-3.20
2	0.00	0.00	0.00	0.00	0.00	0.00
3	-3.20	-3.20	-3.20	-3.20	-3.20	-3.20
4	0.00	0.00	0.00	0.00	0.00	0.00
5	3.20	3.20	3.20	3.20	3.20	3.20
6	3.20	3.20	3.20	3.20	3.20	3.20
7	-3.20	-3.20	-3.20	-3.20	-3.20	-3.20
8	3.20	3.20	3.20	3.20	3.20	3.20
9	-3.20	-3.20	-3.20	-3.20	-3.20	-3.20
10	3.20	3.20	3.20	3.20	3.20	3.20
11	-3.20	-3.20	-3.20	-3.20	-3.20	-3.20
12	3.20	3.20	3.20	3.20	3.20	3.20
13	0.00	0.00	0.00	0.00	0.00	0.00
14	0.00	0.00	0.00	0.00	0.00	0.00
15	0.00	0.00	0.00	0.00	0.00	0.00
16	-3.20	-3.20	-3.20	-3.20	-3.20	-3.20
17	-3.20	-3.20	-3.20	-3.20	-3.20	-3.20
18	0.00	0.00	0.00	0.00	0.00	0.00
19	0.00	0.00	0.00	0.00	0.00	0.00
20	0.00	0.00	0.00	0.00	0.00	0.00
21	0.00	0.00	0.00	0.00	0.00	0.00
22	0.00	0.00	0.00	0.00	0.00	0.00
23	3.20	3.20	3.20	3.20	3.20	3.20
24	3.20	3.20	3.20	3.20	3.20	3.20

[a] Negative values are considered discharging and positive values are charging

Given the new ESS profiles, the resultant expected distribution transformer loss of life is 0.0003%, similarly seen in TOU pricing, which again ensures the distribution transformer experiences loss of life below the maximum daily limit.

Table A.11 shows the resultant energy bill savings for each residential home in the 6 house secondary system, considering both the maximum savings and PAPR ESS scheduling profiles in the case of DLMP pricing given in Table A.8. A comparison of the costs to the electric utility in TOU pricing and DLMP pricing may be made through consideration of Table

A.7 and A.11 for TOU and DLMP pricing respectively. On comparison of Table A.7 and Table A.11 it may be seen that savings for customers are larger under TOU pricing scheme versus the DLMP pricing in Table A.8. As the difference in pricing between on-peak and off-peak times under time-of-use prices are larger than the price differences seen in DLMP pricing, it is given that customers may save more money by charging and discharging each kilowatt-hour of energy. While time-of-use pricing results in larger price differences between the highest price and lowest price for electricity, DLMP pricing offers consumers more opportunities to charge and discharge to result in energy bill savings, which may be seen on inspection of ESS profiles for DLMP pricing in Table A.9.

Finally, it may be seen that electric utility peak-to-average power reduction, as a means of reducing transformer loss of life, is more costly in the case of DLMP pricing than TOU pricing. The cost to the utility to perform PAPR reduction by bidding to each residential ESS owner a cost equal to its lost revenue is found to be larger in the case of DLMP than TOU pricing, as the charging and discharging times for minimum PAPR have resulted in significant reduction in savings to the consumer requiring larger bids by the DSO for PAPR minimization than in the TOU pricing case. Such comparative pricing results between DLMP and TOU residential customer pricing schemes are highly dependent on the DLMP, which varies in profile and magnitude for each day of the year.

Table A.10 Residential ESS Profile for PAPR Minimization

Hour of Day	House 1 ESS (kW)	House 2 ESS (kW)	House 3 ESS (kW)	House 4 ESS (kW)	House 5 ESS (kW)	House 6 ESS (kW)
1	0.00	0.00	0.00	0.00	0.00	0.00
2	0.00	0.00	0.00	0.00	0.00	0.00
3	-0.09	0.00	0.00	0.00	0.00	0.00
4	-0.24	0.00	0.00	0.00	0.00	0.00
5	-0.26	0.00	0.00	0.00	0.00	0.00
6	0.58	0.00	0.00	0.00	0.00	0.00
7	0.00	0.00	0.00	0.00	0.00	0.00
8	0.00	0.00	0.00	0.00	0.00	0.00
9	0.00	0.00	0.00	0.00	0.00	0.00
10	0.00	0.00	-0.06	-1.28	-1.28	-1.28
11	-1.31	-2.01	-1.59	-1.28	-1.28	-1.28
12	-3.12	-2.01	-1.59	-1.28	-1.28	-1.28
13	-1.97	-2.01	-1.59	-1.28	-1.28	-1.28
14	0.00	-0.36	-1.59	-1.28	-1.28	-1.28
15	0.00	0.00	0.00	0.00	0.00	0.00
16	0.00	0.00	0.00	0.00	0.00	0.00
17	0.00	0.00	0.00	0.00	0.00	0.00
18	0.00	0.00	0.00	0.00	0.00	0.00
19	3.20	3.20	1.69	1.28	1.28	1.28
20	-0.46	1.05	1.18	1.28	1.28	1.28
21	1.15	1.05	1.18	1.28	1.28	1.28
22	2.51	1.05	1.18	1.28	1.28	1.28
23	0.00	0.04	1.18	1.28	1.28	1.28
24	0.00	0.00	0.00	0.00	0.00	0.00

Table A.11 Residential ESS Profile Savings for DLMP Pricing

House	Energy Cost Savings for Maximum Savings (¢)	Energy Cost Savings for PAPR (¢)	Electric Utility Bid for Rescheduling (¢)
1	32.49	4.98	27.51
2	32.49	6.24	26.25
3	32.49	3.40	29.09
4	32.49	4.31	28.18
5	32.49	4.31	28.18
6	32.49	4.31	28.18
Total	194.94	27.55	167.39

Appendix B IEEE 123-Bus Standard Test Distribution System Data

Table B.1 Line Segment Data

Node A	Node B	Length (ft.)	Config.
1	2	175	10
1	3	250	11
1	7	300	1
3	4	200	11
3	5	325	11
5	6	250	11
7	8	200	1
8	12	225	10
8	9	225	9
8	13	300	1
9	14	425	9
13	34	150	11
13	18	825	2
14	11	250	9
14	10	250	9
15	16	375	11
15	17	350	11
18	19	250	9
18	21	300	2
19	20	325	9
21	22	525	10
21	23	250	2
23	24	550	11
23	25	275	2
25	26	350	7
25	28	200	2
26	27	275	7
26	31	225	11
27	33	500	9
28	29	300	2
29	30	350	2
30	250	200	2
31	32	300	11
34	15	100	11
35	36	650	8
35	40	250	1
36	37	300	9

Table B.1 Line Segment Data (Continued)

Node A	Node B	Length (ft.)	Config.
36	38	250	10
38	39	325	10
40	41	325	11
40	42	250	1
42	43	500	10
42	44	200	1
44	45	200	9
44	47	250	1
45	46	300	9
47	48	150	4
47	49	250	4
49	50	250	4
50	51	250	4
51	151	500	4
52	53	200	1
53	54	125	1
54	55	275	1
54	57	350	3
55	56	275	1
57	58	250	10
57	60	750	3
58	59	250	10
60	61	550	5
60	62	250	12
62	63	175	12
63	64	350	12
64	65	425	12
65	66	325	12
67	68	200	9
67	72	275	3
67	97	250	3
68	69	275	9
69	70	325	9
70	71	275	9
72	73	275	11
72	76	200	3
73	74	350	11
74	75	400	11
76	77	400	6
76	86	700	3

Table B.1 Line Segment Data (Continued)

Node A	Node B	Length (ft.)	Config.
77	78	100	6
78	79	225	6
78	80	475	6
80	81	475	6
81	82	250	6
81	84	675	11
82	83	250	6
84	85	475	11
86	87	450	6
87	88	175	9
87	89	275	6
89	90	225	10
89	91	225	6
91	92	300	11
91	93	225	6
93	94	275	9
93	95	300	6
95	96	200	10
97	98	275	3
98	99	550	3
99	100	300	3
100	450	800	3
101	102	225	11
101	105	275	3
102	103	325	11
103	104	700	11
105	106	225	10
105	108	325	3
106	107	575	10
108	109	450	9
108	300	1000	3
109	110	300	9
110	111	575	9
110	112	125	9
112	113	525	9
113	114	325	9
135	35	375	4
149	1	400	1
152	52	400	1
160	67	350	6

Table B.1 Line Segment Data (Continued)

Node A	Node B	Length (ft.)	Config.
197	101	250	3

Table B.2 Overhead Line Configuration Data

Config.	Phasing	Phase Conductor (ACSR)	Neutral Conductor (ACSR)
1	A B C N	336,400 26/7	4/0 6/1
2	C A B N	336,400 26/7	4/0 6/1
3	B C A N	336,400 26/7	4/0 6/1
4	C B A N	336,400 26/7	4/0 6/1
5	B A C N	336,400 26/7	4/0 6/1
6	A C B N	336,400 26/7	4/0 6/1
7	A C N	336,400 26/7	4/0 6/1
8	A B N	336,400 26/7	4/0 6/1
9	A N	1/0	1/0
10	B N	1/0	1/0
11	C N	1/0	1/0

Table B.3 Underground Line Configuration Data

Config.	Phasing	Cable
12	A B C	1/0 AA, CN

Table B.4 Transformer Data

Transformer	kVA	kV - high	kV - Low	R(%)	X(%)
Substation	5,000	115-D	4.16-Gr.Y	1.00	8.00
XFM-1	150	4.16-D	0.48-D	1.27	2.72

Table B.5 Three Phase Switch Positions and Status

Node A	Node B	Normal Position
13	152	Closed
18	135	Closed
60	160	Closed
61	610	Closed
97	197	Closed
150	149	Closed
250	251	Open
450	451	Open
54	94	Open
151	300	Open
300	350	Open

Table B.6 Shunt Capacitor Data

Node	Phase A (kVAR)	Phase B (kVAR)	Phase C (kVAR)
83	200	200	200
88	50	0	0
90	0	50	0
92	0	0	50

Table B.7 Regulator Data

ID	Line Segment	Node	Phase	Bandwidth (V)	PT Ratio	Primary CT Rating	R	X	Voltage Level
1	150-149	150	A	2	20	700	3.0	7.5	120
2	9-14	9	A	2	20	50	0.4	0.4	120
3-A	25-26	25	A	1	20	50	0.4	0.4	120
3-C	25-26	25	C	1	20	50	0.4	0.4	120
4-A	160-67	160	A	2	20	300	0.6	1.3	124
4-B	160-67	160	B	2	20	300	1.4	2.6	124
4-C	160-67	160	C	2	20	300	0.2	1.4	124

Table B.8 Spot Load Data

Node	Load Model	Phase 1 kW	Phase 1 kVAR	Phase 2 kW	Phase 2 kVAR	Phase 3 kW	Phase 3 kVAR
1	Y-PQ	40	20	0	0	0	0
2	Y-PQ	0	0	20	10	0	0
4	Y-PR	0	0	0	0	40	20
5	Y-I	0	0	0	0	20	10
6	Y-Z	0	0	0	0	40	20
7	Y-PQ	20	10	0	0	0	0
9	Y-PQ	40	20	0	0	0	0
10	Y-I	20	10	0	0	0	0
11	Y-Z	40	20	0	0	0	0
12	Y-PQ	0	0	20	10	0	0
16	Y-PQ	0	0	0	0	40	20
17	Y-PQ	0	0	0	0	20	10
19	Y-PQ	40	20	0	0	0	0
20	Y-I	40	20	0	0	0	0
22	Y-Z	0	0	40	20	0	0
24	Y-PQ	0	0	0	0	40	20
28	Y-I	40	20	0	0	0	0
29	Y-Z	40	20	0	0	0	0
30	Y-PQ	0	0	0	0	40	20
31	Y-PQ	0	0	0	0	20	10
32	Y-PQ	0	0	0	0	20	10
33	Y-I	40	20	0	0	0	0
34	Y-Z	0	0	0	0	40	20
35	D-PQ	40	20	0	0	0	0
37	Y-Z	40	20	0	0	0	0
38	Y-I	0	0	20	10	0	0
39	Y-PQ	0	0	20	10	0	0
41	Y-PQ	0	0	0	0	20	10
42	Y-PQ	20	10	0	0	0	0
43	Y-Z	0	0	40	20	0	0
45	Y-I	20	10	0	0	0	0
46	Y-PQ	20	10	0	0	0	0
47	Y-I	35	25	35	25	35	25
48	Y-Z	70	50	70	50	70	50
49	Y-PQ	35	25	70	50	35	20
50	Y-PQ	0	0	0	0	40	20
51	Y-PQ	20	10	0	0	0	0
52	Y-PQ	40	20	0	0	0	0
53	Y-PQ	40	20	0	0	0	0

Table B.8 Spot Load Data (Continued)

Node	Load Model	Phase 1 kW	Phase 1 kVAR	Phase 2 kW	Phase 2 kVAR	Phase 3 kW	Phase 3 kVAR
55	Y-Z	20	10	0	0	0	0
56	Y-PQ	0	0	20	10	0	0
58	Y-I	0	0	20	10	0	0
59	Y-PQ	0	0	20	10	0	0
60	Y-PQ	20	10	0	0	0	0
62	Y-Z	0	0	0	0	40	20
63	Y-PQ	40	20	0	0	0	0
64	Y-I	0	0	75	35	0	0
65	D-Z	35	25	35	25	70	50
66	Y-PQ	0	0	0	0	75	35
68	Y-PQ	20	10	0	0	0	0
69	Y-PQ	40	20	0	0	0	0
70	Y-PQ	20	10	0	0	0	0
71	Y-PQ	40	20	0	0	0	0
73	Y-PQ	0	0	0	0	40	20
74	Y-Z	0	0	0	0	40	20
75	Y-PQ	0	0	0	0	40	20
76	D-I	105	80	70	50	70	50
77	Y-PQ	0	0	40	20	0	0
79	Y-Z	40	20	0	0	0	0
80	Y-PQ	0	0	40	20	0	0
82	Y-PQ	40	20	0	0	0	0
83	Y-PQ	0	0	0	0	20	10
84	Y-PQ	0	0	0	0	20	10
85	Y-PQ	0	0	0	0	40	20
86	Y-PQ	0	0	20	10	0	0
87	Y-PQ	0	0	40	20	0	0
88	Y-PQ	40	20	0	0	0	0
90	Y-I	0	0	40	20	0	0
92	Y-PQ	0	0	0	0	40	20
94	Y-PQ	40	20	0	0	0	0
95	Y-PQ	0	0	20	10	0	0
96	Y-PQ	0	0	20	10	0	0
98	Y-PQ	40	20	0	0	0	0
99	Y-PQ	0	0	40	20	0	0
100	Y-Z	0	0	0	0	40	20
102	Y-PQ	0	0	0	0	20	10
103	Y-PQ	0	0	0	0	40	20
104	Y-PQ	0	0	0	0	40	20

Table B.8 Spot Load Data (Continued)

Node	Load Model	Phase 1 kW	Phase 1 kVAR	Phase 2 kW	Phase 2 kVAR	Phase 3 kW	Phase 3 kVAR
106	Y-PQ	0	0	40	20	0	0
107	Y-PQ	0	0	40	20	0	0
109	Y-PQ	40	20	0	0	0	0
111	Y-PQ	20	10	0	0	0	0
112	Y-I	20	10	0	0	0	0
113	Y-Z	40	20	0	0	0	0
114	Y-PQ	20	10	0	0	0	0

Line Configuration Impedances

Line Configuration 1:

$$z = \begin{bmatrix} 0.4576 + j1.0780 & 0.1560 + j0.5017 & 0.1535 + j0.3849 \\ & 0.4666 + j1.0482 & 0.1580 + j0.4236 \\ & & 0.4615 + j1.0651 \end{bmatrix} \Omega / mile$$

$$b = \begin{bmatrix} 5.6765 & -1.8319 & -0.6982 \\ & 5.9809 & -1.1645 \\ & & 5.3971 \end{bmatrix} \mu S / mile$$

Line Configuration 2:

$$z = \begin{bmatrix} 0.4666 + j1.0482 & 0.1580 + j0.4236 & 0.1560 + j0.5017 \\ & 0.4615 + j1.0651 & 0.1535 + j0.3849 \\ & & 0.4576 + j1.0780 \end{bmatrix} \Omega / mile$$

$$b = \begin{bmatrix} 5.9809 & -1.1645 & -1.8319 \\ & 5.3971 & -0.6982 \\ & & 5.6765 \end{bmatrix} \mu S / mile$$

Line Configuration 3:

$$z = \begin{bmatrix} 0.4615 + j1.0651 & 0.1535 + j0.3849 & 0.1580 + j0.4236 \\ & 0.4576 + j1.0780 & 0.1560 + j0.5017 \\ & & 0.4666 + j1.0482 \end{bmatrix} \Omega / mile$$

$$b = \begin{bmatrix} 5.3971 & -0.6982 & -1.1645 \\ & 5.6765 & -1.8319 \\ & & 5.9809 \end{bmatrix} \mu S / mile$$

Line Configuration 4:

$$z = \begin{bmatrix} 0.4615 + j1.0651 & 0.1580 + j0.4236 & 0.1535 + j0.3849 \\ & 0.4666 + j1.0482 & 0.1560 + j0.5017 \\ & & 0.4576 + j1.0780 \end{bmatrix} \Omega / mile$$

$$b = \begin{bmatrix} 5.3971 & -1.1645 & -0.6982 \\ & 5.9809 & -1.8319 \\ & & 5.6765 \end{bmatrix} \mu S / mile$$

Line Configuration 5:

$$z = \begin{bmatrix} 0.4666 + j1.0482 & 0.1560 + j0.5017 & 0.1580 + j0.4236 \\ & 0.4576 + j1.0780 & 0.1535 + j0.3849 \\ & & 0.4615 + j1.0651 \end{bmatrix} \Omega / mile$$

$$b = \begin{bmatrix} 5.9809 & -1.8319 & -1.1645 \\ & 5.6765 & -0.6982 \\ & & 5.3971 \end{bmatrix} \mu S / mile$$

Line Configuration 6:

$$z = \begin{bmatrix} 0.4576 + j1.0780 & 0.1535 + j0.3849 & 0.1560 + j0.5017 \\ & 0.4615 + j1.0651 & 0.1580 + j0.4236 \\ & & 0.4666 + j1.0482 \end{bmatrix} \Omega / mile$$

$$b = \begin{bmatrix} 5.6765 & -0.6982 & -1.8319 \\ & 5.3971 & -1.1645 \\ & & 5.9809 \end{bmatrix} \mu S / mile$$

Line Configuration 7:

$$z = \begin{bmatrix} 0.4576 + j1.0780 & 0.0000 + j0.0000 & 0.1535 + j0.3849 \\ & 0.0000 + j0.0000 & 0.0000 + j0.0000 \\ & & 0.4615 + j1.0651 \end{bmatrix} \Omega / mile$$

$$b = \begin{bmatrix} 5.1154 & 0.0000 & -1.0549 \\ & 0.0000 & 0.0000 \\ & & 5.1704 \end{bmatrix} \mu S / mile$$

Line Configuration 8:

$$z = \begin{bmatrix} 0.4576 + j1.0780 & 0.1535 + j0.3849 & 0.0000 + j0.0000 \\ & 0.4615 + j1.0651 & 0.0000 + j0.0000 \\ & & 0.0000 + j0.0000 \end{bmatrix} \Omega / mile$$

$$b = \begin{bmatrix} 5.1154 & -1.0549 & 0.0000 \\ & 5.1704 & 0.0000 \\ & & 0.0000 \end{bmatrix} \mu S / mile$$

Line Configuration 9:

$$z = \begin{bmatrix} 1.3292 + j1.3475 & 0.0000 + j0.0000 & 0.0000 + j0.0000 \\ & 0.0000 + j0.0000 & 0.0000 + j0.0000 \\ & & 0.0000 + j0.0000 \end{bmatrix} \Omega / mile$$

$$b = \begin{bmatrix} 4.5193 & 0.0000 & 0.0000 \\ & 0.0000 & 0.0000 \\ & & 0.0000 \end{bmatrix} \mu S / mile$$

Line Configuration 10:

$$z = \begin{bmatrix} 0.0000 + j0.0000 & 0.0000 + j0.0000 & 0.0000 + j0.0000 \\ & 1.3292 + j1.3475 & 0.0000 + j0.0000 \\ & & 0.0000 + j0.0000 \end{bmatrix} \Omega / mile$$

$$b = \begin{bmatrix} 0.0000 & 0.0000 & 0.0000 \\ & 4.5193 & 0.0000 \\ & & 0.0000 \end{bmatrix} \mu S / mile$$

Line Configuration 11:

$$z = \begin{bmatrix} 0.0000 + j0.0000 & 0.0000 + j0.0000 & 0.0000 + j0.0000 \\ & 0.0000 + j0.0000 & 0.0000 + j0.0000 \\ & & 1.3292 + j1.3475 \end{bmatrix} \Omega / mile$$

$$b = \begin{bmatrix} 0.0000 & 0.0000 & 0.0000 \\ & 0.0000 & 0.0000 \\ & & 4.5193 \end{bmatrix} \mu S / mile$$

Line Configuration 12:

$$z = \begin{bmatrix} 1.5209 + j0.7521 & 0.5198 + j0.2775 & 0.4924 + j0.2157 \\ & 1.5329 + j0.7162 & 0.5198 + j0.2775 \\ & & 1.5209 + j0.7521 \end{bmatrix} \Omega / mile$$

$$b = \begin{bmatrix} 67.2242 & 0.0000 & 0.0000 \\ & 67.2242 & 0.0000 \\ & & 67.2242 \end{bmatrix} \mu S / mile$$

Appendix C Secondary Distribution System Data

Table C.1 Center-Tapped Distribution Transformer Data

Transformer Rating	kV - high	kV - Low	R(%)	X(%)
25 kVA	4.16-D	0.24-Gr.Y	0.5367	1.0733
50 kVA	4.16-D	0.24-Gr.Y	1.0140	1.7239

Table C.2 Secondary System Line Data

Line Type	Conductor	Length
Secondary Line	1/0 AA	125’
Service Drop	#2 AWG	90’

Table C.3 Secondary Conductor Data

Conductor	GMR	Diameter	Resistance	Insulation Thickness
1/0 AA	0.0111 ft.	0.368 in.	0.97 Ω/mi.	80 mil
#2 AWG	0.00418 ft.	0.361 in.	1.69 Ω/mi.	80 mil

Secondary Line Impedance:

$$z_{SL} = \begin{bmatrix} 1.8149 + j0.0701 & 0.8449 + j0.3530 \\ 0.8449 + j0.3530 & 1.8149 + j0.0701 \end{bmatrix} \Omega / mile$$

Service Drop Impedance:

$$z_{SD} = \begin{bmatrix} 2.2891 + j1.0211 & 0.5991 + j0.7480 \\ 0.5991 + j0.7480 & 2.2891 + j1.0211 \end{bmatrix} \Omega / mile$$